

**DESIGN AND EVALUATION OF CHIP SEALS THROUGH IMAGE-BASED
MICROSTRUCTURAL PARAMETERS AND PERFORMANCE TESTS**

By

Yogesh Shamsunder Kumbarger

A DISSERTATION

Submitted to
Michigan State University
in partial fulfilment of the requirements
for the degree of

Civil Engineering—Doctor of Philosophy

2019

ABSTRACT

DESIGN AND EVALUATION OF CHIP SEALS THROUGH IMAGE-BASED MICROSTRUCTURAL PARAMETERS AND PERFORMANCE TESTS

By

Yogesh Shamsunder Kumbargeri

Chip seal is one of the most popularly adopted pavement preservation strategies. A chip seal treatment is constructed by adding hot asphalt or emulsion on the surface of an existing pavement, spraying aggregates on the top, followed by roller compaction. Extensive research has led to the formulation of various chip seal analysis and design methodologies. These methods are mostly empirical in nature and depend on numerous assumptions related to chip seal microstructure and their expected behavior after compaction in field. Hence, there is a need for in-depth analysis of chip seals to develop performance-based design methods addressing the primary distresses as well as the microstructural parameters such as percent embedment and aggregate orientation. The objective of this research study was to evaluate chip seals through image-based microstructural parameters and performance tests. The results of a comprehensive experimental program lead to development of a holistic approach to chip seal design, encompassing various aspects of chip seal performance through aggregate-binder microstructural perspective. New image processing techniques were developed to understand the percent embedment and aggregate orientation behavior. Additionally, finite element analyses were performed using actual chip seal images to evaluate mechanistic characteristics (e.g., magnitudes of strains at the aggregate/binder interface) responsible for chip seal performance. Further, extensive performance tests were run in laboratory to evaluate the effect of design parameters (e.g. percent embedment, aggregate orientation) on chip seal performance distresses (aggregate loss and bleeding). The results were combined and analyzed to yield new insights into effect of microstructural parameters on chip seal

performance. Furthermore, a performance-based design procedure was developed for design of chip seals. This procedure integrates the chip seal microstructural behavior and its performance.

Copyright by
YOGESH SHAMSUNDER KUMBARGER
2019

ACKNOWLEDGEMENTS

First and foremost, I would like to thank the Almighty God for giving me this opportunity and for His blessings to make this happen. It has been an incredible journey till now. Never did I know that I would be pursuing PhD one day. It was when I was accepted at IIT Kharagpur for Masters program and came in touch with my Masters thesis advisor Dr. Krishna Biligiri, that I started developing a keen interest in research and started dreaming of pursuing PhD. I would like to thank him for kindling that fire in me. I would especially like to thank my family: Dr. Shamsunder Kumbargeri (father), Amruta Kumbargeri (mother), (soon to be Dr.) Amogh Kumbargeri (brother), Nikita Kulkarni Kumbargeri (sister-in-law). I would like to thank my family for being always there for me and inspiring me to follow my passion with God's blessings.

I can vividly remember the joy after receiving the PhD offer letter from Michigan State University (MSU). After being accepted at MSU, I could have never imagined that it would be a beginning of an incredible journey. I would really like to thank my PhD Advisor Dr. M. Emin Kutay for being an amazing professor, mentor and advisor to me. He has been extremely supportive of my research ideas, career development and most of all my personality development. He is a person who wants his students to develop all the skills that are essential to succeed in the world out there. He focusses on each and every aspect of effective development of a student such as learning to perform effective literature review, developing critical thinking, observing other people's work, developing independent ideas and working on them, gaining knowledge as well as disseminating that knowledge through effective oral and written communication. I especially thank him for being so supportive of my plan to pursue summer internship at SME in 2018. Furthermore, the weekly research group meetings have been very useful to keep up the spirit and work harder

towards my research. I have always liked how during the meetings, apart from research related comments, how he also focusses on tips and tricks to achieve success and happiness in personal life as well. He has always tried his best to provide funding to us for attending and presenting at so many conferences and meetings during my PhD tenure. These conferences have helped develop my knowledge, connections, confidence as well as communication skills to a great extent. Furthermore, I would also like to thank my thesis committee members Dr. Neeraj Buch, Dr. Karim Chatti, and Dr. Thomas Pence. They have been very supportive and have provided very good inputs and guidance to me.

I would like to thank my friends Shashwath Sreedhar, Prathmesh Jichkar and Kalyani Kapsikar for being there with me during this journey. Shashwath, Prathmesh and myself used to help each other during the laboratory experiments and field visits for our Masters thesis. It has been great to have them here in the US as well during my PhD journey, although in three different states here. The TRB conferences have always been fun because of you guys. I hope we continue to attend and meet during the future conferences as well. During my initial days of getting used to the college and work life in the US, it was really smooth because of Kalyani who was also exploring it for the first time as part of her Masters program. It has been a great journey including working on assignments, projects, exam preparation etc. I would also like to thank Shardula Gawankar and Shivam Bajaj for the good support and fun time and wish great success to both.

I would like to thank my colleague, lab mate and great friend (soon to be Dr.) Aksel Seitlari. It has been a great journey together. From working on papers as well as the daily lunch sessions to discussions on diverse topics like politics, religion, nationality, career, family, values and principles etc. All those discussions have broadened my view and outlook to a great extent.

My PhD journey would not have been this much fun without a great friend and colleague like Aksel. I wish him all the very best in his career.

I would also like to thank Ilker (Dr. Ilker Boz) for being an amazing mentor, colleague and very nice friend. Ilker's advice and guidance has added value to this dissertation. It has been so much fun working with Ilker over the past couple of years. I hope we stay in touch and potentially work on projects and papers in the future. Also, I would like to thank my former lab mates Dr. Salih Kocak and Sepehr Solemani for their help during my first year of PhD at MSU.

I would like to thank Margaret Conner (former grad secretary) and her husband Dana Conner for so many things that I cannot even start naming. From teaching me how to drive, to the Thanksgiving dinners, first Christmas celebration in America, weekend hangouts, lawn and yard work activities and so many parties, essentially offering me the comfort of home away from home here in America! For me, thanksgiving is incomplete without a visit to Margaret's house! I especially appreciate her efforts to cook vegetarian food just for me whenever I visit her. The day I came to MSU, she used to say "I will retire when you are ready to graduate". And coincidentally, she is retiring in the same semester as that of my graduation. I wish her a very healthy and awesome retired life!

I would also like to thank Laura Post (current grad secretary) for being there, helping out and making my life easier as a graduate assistant all throughout my PhD program. I will definitely miss those talk sessions every morning when I used to come to civil engineering department office to take coffee. Also, I would like to thank Laura Taylor for the professional and personal support as well as the conversations every morning (with her tea!). Laura Taylor is very kind, caring and ensures administrative smoothness for all the graduate students.

Again, I would like to thank the Almighty God without Whose blessings, all this would not have been possible. I pledge to do my best throughout my life to spread the knowledge that I have gained in my PhD and also apply it to make things better for the society and pray to God to give me the strength, commitment and success in this endeavor.

TABLE OF CONTENTS

LIST OF TABLES	xii
LIST OF FIGURES	xiii
1. INTRODUCTION.....	1
2. LITERATURE REVIEW	4
2.1 <i>Chip seal design procedures</i>	5
2.1.1 Hanson design Method	5
2.1.2 Kearby and Modified Kearby Design Method.....	5
2.1.3 McLeod Design Method	6
2.1.4 Modified McLeod Design Method	7
2.1.5 Austroads method	7
2.1.6 South Africa design method.....	8
2.1.7 The United Kingdom design method (road note 39)	8
2.1.8 New Zealand method	8
2.1.9 NCSU Performance-based design method.....	9
2.2 <i>Aggregate loss tests for chip seals</i>	10
2.2.1 Vialit Adhesion Test	11
2.2.2 Frosted Marble Test	12
2.2.3 Australian Aggregate Pull-out Test	12
2.2.4 Pennsylvania Aggregate Retention Test	12
2.2.5 Pneumatic Adhesion Tension Test.....	13
2.2.6 ASTM D7000 Sweep Test.....	13
2.3 <i>Bleeding tests for chip seals</i>	15
2.3.1 Accelerated Chip Seal Simulation Device (HSKSC)	17
2.3.2 Modified Loaded Wheel Test (LWT)	17
2.3.3 Third scale model mobile loading simulator (MMLS3)	18
2.4 <i>Finite element analyses on chip seals</i>	19
2.5 <i>Evaluation of chip seal macrotexture</i>	21
2.6 <i>Summary and problem statement</i>	22
3. OBJECTIVES AND RESEARCH PLAN	25
3.1 <i>Task 1: Development of improved parameters based on image analysis and justification via finite element modelling</i>	25
3.2 <i>Task 2: Performance tests on chip seals</i>	26
3.3 <i>Task 3: Analysis of performance through image processing and finite element modelling approaches</i>	26
3.4 <i>Task 4: Performance based design procedure for chip seals</i>	27
4. EXPERIMENTAL PROGRAM, MATERIALS AND METHODS	28

4.1	<i>Quantification of Aggregate Loss</i>	32
4.1.1	Residual Aggregate Rate (RAR).....	32
4.1.2	Aggregate Loss by Hand Brushing (ALB)	33
4.1.3	Aggregate Loss by Sweep (ALS)	34
4.1.4	Cumulative Aggregate Loss (CAL).....	34
4.1.5	Residual binder application rate (RBAR).....	34
4.2	<i>Quantification of Bleeding</i>	35
4.3	<i>Finite Element Analyses on Chip Seals</i>	42
4.3.1	Finite Element Model Development.....	42
4.3.2	Stage I: Chip Seals with a Single Aggregate	45
4.3.3	Stage II: Chip Seals with Two Bridged Aggregates	45
4.3.4	Stage III: Chip Seals with Multiple Aggregates	46
4.3.5	Evaluation of the Effect of Aggregate Application Rate via FE modelling and Sweep Tests	46
5.	NEW IMAGE-BASED PARAMETERS FOR CHIP SEALS	47
5.1	<i>Orientation distribution of chip seal aggregates</i>	47
5.2	<i>Effective percent embedment (ePE)</i>	48
6.	EVALUATING AGGREGATE LOSS IN CHIP SEALS	50
6.1	<i>Modified sweep test results</i>	50
6.1.1	Aggregate Loss by Hand Brushing.....	50
6.1.2	Aggregate Loss by Sweep.....	51
6.1.3	Cumulative Aggregate Loss.....	52
6.1.4	Residual Aggregate Rate.....	55
6.1.5	Residual Aggregate Gradation.....	55
6.2	<i>Digital image analysis results</i>	58
6.2.1	Percent Embedment and Aggregate Loss	58
6.2.2	Orientation of Aggregates.....	59
6.3	<i>Comparison of hot applied and emulsion-based chip seals in terms of aggregate loss</i> ...	62
6.4	<i>Summary of chapter findings</i>	63
7.	INVESTIGATION OF BLEEDING BEHAVIOR IN CHIP SEALS	65
7.1	<i>Effect of Binder Application Rates (BAR) and Emulsion Application Rates (EAR) on Bleeding</i>	65
7.2	<i>Effect of aggregate application rate (AAR) on bleeding</i>	70
7.2.1	Characterization of effect of AAR on bleeding through 2D PBA criterion	70
7.2.2	Characterization of effect of AAR on bleeding through 3D Mean Profile Depth (MPD) criterion.....	74
7.3	<i>Relation between PE and bleeding</i>	76
7.4	<i>Comparative performance of binder and emulsion with respect to bleeding</i>	78
7.5	<i>Summary of chapter findings</i>	79
8.	DEVELOPMENT OF A PERFORMANCE-BASED DESIGN METHODOLOGY FOR CHIP SEALS	81

8.1 Aggregate orientation	81
8.2 Aggregate loss.....	82
8.3 Bleeding	83
8.4 Performance-based design procedure	84
8.5 Comparison with existing design methods.....	85
8.6 Acceptable Range of Percent Embedment	87
8.7 Summary of chapter findings	87
9. FINITE ELEMENT MODELLING OF CHIP SEALS	89
9.1 Chip Seals with a Single Aggregate.....	89
9.2 Chip Seals with two Aggregates	95
9.3 Chip Seals with Multiple Aggregates (Full Spectrum)	98
9.3.1 Evaluation of Percent Embedment and Aggregate Shape Characteristics.....	98
9.3.2 Evaluation of Aggregate Application Rate	100
9.4 Summary of chapter findings	103
10. CONCLUSIONS	106
REFERENCES.....	110

LIST OF TABLES

Table 4.1 Prony series coefficients for asphalt binder and substrate HMA.....	45
Table 8.1 Comparison of BAR and AAR values obtained by following various Chip Seal design methodologies	86

LIST OF FIGURES

Figure 2.1 Illustration of lever and wedge effect	10
Figure 4.1 Experimental flow chart	30
Figure 4.2 A picture of the sweep test device for chip seal aggregate loss testing.....	34
Figure 4.3 A picture of the modified HWT device for chip seal bleeding testing.....	36
Figure 4.4 Illustration of image analysis steps to compute the bleeding area	37
Figure 4.5 Steps of obtaining Mean Profile Depth of chip seal samples using 3D stereology imaging.	39
Figure 4.6 a) MPD visualization sketch, and b) illustration of relation between MPD and PE ..	40
Figure 4.7 Comparison of MPD values computed from the in-house MATLAB based algorithm to the values obtained from commercial laser scanning equipment	42
Figure 4.8 Stepwise procedure for obtaining finite element model of chip seals.....	44
Figure 4.9 Illustration of the horizontal and vertical stress functions applied to the top of the chip seals: Top graph is the normalized shape functions, and bottom graph is the actual stresses applied	45
Figure 5.1 (a) A screenshot of the CIPS software illustrating the computation of percent embedment using each aggregate method, (b) illustration of orientation of the aggregates	49
Figure 6.1 Aggregate loss by hand brushing (ALB) results for (a) set I- B and (b) set II- B, Aggregate lost by sweep (ALS) for (c) set I-B and (d) set II- B, and Cumulative aggregate loss (CAL) for (e) set I- B and (f) set II- B	53
Figure 6.2 Aggregate loss by hand brushing (ALB) results for (a) set III- B and (b) set IV- B, Aggregate lost by sweep (ALS) for (c) set III-B and (d) set IV- B, and Cumulative aggregate loss (CAL) for (e) set III- B and (f) set IV- B.....	54
Figure 6.3 Residual aggregate application rate (RAR) for (a) set II-B (hot-applied) and (b) set IV- B (emulsion), Δ RAR for (c) set II-B and (d) set IV-B, (e) picture of aggregates lost due to hand brush and (f) picture of initial aggregate sample	57

Figure 6.4 (a) ALS vs PE, (b) ALS vs ePE, (c) CAL vs PE ,and (d) CAL vs ePE including data from hot applied as well as emulsion based chip seals (groups I,II,III and IV)	60
Figure 6.5 (a) CPAF vs BAR for set I-A, (b) CPAF vs AAR for set II-A, (c) CPAF vs BAR for set III-A, (d) CPAF vs AAR for set IV-A, (e) illustration of flat side orientation of aggregates, (f) illustration of change in orientation of aggregates due to lever and wedge effect, (g) a picture showing the binder sticking to the compaction rubber pad resulting in change in orientation of aggregates in case of high BAR.....	61
Figure 6.6 a) Comparison of Cumulative Aggregate Loss by sweep (CAL) for binder and emulsion-based chip seals at RBARs, b) sketch showing concave shape of emulsion surface, c) sketch showing convex shape of emulsion surface.....	63
Figure 7.1 a) PBAs and b) Δ PBA for hot applied chip seals with different BARs	67
Figure 7.2 Aggregate pickup during HWT tests of high BAR (0.4 gal/yd ²).....	68
Figure 7.3 a) PBAs and b) Δ PBA for emulsion-based chip seals with different EARs	69
Figure 7.4 For hot applied chip seal samples: a) PBAs at different cycles b) Δ PBA, c) CPAF for different AARs.....	72
Figure 7.5 For emulsion applied chip seal samples: a) PBAs at different cycles b) Δ PBA, c) CPAF for different AARs	73
Figure 7.6 MPDs at different cycles for hot applied chip seal samples with AAR of 18 lb/yd ² , 20 lb/yd ² , and 22 lb/yd ²	75
Figure 7.7 MPDs at different cycles for emulsion-based chip seal samples AAR of 18 lb/yd ² , 20 lb/yd ² , and 22 lb/yd ²	76
Figure 7.8 a) PBA vs ePE and b) PBA vs ePE at 1500 HWT cycles	77
Figure 7.9 a) PBA and b) Δ PBA for binder and emulsion applied chip seals	78
Figure 8.1 Variation of cumulative percentage of aggregates lying on their flat side (CPAF) for samples of set I-A (hot applied) with different aggregate application rates (AARs)	82
Figure 8.2 Variation of the Cumulative Aggregate Lost by sweep (CAL) for Set II-B (hot applied) samples with different binder application rates (BARs).....	83
Figure 8.3 The change in the Percentage Bleeding Area (PBA) for Set II-C (hot-applied) samples with different binder application rates (BARs).....	84
Figure 8.4 Flowchart depicting the performance-based procedure for chip seal designs.....	86

Figure 8.5 Illustration of determination of acceptable range of percent embedment	88
Figure 9.1 Tensile strain distributions at 25°C around the binder-aggregate interface at various percent embedment for the chip seal with the cubical aggregate	91
Figure 9.2 Maximum tensile strain (ϵ_{Tmax}) at the binder-aggregate interface as a function of temperature and percent embedment for the chip seal with the cubical aggregate	91
Figure 9.3 Tensile strain distributions at 25°C around the binder-aggregate interface at various percent embedment for the chip seal with the flaky aggregate.....	94
Figure 9.4 Maximum tensile strain (ϵ_{Tmax}) at the binder-aggregate interface as a function of temperature and percent embedment for the chip seal with the flaky aggregate.....	94
Figure 9.5 Percent Change in ϵ_{Tmax} with change in PE, for single aggregate at 25°C	95
Figure 9.6 Tensile strain distributions at 25°C around the binder-aggregate interface at various percent embedment levels for the chip seal with two cubical aggregates	96
Figure 9.7 Tensile strain distributions at 25°C around the binder-aggregate interface at various percent embedment levels for the chip seal with two flaky aggregates.....	97
Figure 9.8 Maximum tensile strain (ϵ_{Tmax}) at the binder-aggregate interface at 25°C as a function of percent embedment for the chip seals with two aggregates	97
Figure 9.9 Tensile strain distributions at 25°C around the binder-aggregate interface at various percent embedment levels for the chip seal with multiple aggregates (cubical)	99
Figure 9.10 Tensile strain distributions at 25°C around the binder-aggregate interface at various percent embedment levels for the chip seal with multiple aggregates (flaky).....	99
Figure 9.11 Maximum tensile strain (ϵ_{Tmax}) at the binder-aggregate interface at 25°C as a function of percent embedment for the chip seals with multiple aggregates.....	100
Figure 9.12 Snapshots of FEM meshes of chip seal samples prepared at several AARs.	101
Figure 9.13 Maximum tensile strain (ϵ_{Tmax}) at the binder-aggregate interface as a function of temperature for the chip seals with different aggregate application rates	102
Figure 9.14 Cumulative Aggregate loss from the sweep test at a range of temperatures for the chip seals with cubical and flaky aggregates.	103

1. INTRODUCTION

Chip seals are one of the main pavement preservation treatments. They are used to improve the functional properties of the existing pavements, and often preferred to address pavements exhibiting surface integrity and texture problems (D. Gransberg & James 2005; Abedini et al. 2017; Gransberg & Zaman 2005a; Praticò et al. 2016; Guirguis & Buss 2017). They are also beneficial in extending the service life of the existing pavements by slowing down the oxidation and preventing water to infiltrate into the pavements. The popularity of this treatment stems from their cost-effectiveness and ease of construction. Over the past few years, there has been an increased focus on pavement preservation treatments (Serigos et al. 2017; Johannes et al. 2011; Lee & Kim 2008a; Pierce & Kebede 2015; D. D. Gransberg & James 2005; Haider et al. 2019). Chip seal performance primarily depends on the interaction between its two main constituents: aggregate and binder. An optimal aggregate-binder interaction provides efficient and long-lasting performance. There have been numerous studies to develop design methodologies for chip seals (Epps, C.W. Chaffin, et al. 1980; F. M. Hanson 1934; Kearby 1953; Mcleod et al. 1969; Roberts & Nicholls 2008; Epps & Gallaway 1972; AASHTO-PP82 2016; TNZ-report 2005). These studies focused on the binder and aggregate application rates and included certain assumptions on aggregate-binder interactions. For example, it is assumed that voids in chip seal aggregates get filled with binder at a specific percent embedment level at different stages of construction and service life. These calculations are based on another assumption that all the aggregates lie on a plane parallel to their flattest sides, perpendicular to the average least dimension (ALD).

Kearby's design (Kearby 1953) methodology introduced application rates and percent embedment for designing chip seals. A nomograph was developed for calculating binder and aggregate application rates from percent embedment and voids between aggregates. McLeod design methodology uses empirical equations to estimate binder and aggregate application rates. Percent embedment criteria was indirectly used in the form of traffic correction factor, for computing binder application rates. Based on similar concepts, there have been other chip seal design methodologies (TNZ-report 2005; South-african-national-road-agency-report 2007; AASHTO-PP82 2016; Roberts & Nicholls 2008). Effect of chip seal microstructure on its performance has been acknowledged by all of the above design methodologies, however, the parameters representing the chip seal microstructure have been very simplistic (e.g., average least dimension) and computed indirectly. Aggregate size and orientation distribution were not considered. Percent embedment calculations were based on sand patch test results, which includes assumptions that do not necessarily represent the real chip seal microstructure in the field. Overall, these methods have not been successful in integrating the effect of chip seal microstructure and its performance. Therefore, there is a need for an in-depth evaluation of the relationship between the performance and chip seal microstructural characteristics such as percent embedment and orientation distribution of individual aggregates. This requires development of new image processing techniques to directly measure the percent embedment and orientations of the aggregates as well as conducting extensive performance tests on various chip seal microstructures. This can help develop comprehensive chip seal design and evaluation guidelines encompassing fundamental parameters, performance indicators (distresses) and low-cost innovative methodologies.

This research study is a holistic investigation of factors affecting hot and emulsion-based chip seal performance. Various aspects of chip seal characteristics are presented individually in separate chapters. Chapter 2 includes a comprehensive literature review on various methods of chip seal evaluation and design. The objectives of this research study and a research plan is summarized in Chapter 3. The experimental program and materials and methods used in this study are presented in Chapter 4. New image-based parameters that were developed in this study have been explained in Chapter 5. Chapters 6 and 7 include results of analyses of chip seal aggregate loss and bleeding behavior respectively, achieved through image analysis and performance tests. The new performance-based design procedure that has been developed in this study has been presented in chapter 8. Chapter 9 includes chip seal evaluation through finite element approach. Chapter 10 includes summary and conclusions of this study.

2. LITERATURE REVIEW

This section includes the literature review on chip seal design methods and evaluation of performance distresses. Also, previous efforts on evaluation of chip seals through mechanistic approaches have also been discussed.

In the United States, chip seal design has been reported to be somewhat of an art rather than a science (D. D. Gransberg & James 2005). Initial efforts to design chip seals were based on a purely empirical approach (F. M. Hanson 1934; McLeod 1969; Kearby 1953). With further research, this approach was slightly modified with inclusion of aggregate shape and other morphological characteristics (Johannes et al. 2011; Epps, C W Chaffin, et al. 1980; Epps & Gallaway 1972). McLeod and Kearby design procedures are some of the popular examples of this approach. Geographical differences, variable nature of materials as well as surface conditions were some of the challenges in establishing a nationwide design method. Empirical approaches are used by many road agencies, based on their experience with the local materials. A research study by Gransberg et al. showed that less than one third of total number of states in the US use a formal method to design chip seals. Less than twelve states don't use any formal method and remaining states design chip seals based on their own experience as explained above (D. D. Gransberg & James 2005).

State road agencies often utilize warranty specifications for chip seals (MDOT-warrantyguidelines 2017). In general, short-term performance warranties are in place for approximately 5-10 years period. Some specifications exist a shorter period of around 12 months in case of chip seals or general pavement preservation treatments. Different states have different performance requirements based on the critical conditions faced by the road agencies and historic

performance data (IDOT-guide 2017; NCDOT-manual 2016). As more states move towards performance warranties, it will become imperative for the road agencies as well as contractors to adopt performance-based design approaches for pavement preservation in general and chip seals in particular.

2.1 Chip seal design procedures

2.1.1 Hanson design Method

This method was the first attempt at formal design of chip seal treatments (F. Hanson 1934). The main assumption of this method was that the voids in chip seal aggregates after spreading over the pavement, rolling and traffic condition becomes nearly 50%, 30% and 20%, respectively. Another assumption of this method was that after opening to traffic, aggregates lie on their flattest side and therefore, average least dimension (ALD) is nearly equal to the average thickness of the aggregates after the construction. The concept of ALD was introduced for the very first time by this method. The other design methods developed later are more or less improvements of this method. The improvements mostly relate to correction factors with respect to aggregate types, emulsion residues, amount of traffic, etc.

2.1.2 Kearby and Modified Kearby Design Method

In the United States, one of the first efforts for chip seal design was made by Jerome Kearby in 1953 (Kearby 1953). This method resulted in development of nomograph to obtain binder application rates based on input data of average mat thickness, percent embedment and voids percentage. Aggregate application rate (AAR) is calculated based on results from test board method (AASHTO-PP82 2016). In this method, aggregates are applied on a board with an area of one square yard, such that it achieves single aggregate (one stone thick) layer. This method applies mostly to the uniformly graded aggregates. Also, the range of percent embedment and voids

percentage used for mat thickness calculation is very limited. This method doesn't consider the effect of traffic for adjustment of mat thickness calculations.

Further research by Epps et al. in 1980 lead to a modified nomograph for incorporating synthetic aggregates that are generally porous and lightweight (Epps, C.W. Chaffin, et al. 1980). The revised nomograph also allowed broader range for percent embedment. Correction factors were developed to help account the effects of traffic on mat thickness (Epps & Gallaway 1972). Also test board procedure with AAR was slightly modified by recommending the aggregates to be spread on an area of half square yard instead of one square yard as in Kearby Method. These modifications were incorporated and named as "Modified Kearby Design methodology"(Epps, C W Chaffin, et al. 1980).

2.1.3 McLeod Design Method

This method was developed by Norman McLeod in 1969 (McLeod 1969) and was later adapted by the Asphalt Institute. This method is based on two basic principles:

- Computation of aggregate application rate is based on assumption that the resulting layer would be one-stone thick. Further, all the aggregates are assumed to lie on their flattest sides. In this method, a term called aggregate least dimension (ALD) is used to represent the height of the chip seal, which is equivalent to the average of the shortest dimension of the aggregates used in the chip seal.
- The volume of air voids between the aggregates is assumed to be 50% of the total volume, immediately after the aggregate application, before compaction. This volume reduces to 30% after compaction and eventually to 20% after sufficient trafficking. The binder/emulsion to be applied should fill 65% to 70% of the final 20% of the voids to prevent aggregate loss due to insufficient binder/emulsion application rate.

In this method, the aggregate application rate depends on the aggregate gradation, shape, and specific gravity. The binder application rate depends on the aggregate gradation, absorption and shape, traffic volume, existing pavement condition, and the residual asphalt content of the binder.

2.1.4 Modified McLeod Design Method

The underlying assumption of McLeod design method that the final volume of air voids being 20% was critically investigated by other research studies. It was reported that final volume of air voids in chip seals was higher than 20%, and a value of 40% was recommended (Potter & Church 1969). Research studies have explained that the 20% final void content assumption was only applicable for materials and construction procedures during olden days. Aggregates used were relatively soft and it was hypothesized that steel rollers could have crushed the aggregate particles during compaction. A value of 20% was used to derive the McLeod's design equations for aggregate and binder application (Johannes et al. 2011). Using a smaller value for the final void content in the McLeod's design equations results in a higher aggregate application rate and a lower binder application rate than the actual optimal values. The design equations for this method can be found in (Johannes et al. 2011).

2.1.5 Austroroads method

In this method (Austroroads 2018), some of the earlier general assumptions from Hanson method (F. M. Hanson 1934) are used but with slight modifications. The concepts of ALD and one stone thick layer of aggregates are used in this method as well. Furthermore, only single sized aggregates are used in this method. The basic binder application rate is calculated by percentage of void between aggregates filled with asphalt (VFA), void content between aggregates (VMA), traffic volume and type. The major modification in assumption is that percent embedment during

rolling and initial traffic is 35-40% which increases to 50-65% after two years of construction. Additional correction factors have also been recommended for inculcating the effect of traffic volume.

2.1.6 South Africa design method

This method (South african national road agency report 2007) is based on combination of Hanson and modified Kearby design methods. The principle of binder filling certain assumed percentage of voids and leading to aggregates lying on ALDs is valid for this method as well. Approximately 40% of voids between the aggregates are assumed to be filled. Nomograph for aggregate application rates determination as well as use of residual binder content (in case of emulsions) have been adopted from modified Kearby method.

2.1.7 The United Kingdom design method (road note 39)

The design procedure for United Kingdom is called as Road note 39 (Roberts & Nicholls 2008). In this method, surface hardness of existing pavement is measured using a hardness probe and road hardness (RH) is characterized based on those results. The binder application rates are recommended based on temperature (climate) and traffic with its effect on the hardness of the surface. Apart from the basic assumptions related to chip seals as discussed before, this method also specifies macrotexture and noise related requirements for a safe and quiet chip seal pavement.

2.1.8 New Zealand method

This method (TNZ-report 2005) is a slightly modified version of Hanson's method. At least 35% of the total voids are assumed to be filled until the first winter. Bleeding is the major distress that has been addressed in this method. Hence the assumptions related to amount of filling of voids by the binder are on the lower threshold than that of the other popular international design methods. High binder application rates are strictly discouraged.

2.1.9 NCSU Performance-based design method

This is the most recent chip seal design methodology that considers chip-seal microstructure, in addition to several other tests (Kim et al. 2012). It involves aggregate analysis (specific gravity), volumetric calculations and results from 3D laser profile scanning tests in order to determine the binder and aggregate application rates for chip seals.

In the first step, aggregate application rate is determined using board test. The main objective in this step is to ensure that, at selected aggregate application rate, only a single layer of aggregates is formed without overlapping. In the next step, 3D laser profile tests are run on the aggregate mat to find total volume of the aggregates lying on the surface. Also, aggregate density is measured in accordance with the ASTM C-29 method (ASTM-C29 2009). Using density results, volume of aggregates is calculated. From total volume and aggregate volume results, volume of air is calculated. This is further used in the next step to evaluate the optimum binder application rate.

Main drawbacks of this method are:

- The effect of binder and aggregate application rates on aggregate orientation is ignored. Use of board test to compute aggregate application rates fails to consider the combined effect of aggregate interaction on overall aggregate-binder arrangement after compaction in the field. In the absence of binder and compaction, most of the aggregates align in a plane perpendicular to their shortest dimension. However, aggregate orientation strongly depends on the presence of binder and also on the aggregate-binder interaction during compaction. Over application of aggregates lead to the ‘lever and wedge’ effect, where excessive aggregates push the other aggregates sideways and upwards, causing them to misalign (see Figure 2.1). It has been proved from previous research, that orientation of

aggregates is an important parameter affecting chip seal performance (Y. S. Kumbargeri, Kutay, et al. 2018; Y. Kumbargeri et al. 2018; Y. S. Kumbargeri, Boz, et al. 2018). Hence, aggregate orientation needs to be considered while designing chip seals. This is especially important while determining the aggregate application rates with the objective to ensure that most of the aggregates align to their flattest sides when constructing chip seals.

- This method requires the use of a laser scanning equipment. Most of the road agencies, especially county road departments, do not have access to a laser scanning equipment. Hence, it is important to develop a design methodology that doesn't require use of expensive equipment.

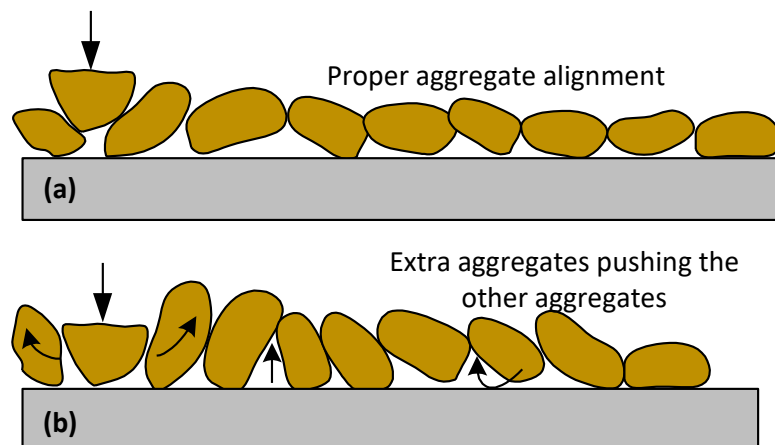


Figure 2.1 Illustration of lever and wedge effect

2.2 Aggregate loss tests for chip seals

Aggregate loss occurs because of weak binder-aggregate bond. This is generally caused by insufficient embedment of aggregates into the binder. Low binder application rates or high aggregate application rates generally lead to occurrence of this distress. The other factors affecting chip loss can be listed as follows:

- High traffic stress: This can happen due to high volumes of activity, excessive weights of vehicles, braking and acceleration.

- Environmental conditions: Precipitation immediately after chip seal construction can have an adverse effect on development of the bonding of aggregates and binder, leading to high susceptibility to aggregate loss.
- High dust content: If the aggregates used for chip seal applications have a high dust content, it adversely affects the bonding of the aggregate and binder. This results in higher susceptibility to aggregate loss.

Several methods have been developed to characterize aggregate loss in chip seals. A summary of each procedure is presented in the following subsections.

2.2.1 Vialit Adhesion Test

The Vialit Adhesion Test was first introduced in France to measure the effect of binder and aggregate type on performance (Louw et al. 2004). It consists of three component metal bases with the vertical rod, a steel ball, and metal test plates. The steel ball is dropped over inverted chip seal sample and aggregate loss is computed through chip seal weight measurement before and after the test. Jordan and Howard (2010) studied applicability of the Vialit test on surface seal treatments with respect to performance (Jordan & Howard 2010). It was concluded that results from the Vialit test are always questionable and it is not sufficient to make conclusions regarding performance of seal treatments. Another study by Epps-Martin et al (2001) also suggested that results from the Vialit test are inconsistent and they cannot differentiate between good and poor performance of the seal treatments (Epps-Martin et al. 2001). Nevertheless, it remains as one of the popular tests for aggregate loss due to the ease of conducting this test. It was used as the major aggregate loss performance test in the recent NCHRP study on performance specification for chip seals (Kim et al. 2017)

2.2.2 Frosted Marble Test

The Frosted Marble Test (FMT) was developed to measure binder adhesion by applying torque to marbles fixed to a base tray with the binder. The test setup consists of a torque wrench, a hooked foot for applying shear and a tray on which binder is spread and marbles are placed, respectively. Howard et al. (2009) made a modification to the FMT setup by including temperature control using an environmental chamber. They also modified the curing procedure. Howard et al. (2009) stated that although the results from the FMT seem to be valuable for evaluating the performance of binder adhesion and curing, it is not enough by itself and other test methods should be used to make comprehensive evaluation.

2.2.3 Australian Aggregate Pull-out Test

This test method was developed to measure the necessary pull-out force to separate aggregates from the asphalt bitumen material in surface seal treatments. After the surface seal treatment is prepared, the embedded aggregates are fixed by a crocodile clip and a 20 g/sec pull-out rate is applied to the stone until it is detached. During this procedure, load measurements are taken continuously. One of the uses of this test method can be found in determining the duration of traffic control after construction. In addition, coated average area of the binder on the aggregate was reported to correlate with the peak tensile stress needed to pull out the aggregate (Sendheera et al. 2006).

2.2.4 Pennsylvania Aggregate Retention Test

The Pennsylvania Aggregate Retention Test (PART) was first developed by National Center for Asphalt Technology (NCAT) at Auburn University (Kandhal & Motter 1991). The test simulates the effect of traffic on surface seal treatments by using a laboratory sieve shaker. A surface seal treatment sample is prepared within the pan and after the compression and curing

process, initial aggregate loss is obtained by turning the pan upside down. Then, the pan is placed in the sieve shaker upside down at an inclination of 45°. After 5 minutes of shaking, aggregate loss is measured and calculated as a percentage.

2.2.5 Pneumatic Adhesion Tension Test

The Pneumatic Adhesion Tension Testing Instrument (PATTI) (ASTM D4541 2009) is used for evaluating bond strength of an asphalt binder by applying direct tension. In this test tensile force is applied to the asphalt binder in a gradual manner until a specified load value is reached or either the asphalt binder layer gets detached from the loading fixture. With respect to general application of this test to all materials, the two common uses of this test are test to fracture (Protocol 1), and tensile bond strength (Protocol 2) as per ASTM D4541. But with respect to asphalt binder, generally the tensile bond strength is measured and reported. This test has been generally used for comparative evaluation of asphalt binders, generally with an intent to test the effects of various PG grades and modifications on asphalt binder properties (Zhou et al. 2014).

2.2.6 ASTM D7000 Sweep Test

The sweep test (ASTM-D7000 2011) is one of the laboratory test methods suggested by the NCHRP Report 680 (Shuler et al. 2011) for evaluation of the performance of asphalt chip seals in terms of aggregate loss. The test procedure includes fabrication of asphalt chip seal samples and testing by applying shear force to the surface of aggregates by using a nylon strip brush affixed to the mixer. Before and after testing, the sample is weighed and the percentage of mass loss is calculated (ASTM-D7000 2011). The goal of the sweep test is to measure the adhesive properties of an emulsion just after the construction, not to simulate the effect of traffic. In other words, this test method is designed to assess the curing characteristics of chip seals. However, researchers have used this method to evaluate the aggregate loss performance of the chip seals.

Among the different test methods mentioned above, sweep test was recommended to be the best for aggregate loss characterization of chip seals. Previous studies compared different asphalt emulsions and binders, and suggested the use of modified binders and emulsions for better performance (Lee & Kim 2012; Aktaş et al. 2013; Rizzutto et al. 2015; Abedini et al. 2017; Gransberg & Zaman 2005b). Furthermore, studies analyzing the effect of binder and aggregate application rates on the aggregate loss of chip seals have also been conducted (Lee & Kim 2008a; Lee et al. 2013). These studies focused on chip seal aggregate loss performance from an empirical perspective. The ASTM D7000 sweep test (ASTM-D7000 2011) was originally intended to investigate the curing characteristics of emulsion-based chip seals to determine the amount time required for the chip seal to sufficiently cure before traffic could be allowed on the surface. Additionally, the sweep test has successfully been utilized (with slight modifications) by various researchers to study the effect of several other factors on performance characteristics of chip seals, including hot applied chip seals (Aktaş et al. 2013; Rizzutto et al. 2015). The sweep test was found to be effective in discerning the performance of chip seals due to differences in aggregate mineralogy and gradation, curing temperature, humidity, type of emulsions, aggregate pre-coating and moisture content (Miller et al. 2010; Wasiuddin et al. 2013; Howard et al. 2017; Johannes et al. 2011). Ranking of field performances of emulsion-based and hot applied chip seals were also evaluated based on the aggregate loss calculated from the sweep test. It was found that the sweep test performed in the laboratory can properly rank specimens to match the field performance (Wasiuddin et al. 2013). Moreover, the sweep test was recommended as the optimal aggregate retention test method among other performance tests (the Vialit and FMT) for emulsion-based chip seals (Howard et al. 2017).

2.3 *Bleeding tests for chip seals*

Bleeding is one of the major chip seal distresses. It is the reduction in the surface texture depth due to asphalt binder rising (or oozing) to the surface. Excessive bleeding can cause significant reduction in skid resistance. This distress is usually observed along the wheel path and around the areas of frequent loading such as intersections where slow traffic and turning movements lead to high stresses. Also due to bleeding, oozed binder can adhere to tires (especially at elevated temperatures), causing them to pick up aggregates and lead to further damage on chip seals. High binder application rates or low aggregate application rates coupled with high temperature conditions lead to bleeding. A survey of US public road agencies was conducted by Gransberg (Gransberg 2005). This survey covered the agencies that use chip seals as an important pavement preservation solution. It identified bleeding and aggregate loss as the two most common distresses for chip seals. Further, bleeding was pointed out to be the most common distress by 81% of respondents which was followed by aggregate loss (67%) (Gransberg 2005). This survey further highlighted the importance of bleeding, as a major distress in chip seals. Susceptibility of chip seals to bleeding depends on several factors described below:

- Aggregate properties: Aggregate properties such as gradation, shape, size and toughness are factors affecting bleeding performance (Chaturabong et al. 2015). Non-uniform gradation (i.e., well graded aggregates) is an important concern in chip seals (Senadheera et al. 2000). This is because aggregates with different sizes will embed into binder at different extents. Some of the small aggregates may be fully embedded and others (especially large aggregates) may be embedded insufficiently (Shuler et al. 2011). Such non-uniformity in embedment creates localized distresses which later spreads to the whole surface due to tire-pickup phenomenon.

- Type of binder :Type and grade of asphalt binder significantly influences the susceptibility of chip seals to bleeding (Shuler et al. 2011). Modified binders typically improve the performance of chip seals with respect to bleeding. Recently, performance related specifications have been developed to choose appropriate emulsion for particular climatic conditions (Kim et al. 2017). Similar studies need to be performed for hot applied chip seals as well.
- Binder application rate: Optimum binder application rate is extremely important to adequate performance of chip seals. Very high content of binder leads to bleeding. Furthermore, traffic volumes play an important role in selection of the binder application rates. It has been reported by some studies that roads with high traffic volumes need lower binder application rates. It is because the heavy traffic can cause aggregates to penetrate into underlying surface after the road is opened to traffic (Texas Department of Transportation 2010).
- Climate: Climate plays a key role in potential for chip seal bleeding. In order to properly address the effect of climate on chip seals, an emulsion performance grading procedure has been developed as part of a recent NCHRP study (NCHRP project 9-50) (Kim et al. 2017).
- Existing pavement surface: Existing pavement surface should not be treated with chip seals during excessively hot days. Soft HMA surface may cause lead to aggregate penetration into substrate.

It is clear that characterization of chip seal bleeding phenomenon is a complicated task. Effect of all or most of the above factors must be taken into consideration. There has been a comprehensive and successful attempt to develop performance related specifications for selection of emulsions for different geographical regions and climatic conditions (Kim et al. 2017). Also,

many chip seal design methodologies have attempted to suggest binder and aggregate application rates based on many assumptions.

Few research studies have focused on characterizing bleeding in the laboratory. These studies used several kinds of small scale loaded wheel tracking devices described below:

2.3.1 Accelerated Chip Seal Simulation Device (HSKSC)

Accelerated Chip Seal Simulation Device (abbreviated in Turkish language as HSKSC) is a vehicle load simulator that was developed in Turkey (Aktaş et al. 2013) to assess the chip seal performance in the laboratory. The loading system is built inside a temperature-controlled cabin, so that moving load can be applied under different temperatures. It provides back and forth movement of the wheel through a pneumatic piston. The diameter of the tire is 48.5 cm, and it is inflated to 70 psi. The wheel travels at a speed of about 1500-wheel application per hour. More than one wheel can be fixed to the transverse shaft to allow for testing of multiple samples at the same time. These units are operated by an external microprocessor-controlled, programmable electronic panel. Although this device considers the effect of moving loads and temperatures, it does not account for real field loads and loading pattern. It has been mostly used to understand performance of surface treatments on a comparative basis.

2.3.2 Modified Loaded Wheel Test (LWT)

The loaded wheel test (LWT) has been specified in ASTM D6372 (ASTM-D6372 2005) and is intended for use to assess bleeding potential in slurry seal and microsurfacing applications. The test applies a rubber-tired wheel (7.62 cm in diameter) with a load of approximately 57 kg to a microsurface for 1,000 cycles at a frequency of 44 cycles per minute. The weight of the dry sample is recorded, and hot sand, heated to 85°C, is added to the sample. The sample is further subjected to 100 cycles with the sand on top of it. The sand is dusted off the sample at the end of

100 cycles, and the weight of the sample is recorded again. Bleeding is determined indirectly through limitation of the amount of sand that adheres to the samples. In a study by Chaturabong et al. (2015), LWT was modified in order to be applied to chip seal bleeding characterization. The test was modified to better represent field conditions through the provision of a mechanism to control. During initial testing, significant raveling (i.e., aggregate loss) was observed. This behavior was attributed to the stiffness of the steel plate used to support the sample in the original LWT device. One cause of bleeding was embedment of aggregate chips into the existing pavement. For the representation of this condition and to provide a flexible support, a neoprene foam pad was placed between the steel plate and sample.

2.3.3 Third scale model mobile loading simulator (MMLS3)

The third scale model mobile loading simulator (MMLS3) is one of accelerated pavement testing devices for determining performance of different kinds of pavements by simulating traffic effect in a determined scale. Lee (2003) first introduced the MMLS3 to measure hot mix asphalt (HMA) performance with respect to fatigue cracking and rutting. This test machine consists of 4 bogies, 1 axle per bogie and 1 wheel/tire per axle (Bhattacharjee et al. 2004). Each wheel has a diameter of 80 mm and can apply a maximum of 800 kPa pressure, and between 1.9 kN and 2.7 kN load. Since the MMLS3 is inside an environmental chamber, the desired temperature can be sustained. In addition to applicability of MMLS3 to HMA pavements, this test is also applicable to surface seal treatments. MMLS3 has been extensively used to characterize bleeding performance of chip seals in recent years. The latest NCHRP project 9-50 (Kim et al. 2017) used MMLS3 as the sole bleeding analysis tool for chip seal pavements.

The above studies developed customized equipment to test and analyze bleeding performance. Although these studies showed promising results, it may not be economically

feasible for the road agencies to buy a specialized equipment for chip seal bleeding evaluation. Because chip seals are applied to low volume roads, road agencies and companies may not be keen on investing additional money on such equipment. Thus, it is important to use readily available equipment to save additional cost of procuring a new equipment. Hamburg wheel tracking device (HWT) is one of the most popular pieces of equipment used to characterize rutting in asphalt pavements. Many road agencies and laboratories have access to HWT. Consequently, it is a feasible option to characterize chip seal bleeding through HWT.

2.4 Finite element analyses on chip seals

One of the first mechanistic analyses of chip seals was done by Huurman et.al. (Huurman et al. 2003), where stress and strain development at the aggregate-binder interface was investigated via a finite element (FE) model. Herrington and Henderson (Herrington & Henderson 2004) developed a 2D FE model using cross-sectional images obtained from chip seal core slices. Consistent with the observations from Huurman's study (Huurman et al. 2003), Herrington and Henderson (Herrington & Henderson 2004) showed that the critical stress and strain conditions develop at the interface of binder and aggregate chips. Huurman (Huurman 2010) later developed an improved model of chip seals, with better meshing of aggregate chips and more realistic spacing between aggregate. Furthermore, a base layer was also included in this model to simulate real field conditions. The study investigated changes of stress and strain in chip seal microstructure by varying the shape of aggregates and load conditions. A study undertaken by Kathirgamanathan & Herrington (Kathirgamanathan & Herrington 2014) focused on developing a 3D FE model to predict the deformation behavior of chip seals for low-volume roads. 3D images obtained using X-ray computed tomography of a real chip seal core was utilized in building the FE model. The study revealed that aggregate interlock reduced the maximum stress levels developed in the binder.

Gerber & Jenkins (Gerber & Jenkins 2017) analyzed individual failure mechanisms (adhesive damage, cohesive damage, and surface texture loss) at a component level for single, double, and cape seals using a 2D FE chip seal model. The results of the study quantified the changes in stress and strain responses of chip seals with respect to changes in the traffic and material properties. The percent embedment (PE) of aggregates is one of the most important parameters governing the chip seal performance. Although its importance has been repeatedly indicated, there are a very limited number of research studies focused on the PE as an important parameter for chip seal design, analysis, and evaluation (Boz et al. 2019; Boz et al. 2018; Ozdemir et al. 2018; Y. S. Kumbargeri, Kutay, et al. 2018; Y. Kumbargeri et al. 2018). While the previous studies have contributed significantly towards the development of a mechanistic evaluation of chip seals, they were not able to incorporate the effect of the PE on chip seal performance.

Another important characteristic that impacts the performance of chip seals is the shape of aggregates. In the current state of practice, most designs do not adequately consider the shape characteristics of aggregates used in chip seals. Additionally, the lever and wedge effect (see Figure 2.1) in chip seal aggregate structure is hypothesized to be the cause of detrimental performance of chip seals when high aggregate application rates are used (Boz et al. 2018; Ozdemir et al. 2018; Y. S. Kumbargeri, Kutay, et al. 2018). Due to the lever and wedge effect, excessive aggregate application rates lead to distortion of aggregate orientation. As a result, aggregates do not necessarily lie on their flattest plane at the end of compaction.

On the other hand, since the mechanical response of an asphalt binder to loading highly depends on temperature, understanding the effect of temperature on chip seal performance is also of a great importance. Hence, in-depth understanding of the percent embedment, aggregate shape characteristics, temperature, and aggregate application rates on the performance of chip seals

through a finite element approach are needed to further shed light on chip seal design characteristics.

2.5 Evaluation of chip seal macrotexture

Pavement texture has often been defined as deviation of pavement surface from a true planar surface (Bitelli et al. 2012). Characteristics related to texture have been reported to affect several functions: safety, friction, noise emission, driving comfort, rolling resistance, wear of tires, gas emissions (Praticò et al. 2013; Ejsmont et al. 2017; Sakhaeifar et al. 2018; Noyce et al. 2005; Henry 2000). Hence pavement texture characterization is an important task. It becomes especially important for chip seal treatments, because one of the primary functions of chip seal includes providing well textured surface for adequate tire/pavement friction. Texture characterization can be divided into 2 categories: micro texture and macro texture. Micro texture corresponds to wavelengths less than 0.5 mm and peak-to-peak amplitudes of the profile ranging between 1 micron and 0.2 mm. Macro texture corresponds to wavelengths between 0.5 mm and 50 mm, with peak-to-peak amplitudes between 0.2 mm and 10 mm (Praticò & Vaiana 2015; Bitelli et al. 2012). For chip seal related surfaces macro texture characterization is performed.

Traditionally, volumetric measuring techniques have been adopted to indirectly compute the texture related characteristics of chip seals. New Zealand sand circle test (TNZ 1981) and the US Sand patch tests (ASTM-E965 2015) have been popular volumetric techniques for texture characterization. In these methods, sand or glass beads are spread on a pavement surface in a circular motion, and the diameter of the resultant shape is measured. The measured diameter and initial volume of sand (or glass bead) are used to compute of the average depth of the sand, which is equivalent to macro texture depth. There are two major disadvantages of these methods. Firstly, it is an indirect way (based on assumptions) to compute texture. Secondly, they have been reported

to not have a good repeatability, due to the strong dependency on the experience of the operator (Flintsch et al. 2003; Bitelli et al. 2012).

In order to overcome these drawbacks, many laser-based techniques have been introduced. Several research studies have been performed to either develop new laser scanning equipment or algorithms related to analysis of laser related measurements for texture computations (Kim et al. 2013; Wang et al. 2011; Ran et al. 2015; Javon M. Adams & Kim 2014; Meegoda & Gao 2015; Čelko et al. 2016; Praticò et al. 2016; Bitelli et al. 2012). Also, commercial laser scanning equipment are currently used in certain road agencies. The major drawback of these equipment is that they are very expensive. There is a need to develop simple and low-cost techniques to compute macro texture characteristics.

2.6 Summary and problem statement

Aggregate orientation and percent embedment (Seitllari & Kutay 2018) are two major microstructural parameters affecting the performance of chip seals. Therefore, they need to be considered in chip seal design. An ideal chip seal is the one whose aggregates embedded adequately into the binder and aligned along their flattest sides. There have been many attempts to develop rational approaches to design chip seals. Modified Kearby method and McLeod method are the most popular design procedures that have been adopted by various agencies (McLeod 1969; Texas Department of Transportation 2010). Also, researchers have modified the McLeod Method (Johannes et al. 2011) to eliminate some of the basic assumptions, but didn't go far enough to correct for the assumptions related to aggregate alignment as well as the substrate surface properties. The Modified Kearby method is used by Texas Department of Transportation and many other road agencies. The so-called 'Board test' is used to find aggregate quantity that fit one-layer thick aggregates in one square yard. All these methods have assumed formation of such an ideal

(or close to ideal) microstructure to be achieved in the field. But there has been limited research on designing chip seals by ensuring an ideal microstructure. There is a need to develop a design procedure that addresses primary distresses (aggregate loss and bleeding) and directly considers aggregate-binder microstructural characteristics (e.g., aggregate orientation and embedment). In order to meet this need, it is important to evaluate the effects of different binder types, aggregate types and application rates on the chip seal microstructure and performance. There have been research studies in the past that evaluated aggregate loss and bleeding through empirical perspective (laboratory tests). But, their relation to percent embedment and aggregate orientation have not been quantitatively evaluated.

Furthermore, macro-texture characteristics of chip seal treatments have traditionally been evaluated either using volumetric indirect methods (based on various assumptions) or using laser scanning based approaches which are very expensive. Hence, there is a need for simple techniques to compute macro texture characteristics and relate to bleeding potential for chip seals.

There is also a need to improve the understanding of chip seal performance via mechanistic principles. There have been a few research studies focusing on analysis of chip seal properties through 2D and 3D finite element analyses. All the chip seal design methodologies acknowledge percent embedment as one of the most important microstructural parameters. However, an investigation of the effect of percent embedment of aggregates in chip seals has not been conducted till now. Furthermore, aggregate shape has a significant impact on chip seal performance. In the current state of practice, limited attention was given to the type and shape of aggregates used in chip seals. It is well known that flaky aggregates have a detrimental effect on hot mix asphalt performance (Tutumluer et al. 2005; Escalada 1995). However, there is very limited information on the effect of flaky aggregates on chip seal performance. Since asphalt binder performance

highly depends on temperature, it is important to incorporate the effect of temperature on chip seal performance in finite element analyses. Also, there is anecdotal evidence on the negative effect of adding excessive aggregates on chip seal performance in literature. This issue needs to be investigated via more mechanistic means, such as the finite element analyses.

3. OBJECTIVES AND RESEARCH PLAN

Overall goal of this study was to develop a holistic approach to chip seal analysis and design, encompassing various aspects of chip seal performance through aggregate-binder microstructural perspective. In order to achieve this goal, the following specific objectives were established:

- Development of advanced image-based parameters to quantify chip seal microstructure (percent embedment and orientation)
- Evaluating effect of binder, emulsion and aggregate application rates on major performance distresses in chip seals (aggregate loss and bleeding) through performance (laboratory tests) and microstructural (image processing and finite element analysis) perspective.
- Investigating effect of binder and aggregate type on chip seal performance
- Development of performance-based chip seal design procedure encompassing microstructural analyses as well as empirical performance parameters.

A research plan was devised to materialize these objectives. The tasks for the research plan are summarized in the sub-section below:

3.1 Task 1: Development of improved parameters based on image analysis and justification via finite element modelling

As part of this task, several image analysis algorithms were developed to compute the following new/improved parameters:

- Effective percent embedment (ePE): This parameter was developed to normalize the effect of non-uniform gradation on analysis of chip seal behavior through PE (Percent Embedment) criteria.
- Cumulative percentage of aggregates lying on flattest side (CPAF): This parameter is computed from the orientation distribution of chip seal aggregates. Ideal chip seals are the ones that have all of their aggregate particles aligning on their flat sides, i.e., CPAF = 100%.
- Additionally, actual 2D chip seal images were converted into finite element meshes and analyzed for the mechanistic parameters. These mechanistic parameters were evaluated for different aggregate shapes and percent embedment conditions.

3.2 Task 2: Performance tests on chip seals

Aggregate loss and bleeding are the most important distresses for chip seals. Chip seal samples were prepared at a range of binder and aggregate application rates. These samples were tested for aggregate loss using sweep test at different temperatures. Also, Hamburg Wheel Tracking tests (HWT) were run on a separate set of chip seal specimens to evaluate the bleeding behavior of chip seals. Comparative analysis of hot applied and emulsion-based chip seals was undertaken as part of this task.

3.3 Task 3: Analysis of performance through image processing and finite element modelling approaches

The results from task 1 (image analysis and finite element methods) and task 2 (performance tests) were analyzed and correlated to yield important inferences regarding the effect of chip seal microstructural parameters on its performance.

3.4 Task 4: Performance based design procedure for chip seals

The important inferences and insights obtained from task 3 were utilized to develop a performance-based design procedure for chip seals. This procedure considers the actual chip seal microstructure and its effect on performance without the assumptions that have been made by the previous empirical design procedures.

4. EXPERIMENTAL PROGRAM, MATERIALS AND METHODS

A laboratory experimental matrix was developed by varying binder/aggregate application rates, using two types of aggregates (elongated/flaky and cubical) and two types of asphalt binders (hot applied PG 70-28 and HFRS2M emulsion). Base binder used in both of the binders (before modification) was a plain PG58-28 binder. Figure 4.1 illustrates the overall experimental flowchart.

The experimental program can be broadly divided into two phases. In the first phase, effect of binder type and aggregate and binder application rates was investigated. In this phase, the chip seal samples were prepared using the commonly used flaky aggregates in Michigan (gerkin 29A). The specimens prepared and tested in this phase were divided into five groups: Group I, II, III, IV, and V. Group I and II were used to study the effect of aggregate and binder application rates on chip seal performance with hot applied binder. Group I specimens were produced with a constant aggregate application rate (AAR) of 18 lb/yd² at four different binder application rates, ranging from 0.25 gal/yd² to 0.4 gal/yd² with increments of 0.05 gal/yd². Group II encompassed specimens with a constant binder application rate (BAR) of 0.3 gal/yd² at the AARs of 16, 18, 20, and 22 lb/yd². These groups were further divided into sets: I-A, I-B, I-C, and II-A, II-B, II-C. Sets I-A and II-A specimens were sliced and used to determine the percent embedment and orientation of aggregates through digital image processing methodology. Set I-B and Set II-B specimens were tested for aggregate loss using the sweep test. Set I-C and II-C specimens were tested for bleeding performance using the Hamburg wheel tracking (HWT). Two replicates were prepared for each set. Group III and IV specimens were prepared using HFRS2M emulsion. Group III specimens consisted of a constant aggregate application rate (AAR) of 18 lb/yd² at five different emulsion

application rates, ranging from 0.25 gal/yd² to 0.45 gal/yd² with increments of 0.05 gal/yd². Group IV encompassed specimens with a constant emulsion application rate (EAR) of 0.3 gal/yd² at the AARs of 16, 18, 20, and 22 lb/yd². These groups were further divided into sets similar to those in the case of groups I and II. Specimens belonging to Group I and Group II have been referred to as AAR specimens with binder and emulsion, respectively in the further sections. It is because these specimens have change in AAR with a constant BAR or EAR. Similarly, specimens from Group II and Group IV have been referred to as BAR and EAR specimens respectively due to their variations in BAR and EAR with constant AAR.

The second phase of this study was undertaken with an objective to evaluate effect of aggregate type (cubical and flaky) and aggregate application rates on chip seal performance using image based finite element approach. Group V consisted of FE meshes created by images of chips seal samples prepared with AAR of 18 lb/yd² and BAR of 0.3 gal/yd² binders. The FE analysis was conducted stepwise, focusing on FE meshes of single aggregate, two aggregates and full chip seal samples. This approach was undertaken to understand the contribution of a single aggregate as well as aggregate interlock on chip seal performance. Furthermore, the images of group II specimens were converted to FE meshes and tensile strain results at various AARs were compared against sweep test results to evaluate effect of AAR on chip seal aggregate loss performance.

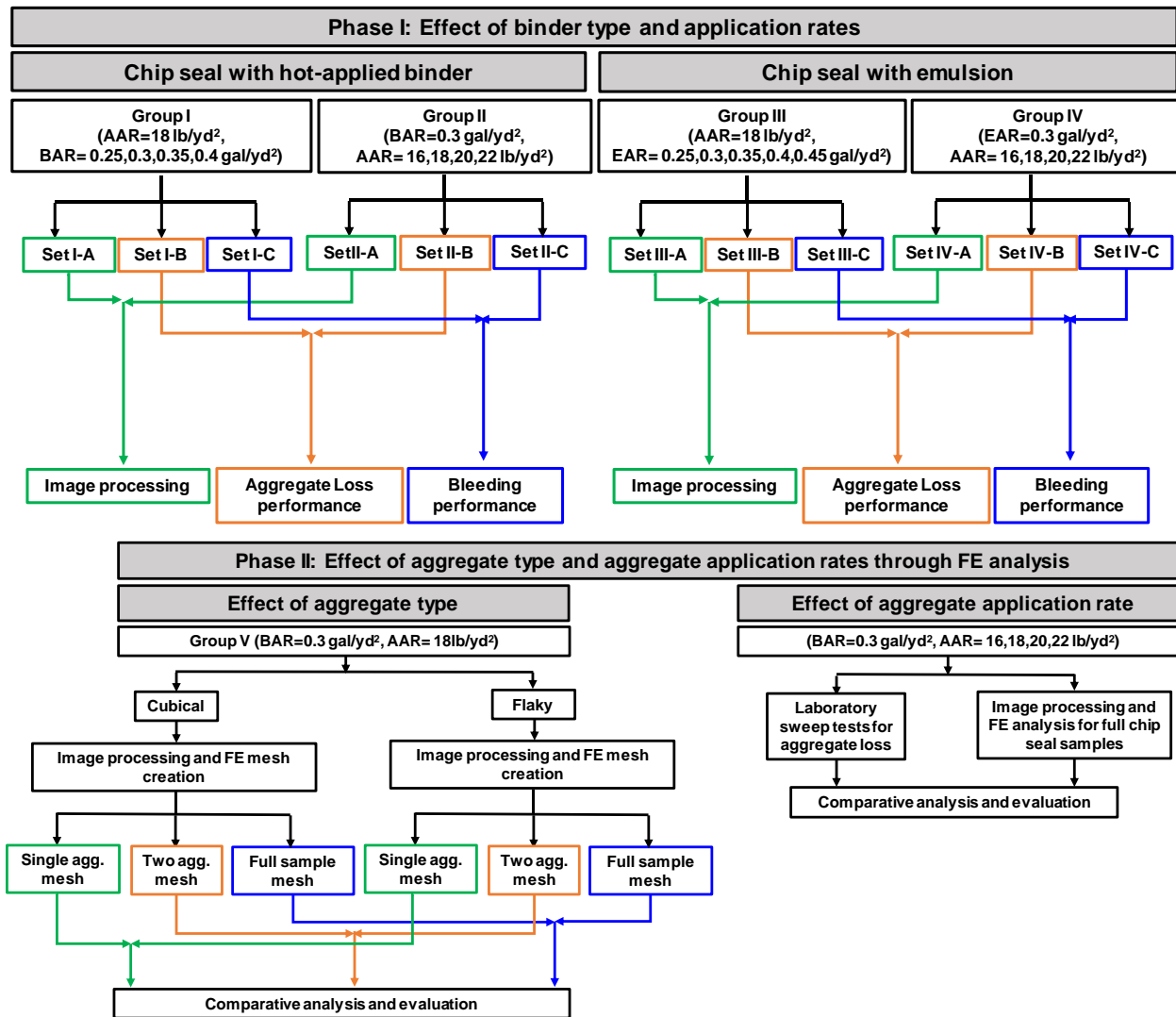


Figure 4.1 Experimental flow chart

Chip seal samples were prepared in the laboratory by applying binder (or emulsion) and aggregates on cylindrical asphalt specimens compacted in the laboratory using the Superpave gyratory compactor. Asphalt concrete substrates had a diameter of 150-mm and a height of 30-mm. The procedure outlined by Kutay et al. (2017) was generally followed while applying the binder and aggregates on the chip seal substrates. The main deviation from the procedure outlined by Kutay et al. (2017) was the binder and aggregate application temperatures, which were 175 and 45°C for the binder and aggregate, respectively.

Once the binder and aggregates were applied, the specimens were first compacted using the hand-kneading compactor, as specified in ASTM D 7000, for three half cycles in one direction and three half cycles in a perpendicular direction. Then, the specimens were subjected to an additional compactive effort by a servo-hydraulic Material Testing System (MTS) to simulate the cyclic pressure in the field. The pressure level used in the Superpave Gyratory Compactor (i.e., 600kPa) was applied to the specimens in a cyclic haversine mode at a frequency of 0.1 Hz for 25 cycles.

The specimens for image analysis were cut using a small tile saw such that five (5) slices were obtained for the image analysis. In addition, a blue playdough was applied on the top of slices for the purpose of creating a color contrast. Images of the vertical cross section of each side of the slices were acquired using a document camera. This process resulted in eight (8) images for each specimen. Further details on sample preparation for image acquisition can be found elsewhere (Kutay et al. 2017). The methods and terminologies developed for different aspects of this study have been presented in the following subsections.

4.1 Quantification of Aggregate Loss

Chip seal specimens prepared at various binder and aggregate application rates were tested for aggregate loss using the sweep test. In this study, the sweep test was performed in general accordance with ASTM D7000, with the following modifications:

- An asphalt mixture substrate was used instead of the felt disk
- Aggregate gradation representative of field aggregate was utilized rather than the required fixed aggregate size in the standard
- Additional compactive effort was applied using a Material Testing System (MTS), in addition to the hand-held compactor as prescribed by ASTM D7000

The surface abrasion procedure followed in this study was the same as described in ASTM D7000. The specimens were subjected to abrasion for 60 seconds at a brush speed of 0.83 gyrations per second, after specimen conditioning at 25°C for 60 minutes. Furthermore, these specimens were analyzed using image analysis techniques to better understand the effect of percent embedment and orientation on aggregate loss performance. Percent embedment and orientation of aggregates were calculated for specimens of set I-A, II-A, III-A, and IV-A. These terms have been explained and illustrated in the next chapter.

Several parameters were developed as part of this study to better evaluate the aggregate loss. These parameters include the residual aggregate rate (RAR), aggregate loss by hand brushing (ALB), aggregate loss by sweep (ALS), and cumulative aggregate loss (CAL).

4.1.1 Residual Aggregate Rate (RAR)

Design application rate is defined as the amount (weight) of aggregates spread over a unit area. A portion of the aggregates is always lost both in laboratory (by hand brush and sweep test) and field-based (by brooming and initial trafficking) chip seal applications. The residual aggregate

rate (RAR) is the amount of aggregates that is retained on the chip seal surface, and is the actual component of aggregates that take part in chip seal performance. In order to understand the effect of application rates on change in residual aggregate rate, the percent change in the RAR (ΔRAR) was calculated and evaluated with respect to the change in consequent AARs. The ΔRAR was calculated using the following equation:

$$\Delta RAR_{(1)-(2)} = \frac{RAR_{(2)} - RAR_{(1)}}{AAR_{(2)} - AAR_{(1)}} \times 100 \quad (4.1)$$

where, $\Delta RAR_{(1)-(2)}$ is the change in the RAR from condition 1 (a given AAR) to condition 2 (subsequent AAR), $RAR_{(1)}$ is the RAR at condition 1 and $RAR_{(2)}$ is the RAR at condition 2. For example, $\Delta RAR_{(16)-(18)}$ refers to change in RAR from AAR of 16 to 18 lb/yd². In this case, AAR of 16 lb/yd² can be termed as condition 1 and AAR of 18 lb/yd² can be termed as condition 2.

4.1.2 Aggregate Loss by Hand Brushing (ALB)

As a part of the sweep test procedure in ASTM D7000 (see Figure 4.2), the chip seal specimen is turned upside down at the end of conditioning time and slightly hand brushed without applying any remarkable amount of force. This is believed to ensure that the aggregates that have no bond with asphalt layer are removed from the specimen without being stuck due to mere aggregate interlocking. This procedure assures accurate results from the sweep test, where only the aggregates embedded in asphalt layer take part in the test. The percent aggregate loss by hand brushing (ALB) was calculated using Equation 4.2:

$$ALB = 100 \times \frac{A-B}{A-C} \quad (4.2)$$

where, A is the weight of chip seal specimen before hand-brushing, B is the weight of chip seal specimen after hand brushing, and C is the weight of the substrate and added binder.

4.1.3 Aggregate Loss by Sweep (ALS)

Aggregate loss by sweep is the mass loss occurred after abrasion for 60 seconds at a brush speed of 0.83 gyrations per second. The percentage of aggregate loss by sweep (ALS) was calculated with Equation 4.3:

$$ALS = 100 \times \frac{B-D}{B-C} \quad (4.3)$$

where D is the weight of the chip seal specimen after the sweep test, and B and C are the same variables defined in Equation 4.2.



Figure 4.2 A picture of the sweep test device for chip seal aggregate loss testing

4.1.4 Cumulative Aggregate Loss (CAL)

The cumulative aggregate loss (CAL) is the total loss as a result of hand brushing and sweep, and was computed by Equation 4.4:

$$CAL = 100 \times \frac{A-D}{A-C} \quad (4.4)$$

4.1.5 Residual binder application rate (RBAR)

The parameter residual binder application rate (RBAR) is defined herein to be able to hot applied and emulsion-based chip seals. Since emulsions lose their water after construction, asphalt

binder residue is the part of emulsion that actually interacts with aggregates during the service life of a chip seal. Hence the accurate comparison between hot applied and emulsion-based chip seals can be made when the emulsion application rates (EAR) are converted into corresponding RBAR which is defined as follows:

$$\text{RBAR} = \text{EAR} \times \% \text{residue} \quad (4.5)$$

where RBAR is the residual binder application rate, %residue is the percentage of asphalt binder residue present in the emulsion. The %residue is typically about 65%, and it is measured in accordance with (AASHTO:T59 2016)

4.2 Quantification of Bleeding

Hamburg Wheel Tracking (HWT) test was used to evaluate the bleeding susceptibility of the chip seals. A series of modifications were made to the HWT device so that it is useful in evaluation of chip seals. A picture of the modified HWT device for chip seal bleeding testing is shown in Figure 4.3. As shown, an 8-inch diameter rubber wheel is used instead of the steel wheel. The rubber wheel had a tire pressure of 34 psi, and the load on the wheel was 125 lbs., which corresponds to the weight of a loaded wheel track used for assessing bleeding of micro surfacing mixtures (ASTM D 6372). HWT tests were run at a temperature of 54°C under wet condition. The particular temperature was chosen since 54°C being the maximum summer pavement temperature in Michigan. A total of 1500 HWT cycles (3000 passes) were applied and 2D images were captured at start and end of the test. At first, the images were acquired using smart phones. These images were cropped to obtain the portion of wheel path. Further, they were converted into binary images to yield percent binder area. Due to the glare (from binder portion) in directly obtained images, discrepancies were observed in the corresponding binary images and percent bleeding area results. In order to solve this problem, a 3D photogrammetric software (3DF Zephyr®) was used. The

images obtained from smartphone served as input for this software package, to yield a 3D image. The problem of glare in the previous images was solved through 3DF Zephyr[®]. Figure 4.4 illustrates the image acquisition and processing phase using 3DF Zephyr[®]. These images were cropped and processed to yield binary images. From the binary images, the parameter Percent Binder Area (PBA) was calculated using the following equation:

$$PBA = \frac{A_{\text{black}}}{A_{\text{total}}} \times 100 \quad (4.6)$$

where A_{black} is the area covered by black pixels (representing the binder), A_{total} is the total area of the image. The PBA is effective in understanding the 2D bleeding behavior of chip seal samples. Higher the PBA, higher is the amount of bleeding for a particular chip seal specimen.



Figure 4.3 A picture of the modified HWT device for chip seal bleeding testing

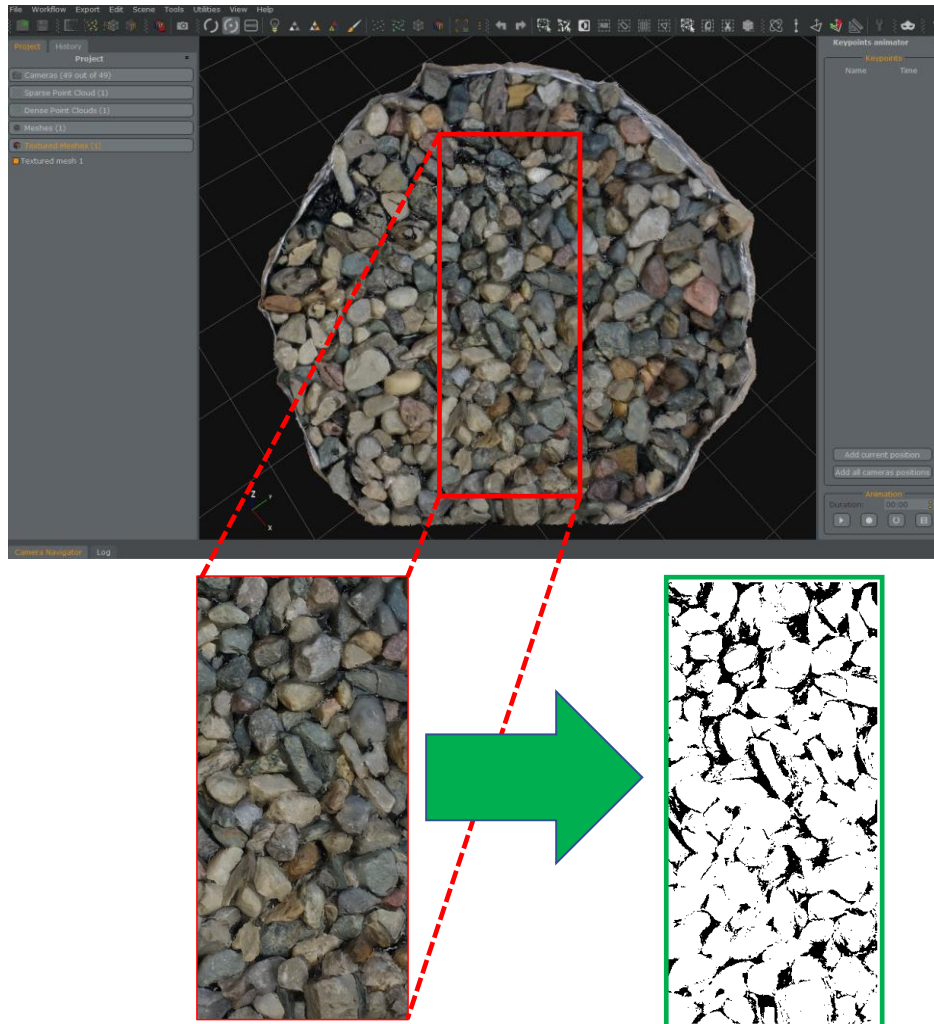


Figure 4.4 Illustration of image analysis steps to compute the bleeding area

Determination of chip seal macrotexture depth after subjecting to Hamburg Wheel Tracking (HWT) tests is another way of quantifying the effect of bleeding. In this study, a low-cost method to evaluate chip seal macrotexture was developed. Figure 4.5 illustrates the general concept of this method. In order to obtain the 3D coordinates of surface of an object, at least two cameras are needed, however, multiple images captured using a single camera from different fields of view can also be used. By knowing the relative location and intrinsic parameters of the cameras, 3D coordinates of the object can be computed (Buttlar et al. 2014). This method was also

successfully used in a previous study to characterize surface of the chip seals to compute mean profile depth and percent bleeding (Boz et al. 2018). The images obtained from a smartphone served as input for 3DF Zephyr® software package which used stereo algorithms to generate 3D images.

These surface coordinates were extracted and input into an in-house algorithm using MATLAB® to compute mean profile depths (MPD) using the following equation (Javon M Adams & Kim 2014):

$$\text{MPD} = \frac{\text{Peak level (first)} + \text{Peak level (second)}}{2} - \text{Aggregate level} \quad (4.7)$$

The peak level is defined as the maximum point along the profile of the chip seal surface. MPD calculation method has been illustrated in Figure 4.6(a). In this study, MPDs were computed along many profiles in a given sample and average value is reported. The single profile lines are equivalent to each line of laser data in case of MPD computation using line lasers. At the end of certain HWT cycles, this technique was utilized to compute mean profile depth (MPD) to characterize the effect of aggregate application rate on bleeding behavior of chip seals. Furthermore, MPD is inherently related to PE. MPD is generally inversely proportional to PE. The relation between MPD and PE has been depicted in Figure 4.6(b).

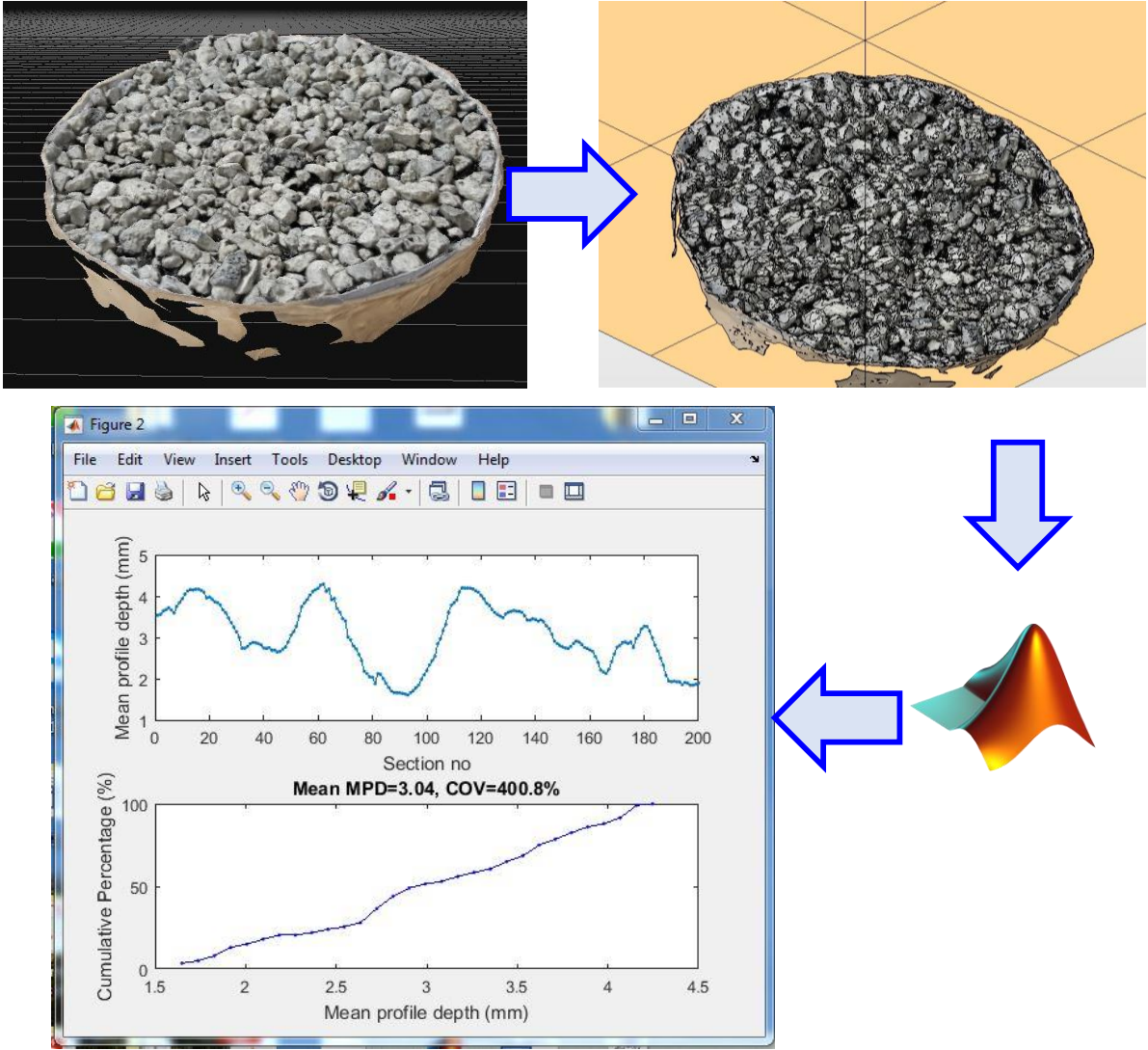


Figure 4.5 Steps of obtaining Mean Profile Depth of chip seal samples using 3D stereology imaging.

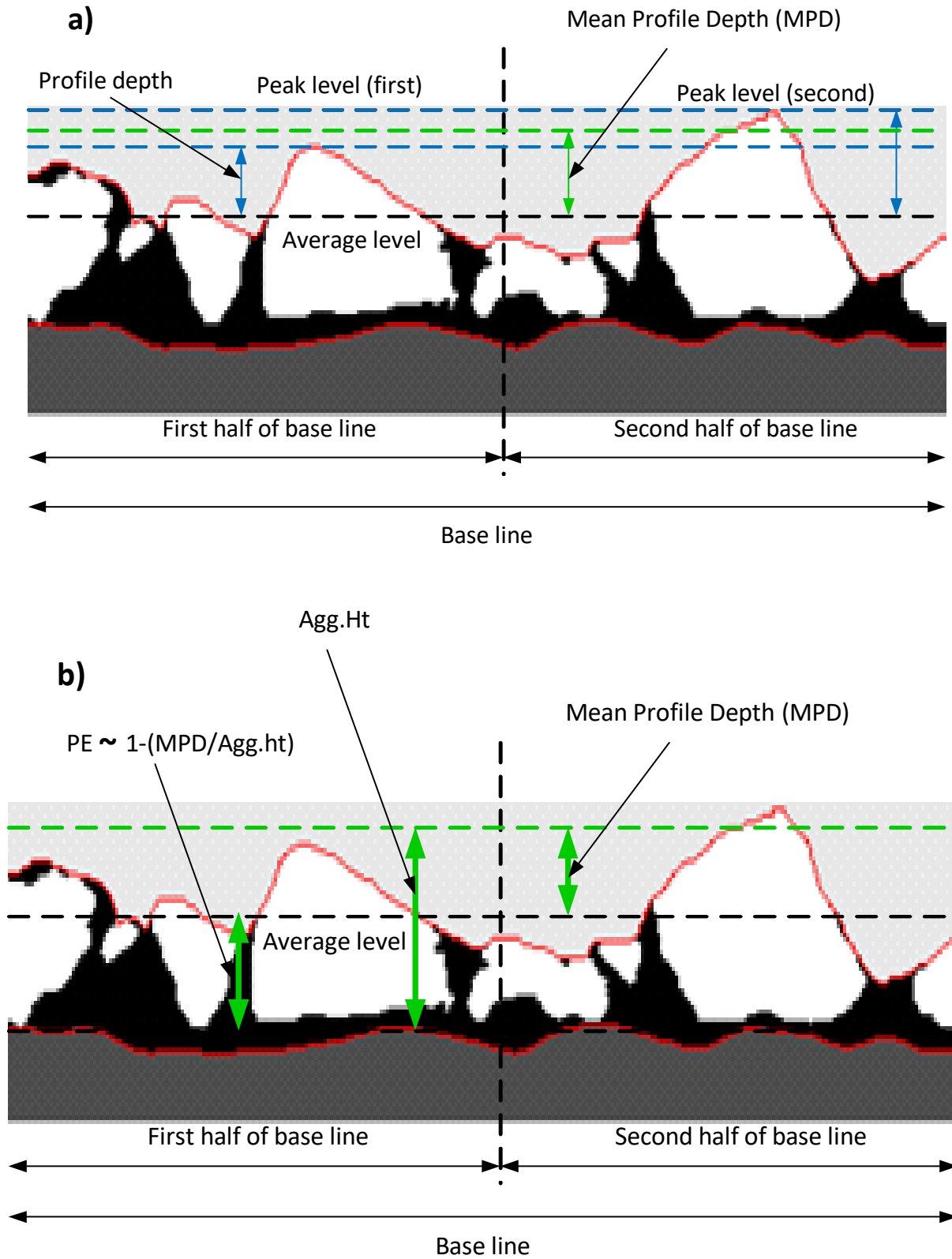


Figure 4.6 a) MPD visualization sketch, and b) illustration of relation between MPD and PE

Before using the 3D MPD computation technique to characterize chip seal bleeding behavior, a verification analysis was conducted. The chip seal samples of group II (hot applied) and IV (emulsion based) with different aggregate application rates were evaluated for macrotexture properties. A commercial laser scanner was used to calculate MPDs of these samples. They were compared against the corresponding MPD valued obtained by the innovative image processing technique (with in house MATLAB based program). The results of this verification study have been presented in Figure 4.7. Based on the limited data set that was available, it can be seen that the values obtained by image processing technique are well in alignment with those calculated using commercial laser scanning equipment. Although in a very few cases, the image processing technique yielded slightly lower values of MPD than that of the laser scanning equipment. But the difference in magnitudes in these cases were very small. This trend has also been observed in a similar study by Puzzo et al. (2017) where a similar photographic MPD evaluation method was compared to commercial scanners. But overall, the image processing technique developed in this study can be used to compute MPD of chip seal specimens for successful characterization of bleeding behavior of chip seals.

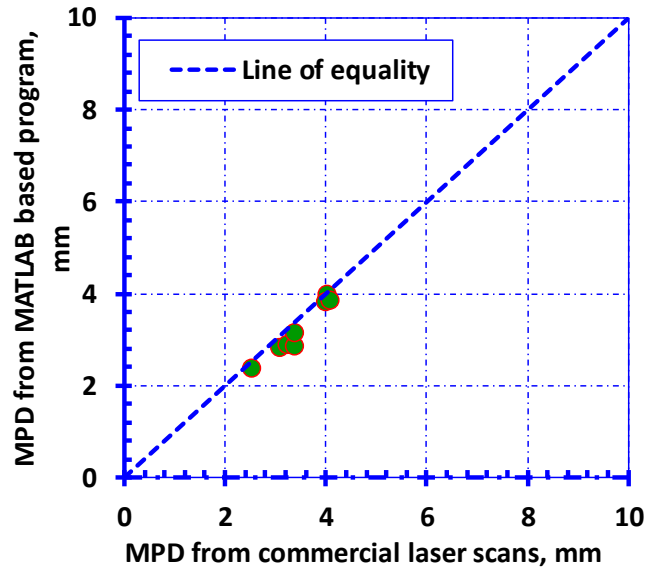


Figure 4.7 Comparison of MPD values computed from the in-house MATLAB based algorithm to the values obtained from commercial laser scanning equipment

4.3 Finite Element Analyses on Chip Seals

The Finite Element Analyses (FEA) on chip seal samples were performed in three stages. The scope of the first stage (stage I) included the study of the effect of percent embedment and temperature on the stability of a single aggregate with different shapes (cubical and flaky). In the second stage (stage II), a hypothetical case of perfectly bridged/interlocked two aggregates were simulated. This case represented the best-case scenario in terms of aggregate interlocking. In the last stage (stage III), entire chip seal cross-section was modeled in FE. Finally, the observed trends were compared to the trends in the results of aggregate loss tests (ASTM-D7000 2011).

4.3.1 Finite Element Model Development

Once chip seal specimens were prepared, they were cut using a small tile saw such that five (5) slices were obtained for the image analysis step (see Figure 4.8a and Figure 4.8b). In addition, a blue playdough was applied on the top of slices for the purpose of creating a color contrast at the surface. Then, the images (Figure 4.8c) of each side of the slices were captured using a document

camera. These images were further processed to specify certain pixel intensities to the different zones of the cross section (Figure 4.8d). It is noted that the tire is not actually simulated in the FE model. Instead, the load is applied at the surface nodes where the tire and the aggregate intersect. The images were then converted into a finite element mesh as shown in Figure 4.8e, using an in-house algorithm developed in MATLAB®. Material properties for the FE mesh were assigned based on the pixel intensity shown in Figure 4.8d. Aggregates were modelled as an elastic material, whereas the asphalt binder and substrate were assigned viscoelastic properties using Prony series coefficients.

Table 4.1 shows the relaxation times (τ_i) and dimensionless elastic coefficients (g_i) of the generalized Maxwell model (Prony series) at a reference temperature of 25°C. The relaxation modulus Prony series coefficients for the binder were obtained through interconversion from dynamic shear modulus ($|G^*|$) master curve. Similarly, the asphalt mixture substrate dynamic modulus ($|E^*|$) master curve was measured in the laboratory and used to compute the Prony series coefficients of the substrate. The shape of the tire loading was based on the functions recommended from previous researchers (Huurman 2010). Figure 4.9 shows the stress functions, which are based on actual stress measurements from a moving tire. The loading pulse was a combination of two individual functions: 1) a step-like function representing the vertical (normal) load, 2) a sinusoidal function representing the lateral (shear) load. Further details on these loading functions can be found in elsewhere (Huurman 2010).

In order to evaluate chip seal performance through FE analysis maximum tensile strains (ϵ_T^{max}) have been computed and used in this study. Furthermore, in order to quantify change in tensile strains for comparing between different conditions, percent change in tensile strains ($\Delta\epsilon_T^{max}$) has been used and is computed as follows:

$$\Delta\epsilon_T^{max} (\%) = \frac{\epsilon_{T_2}^{max} - \epsilon_{T_1}^{max}}{\epsilon_{T_1}^{max}} \times 100 \quad (4.8)$$

where $\epsilon_{T_2}^{max}$ and $\epsilon_{T_1}^{max}$ are the max tensile strain at conditions T1 and T2, respectively

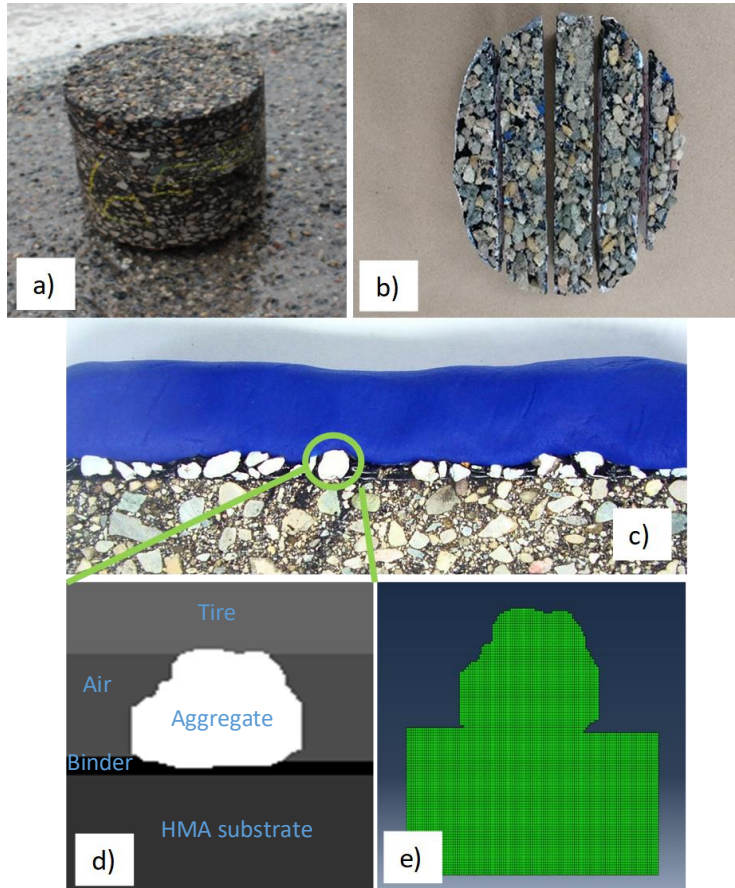


Figure 4.8 Stepwise procedure for obtaining finite element model of chip seals

Table 4.1 Prony series coefficients for asphalt binder and substrate HMA

Asphalt Binder		Asphalt Mixture (substrate)	
G_o (Pa) =	8.42E+06	G_o (Pa) =	6.20E+09
τ_i (s)	g_i	τ_i (s)	g_i
1.000E-03	0.3952945	1.000E-07	0.1520131
4.642E-03	0.2456874	1.668E-06	0.1374991
2.154E-02	0.1745623	2.783E-05	0.1771304
1.000E-01	0.1004653	4.642E-04	0.1847754
4.642E-01	0.0520705	7.743E-03	0.1553424
2.154E+00	0.0213404	1.292E-01	0.1028287
1.000E+01	0.0079164	2.154E+00	0.0527216
4.642E+01	0.0020123	3.594E+01	0.0227300
2.154E+02	0.0005539	5.995E+02	0.0076755
1.000E+03	0.0000970	1.000E+04	0.0060309

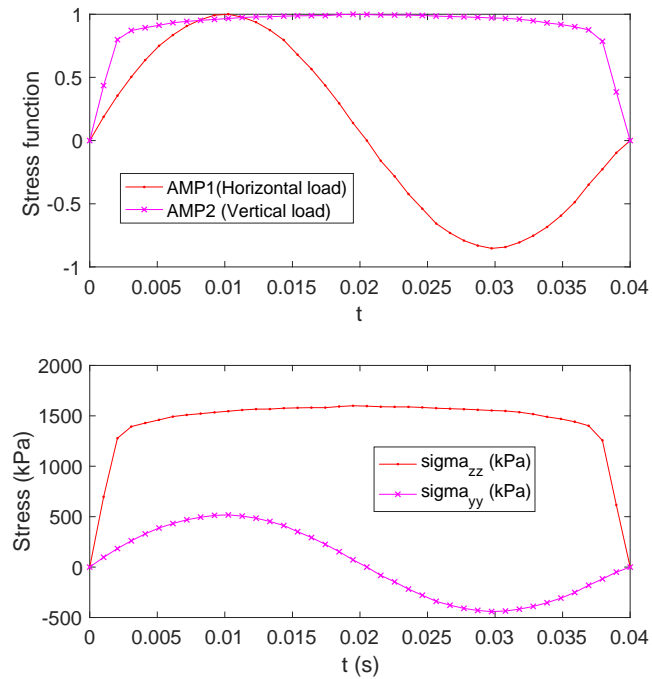


Figure 4.9 Illustration of the horizontal and vertical stress functions applied to the top of the chip seals: Top graph is the normalized shape functions, and bottom graph is the actual stresses applied

4.3.2 Stage I: Chip Seals with a Single Aggregate

Digital images of cubical and flaky aggregates were isolated and processed to create multiple artificial images representing various percent embedment (PE) levels: 25, 50, 72, and 94%. The FE model results were analyzed to determine the maximum tensile strains at the aggregate-binder interface at three temperatures: 25, 30, and 35°C. This theoretical exercise represented the worst possible condition of chip seals, where the aggregate to aggregate interlock is not present.

4.3.3 Stage II: Chip Seals with Two Bridged Aggregates

In this stage, artificial images were generated out of two aggregates used in the previous phase such that they create a stable bridge-like structure. This theoretical case represents one of the best-case scenarios for flaky aggregates, where there is a bridging effect between the two

aggregates, making them potentially more stable. The images were further processed to generate multiple artificial images with the percent embedment levels of 25, 50, 72 and 94%. Similar to stage I, the FE simulations for each aggregate type were performed on chip seals with two aggregates to compute the maximum tensile strains at aggregate-binder interface at a temperature of 25°C. The main objective was to study the effect of aggregate interlocking (i.e., bridging) on the critical strain levels of chip seals with cubical and flaky aggregates.

4.3.4 Stage III: Chip Seals with Multiple Aggregates

In the third stage of the study, cross sectional images of the entire chip seal specimens with cubical and flaky aggregates were taken and converted to the FE meshes. The chip seal specimens for this phase were prepared at an aggregate application rate of 18 lb/yd² and the binder application rate 0.3 gal/yd². The FE simulations were conducted at a temperature of 25°C. Similar to the previous phases, simulations were performed at several percent embedment levels. The maximum tensile strains at the aggregate-binder interface were determined at each percent embedment level.

4.3.5 Evaluation of the Effect of Aggregate Application Rate via FE modelling and Sweep Tests

The aggregate loss results of group II specimens were compared with the FE results obtained from the meshes created by the respective 2D images. The tensile strain results from FE analysis were compared against Cumulative Aggregate loss (CAL) results from sweep test. The negative effect of excessive aggregate application was confirmed analytically as well as experimentally.

5. NEW IMAGE-BASED PARAMETERS FOR CHIP SEALS

In order to be able to quantify chip seal microstructure, new parameters have been developed in this study. These parameters are based on advanced image analysis techniques that use 2D images of chip seal samples taken using a simple document camera.

5.1 *Orientation distribution of chip seal aggregates*

In a previous study (Kutay et al. 2017), a digital image analysis software (CIPS) was developed to calculate percent embedment (PE) of chip seal aggregates into the asphalt binder. The algorithms in the CIPS software were further improved to compute new parameters described in this chapter. Figure 5.1(a) illustrates a screen shot of the chip seal analysis software (CIPS). Orientation of aggregates is an important parameter for performance of asphalt mixtures. A well compacted asphalt mixture has a uniformly distributed aggregate orientation. Similarly, in the case of chip seal applications, it is important that all or most of the aggregates lie on their flattest side forming a one-stone thick seal after compaction for achieving satisfactory performance. The orientation angle of aggregates can be defined as the angle between major axis and the horizontal axis as illustrated in Figure 5.1(b). In this study, the orientation angle of 20° was selected as a threshold angle for determination of aggregates lying on their flattest side. In other words, aggregates with angle of 20° and less are considered to be lying on their flattest side on the pavement substrate. The cumulative percentage of aggregates lying on flattest side (CPAF) was calculated by using the following equation:

$$\text{CPAF} = 100 \times \frac{\sum_0^{20} N_\theta}{N} \quad (5.1)$$

where N_θ is the number of aggregates with orientation angle θ , and N is the total number of aggregates on the specimen. Higher the number of aggregates lying on flattest sides, higher the

value of CPAF. If all the aggregates lie on their fattest sides, the CPAF will be equal to 100%, indicating a well compacted chip seal.

5.2 *Effective percent embedment (ePE)*

In an ideal case, the chip seal aggregates should have uniform gradation. But, in practice, road agencies don't pay much attention to gradation of chip seal aggregates. During this study, it was observed that the aggregates lost due to the hand brush procedure usually belonged to a coarser fraction which, in turn, results in finer gradation on the specimen surface. Hence, in order to effectively discern the effect of application rates on percent embedment of chip seals, it is important to normalize the anomaly caused by differences in residual aggregate rate and gradation for more proper analysis between the effect of percent embedment, aggregate loss and bleeding. This could be achieved by taking the aggregate loss by hand brush into account.

Hence, a term named "Effective percent embedment (ePE)" was introduced in this study. As discussed above, the aggregates lost due to hand brush had a coarser gradation. Thus, it was assumed that the size of each lost aggregate be of a 4.75 mm equivalent diameter. With this assumption, the weight of one aggregate particle was also calculated. Then, the number of aggregate particles that are lost were calculated. It was also assumed that these aggregates have zero (0) percent embedment. This way it is postulated that calculating a weighted average of the PE of all aggregates that are retained and lost after hand brushing takes into account the changes of residual aggregate rate and gradation. The ePE was calculated using the following equation:

$$ePE = \frac{PE_l \times N_l + PE_r \times N_r}{N_l + N_r} \quad (5.2)$$

where, PE_l is the Percent embedment for lost aggregates (assumed to be zero), N_l is the number of lost aggregates, PE_r is the percent embedment for the retained "on specimen" aggregates, and N_r is the number of retained aggregates.

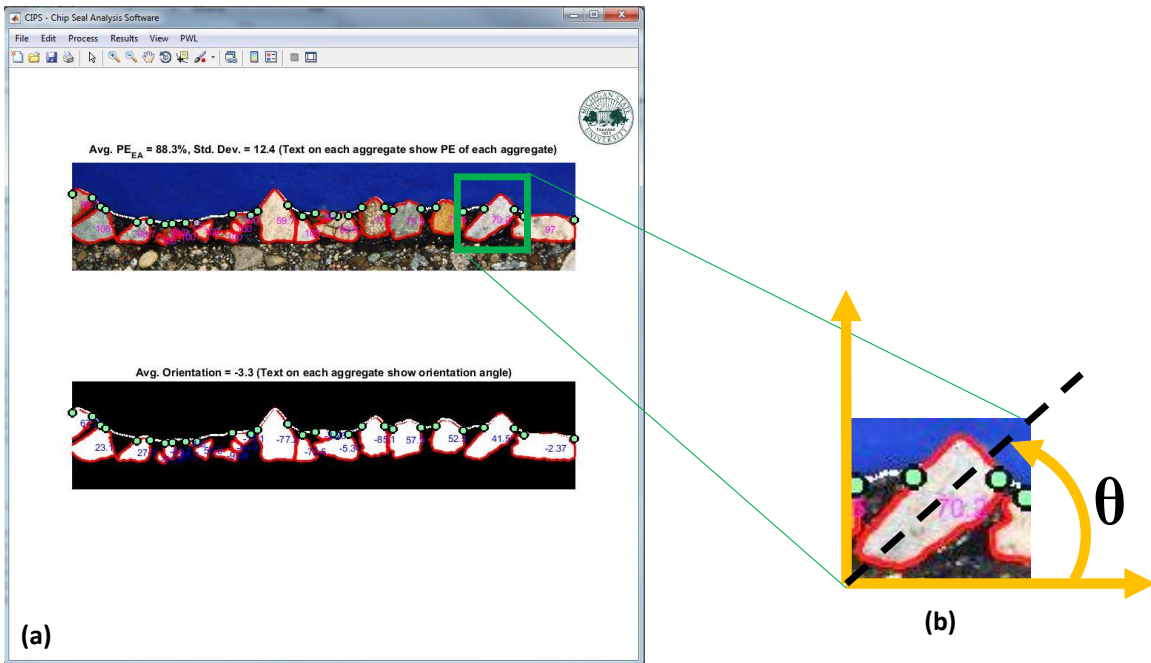


Figure 5.1 (a) A screenshot of the CIPS software illustrating the computation of percent embedment using each aggregate method, (b) illustration of orientation of the aggregates

6. EVALUATING AGGREGATE LOSS IN CHIP SEALS

The objective of this part of the study was to evaluate the impact of binder and aggregate application rates on aggregate loss. A series of hot-applied and emulsion-based chip seal specimens with varying aggregate and binder application rates were prepared. Then, the percent embedment (PE) and aggregate orientation of chip seal specimens were determined by digital image analysis. Additionally, chip seal specimens were subjected to the modified sweep test to determine the aggregate loss.

6.1 *Modified sweep test results*

6.1.1 Aggregate Loss by Hand Brushing

Figure 6.1(a) and depicts the percent aggregate loss by hand brushing (ALB) for hot-applied chip seals (Set I-B). Percent ALB decreases and becomes relatively constant as the BAR increases. The results suggest that once a certain binder application rate is achieved, or a certain percent embedment threshold is achieved, any further increase in the BAR would have no remarkable effect on the bond between the aggregates and the binder, and consequently on aggregate loss by hand brushing. Figure 6.1(b) presents the percent ALB values for Set II-B specimens (with the constant BAR of 0.30 gal/yd² at varying AARs). The percent ALB exhibits a steep increasing trend with an increase in the AAR from 20 to 22 lb/yd², thus revealing that there is a certain aggregate rate threshold point, after which any further increase in the AAR results in no bond with binder and subsequent drastic increase in aggregate loss during hand brushing. It can be deduced from Figure 6.1(b) that such threshold exists around the AAR of 20 lb/yd² for the aggregate type and gradation used in this study. Moreover, similar trends were also reported in

literature for the effect of binder and aggregate application rates on aggregate loss by hand brushing for emulsion-based chip seals (Lee et al. 2006; Lee & Kim 2008a)

Figure 6.2(a) illustrates ALB results for emulsion-based chip seals (set III-B). Similar to the case of hot applied chip seals, ALB decreases with increase in EAR and a constancy is achieved after reaching a threshold EAR of 0.4 gal/yd². The ALB results for set IV-B have been presented in Figure 6.2(b). The magnitude of increase in ALB is higher after 18 lb/yd², but the change is not as steep as in the case of hot applied chip seal. The threshold seems to be shifting towards 18 lb/yd². The reason for such observation could be due to the fact that EAR of 0.30 gal/yd² (for set IV-B) is slightly lower than the typical EARs. This results in less amount of aggregates bonding to the residual binder and hence most of those non-bonded aggregates typically get lost during the initial hand brushing stage.

6.1.2 Aggregate Loss by Sweep

The specimens were subjected to the sweep test following the removal of loose aggregates on the surface by hand brushing. The percent of aggregate loss by the sweep (ALS) is plotted in Figure 6.1(c),(d), Figure 6.2(c), and (d) respectively for Set I-B ,Set II-B, Set III-B and Set IV-B specimens. Overall, in case of hot applied binder, there is a general decreasing trend of aggregate loss with an increase in the BAR, except the BAR of 0.35 gal/yd² in set I-B (Figure 6.1(c)). As shown in Figure 6.1(d), the percent ALS, in general, increased as the AAR is increased (except at AAR = 22 lb/yd²). Very similar trend is observed in case of emulsion based chip seals as well (Figure 6.2(c) and (d)). Despite the overall expected trend in the percent ALS, the results, at a first glance, suggest that the sweep test may not be sensitive to changes in binder (or emulsion) and aggregate application rates. In other words, the sweep test may not have the ability to identify an optimum application rate based on aggregate loss, for both the BAR (or EAR) and AAR. A similar

finding in the literature was reported on the sweep test's ability to differentiate emulsion application rates (Johannes et al. 2011). However, such finding can be explained by the changes in residual aggregate rate (RAR) and gradation due to the aggregate lost by hand brush. In other words, the ability of the sweep test to discern the performance of chip seals among the application rates may have been affected by the RAR and gradation.

6.1.3 Cumulative Aggregate Loss

Cumulative aggregate loss (CAL) takes the combined aggregate loss into account from hand brush and the sweep test. Figure 6.1(e) and (f) display the percent CAL for the set I-B and set II-B respectively in case of hot applied chip seals. Figure 6.2 (e) and (f) illustrate similar results in case of emulsion-based chip seals. The expected trends in aggregate loss with respect to the application rates are clearly visible, suggesting that the percent cumulative aggregate loss in the sweep test is a good aggregate loss index when the performance of chip seals with respect to aggregate loss is of concern.

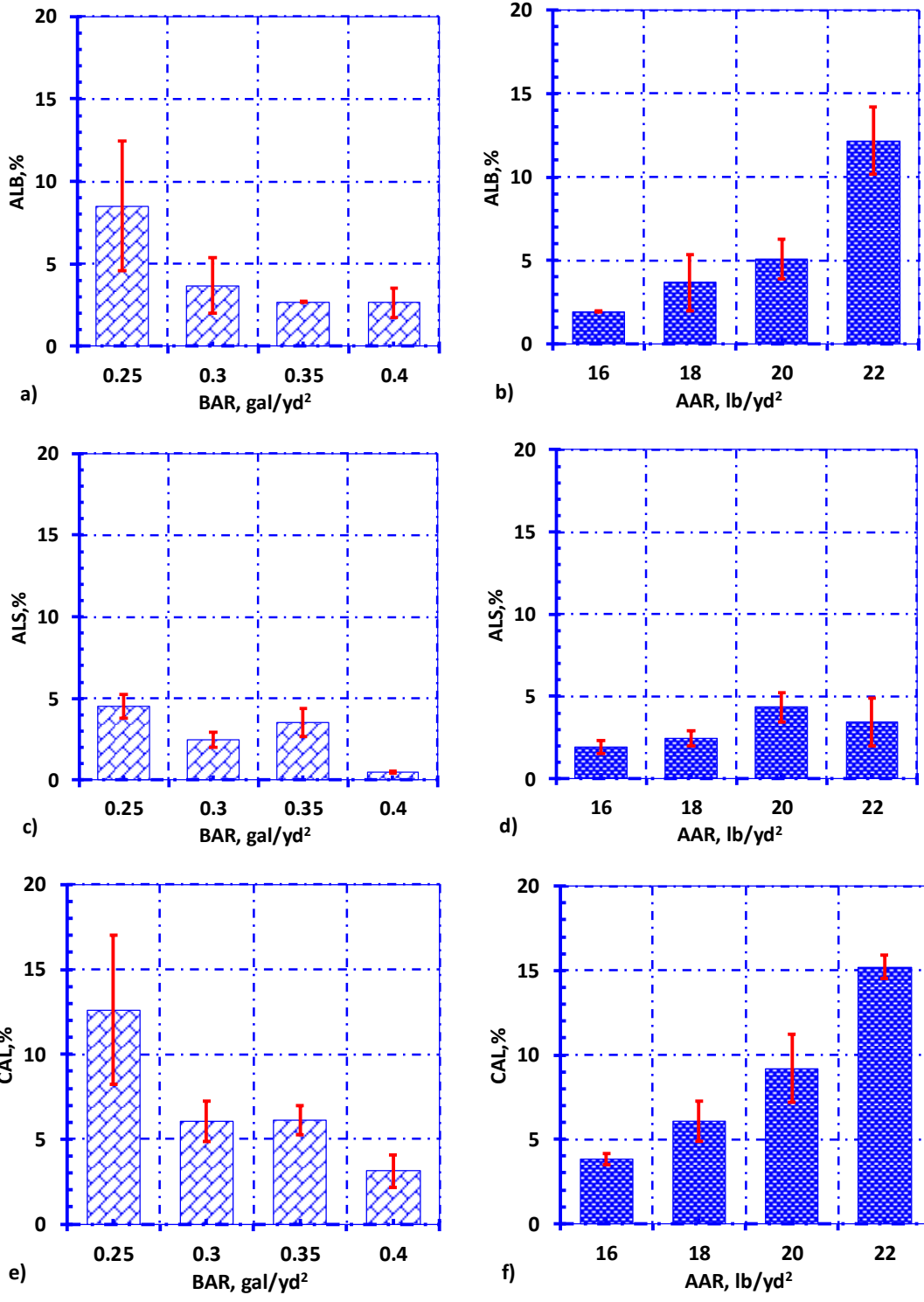


Figure 6.1 Aggregate loss by hand brushing (ALB) results for (a) set I- B and (b) set II- B, Aggregate lost by sweep (ALS) for (c) set I-B and (d) set II- B, and Cumulative aggregate loss (CAL) for (e) set I- B and (f) set II- B

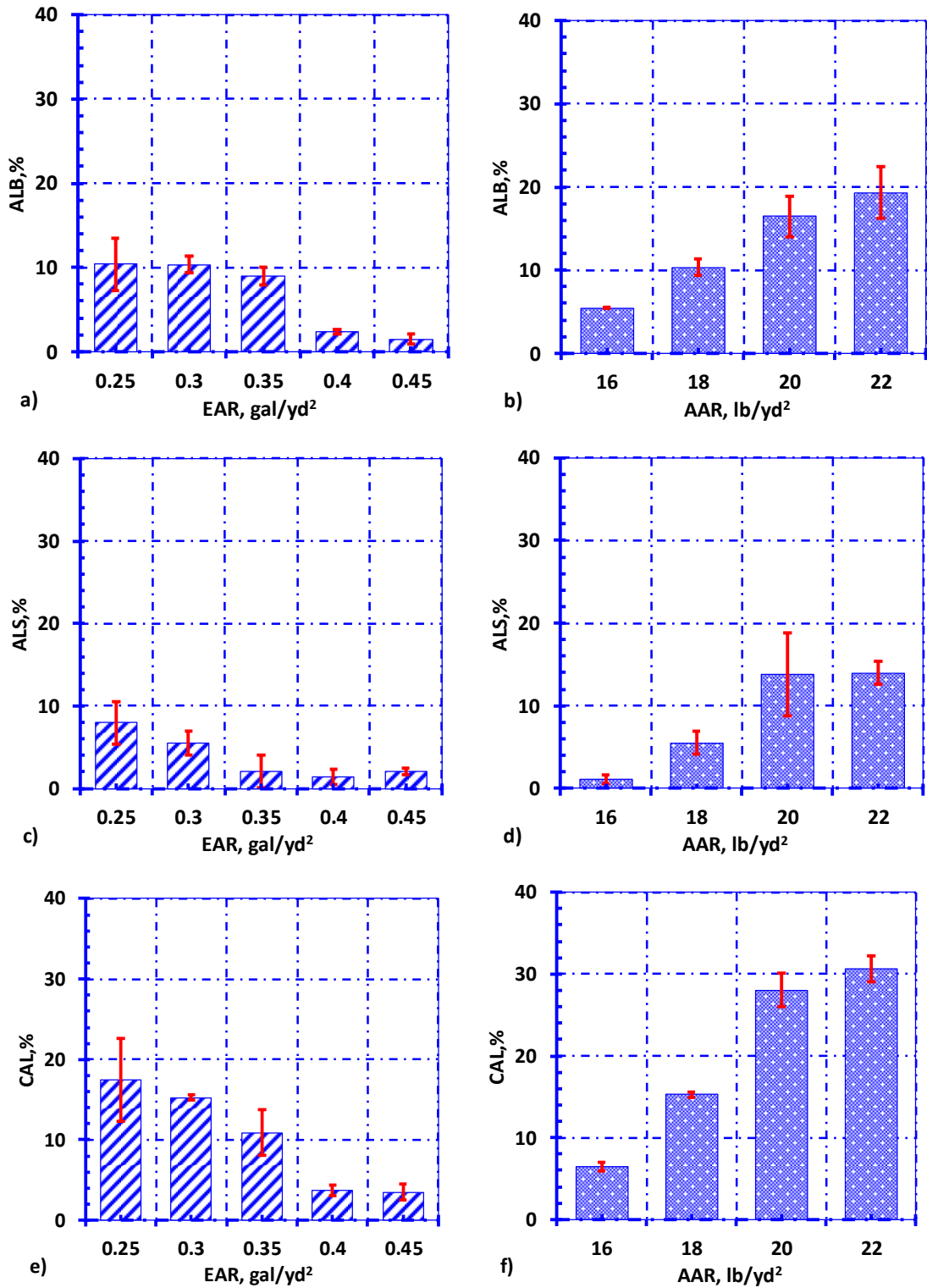


Figure 6.2 Aggregate loss by hand brushing (ALB) results for (a) set III- B and (b) set IV- B, Aggregate lost by sweep (ALS) for (c) set III-B and (d) set IV- B, and Cumulative aggregate loss (CAL) for (e) set III- B and (f) set IV- B

6.1.4 Residual Aggregate Rate

Figure 6.3(a) and Figure 6.3(b) show the residual aggregate rates respectively for the hot applied and emulsion-based AAR specimens. As shown, there are variations in the RARs across the application rates, with noticeable variations in the AAR specimens. In order to specify the aggregate application rate threshold point, the percent change in the RAR (Δ RAR) was calculated and evaluated with respect to the change in consecutive AARs (see equation 4.1).

The Δ RAR is shown in Figure 6.3 (c) and (d) respectively for the hot applied and emulsion-based AAR specimens. This parameter represents, in a sense, the efficiency of application of additional amounts of aggregates. If the increase in the AAR is the same as (or nearly same as) the increase in corresponding RARs, then it is efficient to apply the higher AAR. If Δ RAR has a low value, there is no reason of adding additional aggregates, as the specimen already achieved a saturation in terms of the AAR. Any additional aggregate added after this saturation will be brushed off by the broom, or will cause the so-called ‘lever and wedge’ effect (see Figure 2.1).

As it can be clearly seen from Figure 6.3 (c) that, there is a negligible change in the RAR as the AAR was changed from 20 to 22 lb/yd². Similarly, in case of emulsion-based AAR specimens (Figure 6.3 (d)) a negligible change is observed with the change in AAR from 18 to 20 lb/yd². It can be inferred from this observation that a mere increase in the AAR does not result in a definitive change in the RAR. After a threshold AAR value, the higher AAR has a negligible effect on the amount of retained aggregates.

6.1.5 Residual Aggregate Gradation

It was observed that the aggregates lost due to the hand brush procedure usually belonged to a coarser fraction which, in turn, results in finer gradation on the specimen surface. For comparison purposes, Figure 6.3 (e) shows a picture of aggregates lost due to the hand brush and

Figure 6.3 (f) exhibits initial aggregate sample, where the difference in the gradation of the aggregates is clearly visible. Hence, it is then anticipated that the on-specimen gradation would be finer, for example, for the BAR of 0.25 gal/yd² compared to the BAR of 0.40 gal/yd². Likewise, it is anticipated that the on-specimen gradation would be finer with an increase in the AAR. On the other hand, in the case of excessive aggregate application rates, the notion that coarser aggregates are lost during hand brushing may not always hold true. This is because other variables, for example, residual aggregate rate, spatial aggregate distribution and aggregate orientation can affect the results due to potential complex interaction among them.

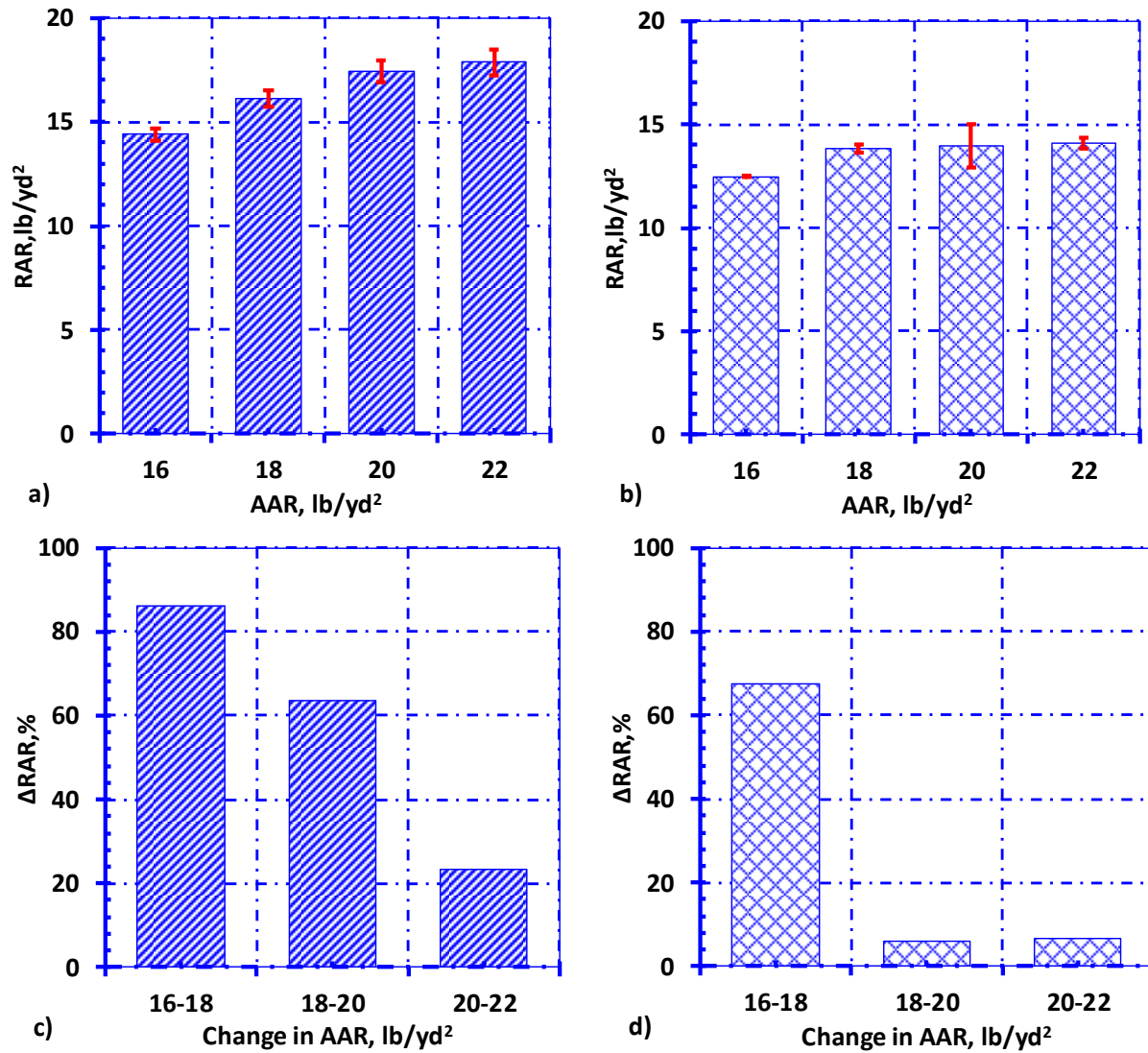


Figure 6.3 Residual aggregate application rate (RAR) for (a) set II-B (hot-applied) and (b) set IV-B (emulsion), Δ RAR for (c) set II-B and (d) set IV-B, (e) picture of aggregates lost due to hand brush and (f) picture of initial aggregate sample

6.2 *Digital image analysis results*

6.2.1 Percent Embedment and Aggregate Loss

Percent embedment (PE) was calculated for hot applied as well emulsion-based specimens using ‘each aggregate method’ algorithm of the CIPS software. The ‘each aggregate method’ algorithm essentially computes the percent embedment of individual aggregates and reports the average and standard deviation of the percent embedment distribution, based on eight slices per chip seal sample. In this study, the PE was computed individually for aggregates belonging to size fraction corresponding to 4.75-9.5 mm. This size range was selected because, as indicated in the previous section, the aggregate loss was mostly noted for coarse aggregate fractions, and coarse aggregates (i.e., aggregates within the range 4.75-9.5 mm) would reflect the effect of the PE on the aggregate loss.

The correlation between PE and ePE respectively with aggregate loss by sweep (ALS) have been presented in Figure 6.4(a) and Figure 6.4(b). Further, relation between PE and ePE respectively with Cumulative aggregate loss (CAL) have been presented in Figure 6.4(c) and Figure 6.4(d). It has to be noted that these relations were developed including data from hot applied as well as emulsion-based chip seals. With the magnitude and range of PE measured, it is not surprising to see that the sweep test did not provide definitive ranking with respect to the application rates in the case of ALS (Figure 6.4(a)). As seen, the magnitude of the measured PE is beyond a point, i.e. 70 percent, that aggregate loss is not likely to be dominating chip seal distress, at least to a differentiable extent. Moreover, the measured PE for one application rate to another one is within a close approximate, about 10 percent range, such that the aggregate loss is not within differentiable range, especially considering the magnitude of the PE being larger than, for example, 70 percent. Although the trend is slightly better when ALS and ePE are correlated (Figure 6.4(c)),

but overall ALS doesn't seem to quantify aggregate loss very efficiently. Nevertheless, the expected trend of ALS increasing with decrease of PE and ePE, is reflected in the Figure 6.4(a) and Figure 6.4(c).

From the relation of CAL with PE (Figure 6.4(b) and ePE (Figure 6.4(d)), it can be inferred that in general ePE is a better fundamental parameter for characterizing aggregate loss behavior. And in terms of laboratory performance test parameters, CAL seems to provide the best relation. Hence, ePE and CAL should be used to characterize chip seal aggregate loss behavior.

6.2.2 Orientation of Aggregates

Orientations of aggregates were calculated using the image analysis procedure explained earlier and the CPAF values were computed using the Equation 5.1. The CPAF results for hot applied chip seal samples as a function of BAR and AAR are presented in Figure 6.5(a) and Figure 6.5(b), respectively. For the BAR specimens, the CPAF increases as BAR increases until $\text{BAR} = 0.35 \text{ gal/yd}^2$, after which CPAF decreases. Overall trend is somewhat logical since aggregates can move (rotate and translate) and compact easier because of higher amount of binder (working as lubricating fluid). The reason for the decrease in CPAF when $\text{BAR} = 0.4 \text{ gal/yd}^2$ was that when there is too much binder, the binder oozes out the surface during compaction and sticks to rubber pad as shown in the Figure 6.5 (g). Then, the action of removing the rubber pad after the compaction exerts a pulling action on the stuck binder which, in turn, exerts an upward force on the aggregates, and rotates them vertically. Similar trend is observed in case of emulsion-based chip seals as well (Figure 6.5(c), and (d)).

There is an increase in CPAF as AAR increases from 16 lb/yd^2 to 18 lb/yd^2 , then the CPAF decreases as AAR increases. This indicates that the optimum aggregate application rate for these specimens is about 18 lb/yd^2 , after which the aggregates 'disorient'. This disorientation can be

explained as follows: The increase in the AAR results in the ‘lever and wedge’ effect as noted by previous researchers (Caltrans 2003), where the excessive aggregates bridge over the single layer aggregates and push and disorient them from their flattest sides. This effect is illustrated in Figure 6.5(e) and Figure 6.5(f). Therefore, it is very important not to apply more aggregates than needed.

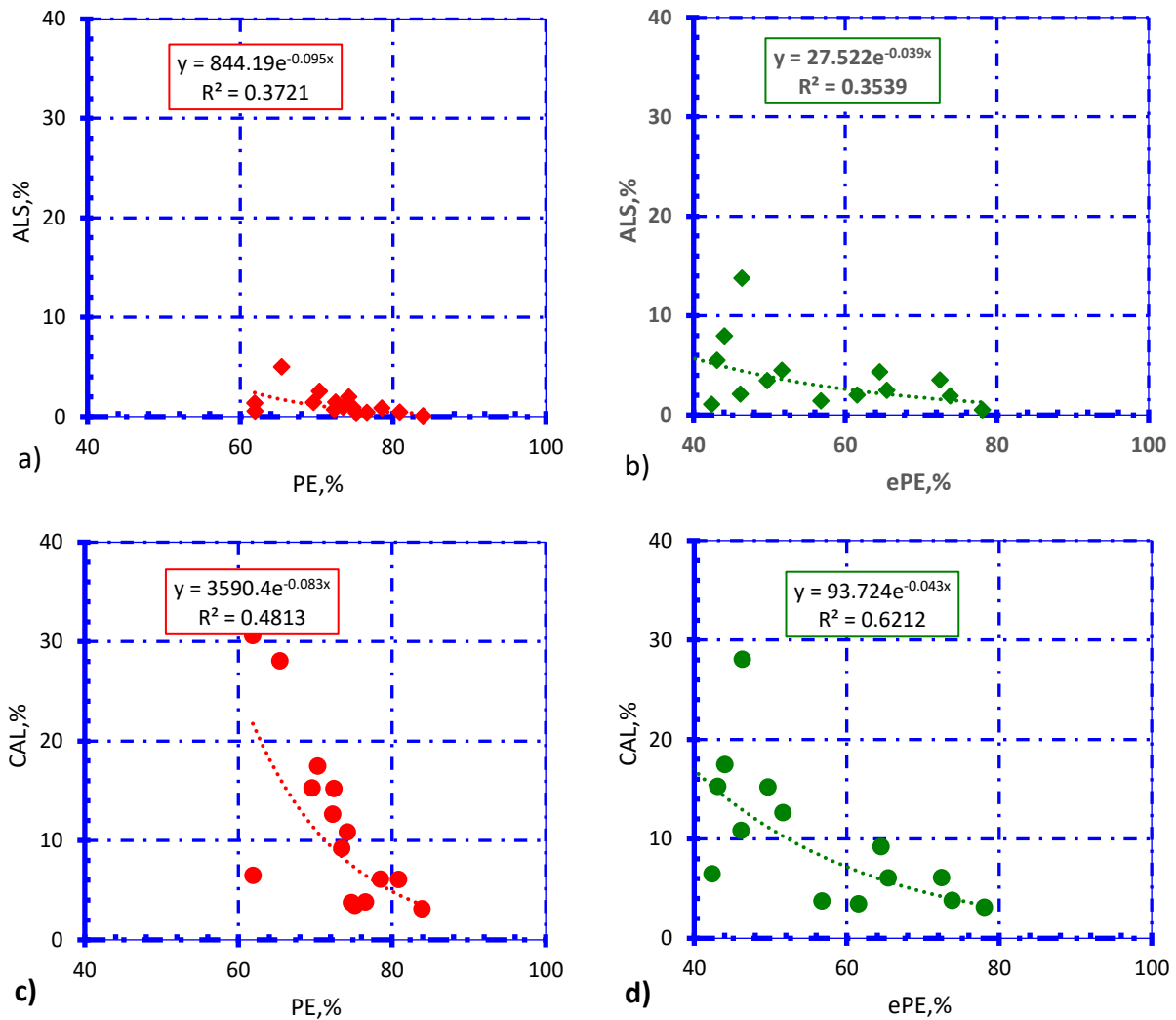


Figure 6.4 (a) ALS vs PE, (b) ALS vs ePE, (c) CAL vs PE ,and (d) CAL vs ePE including data from hot applied as well as emulsion based chip seals (groups I,II,III and IV)

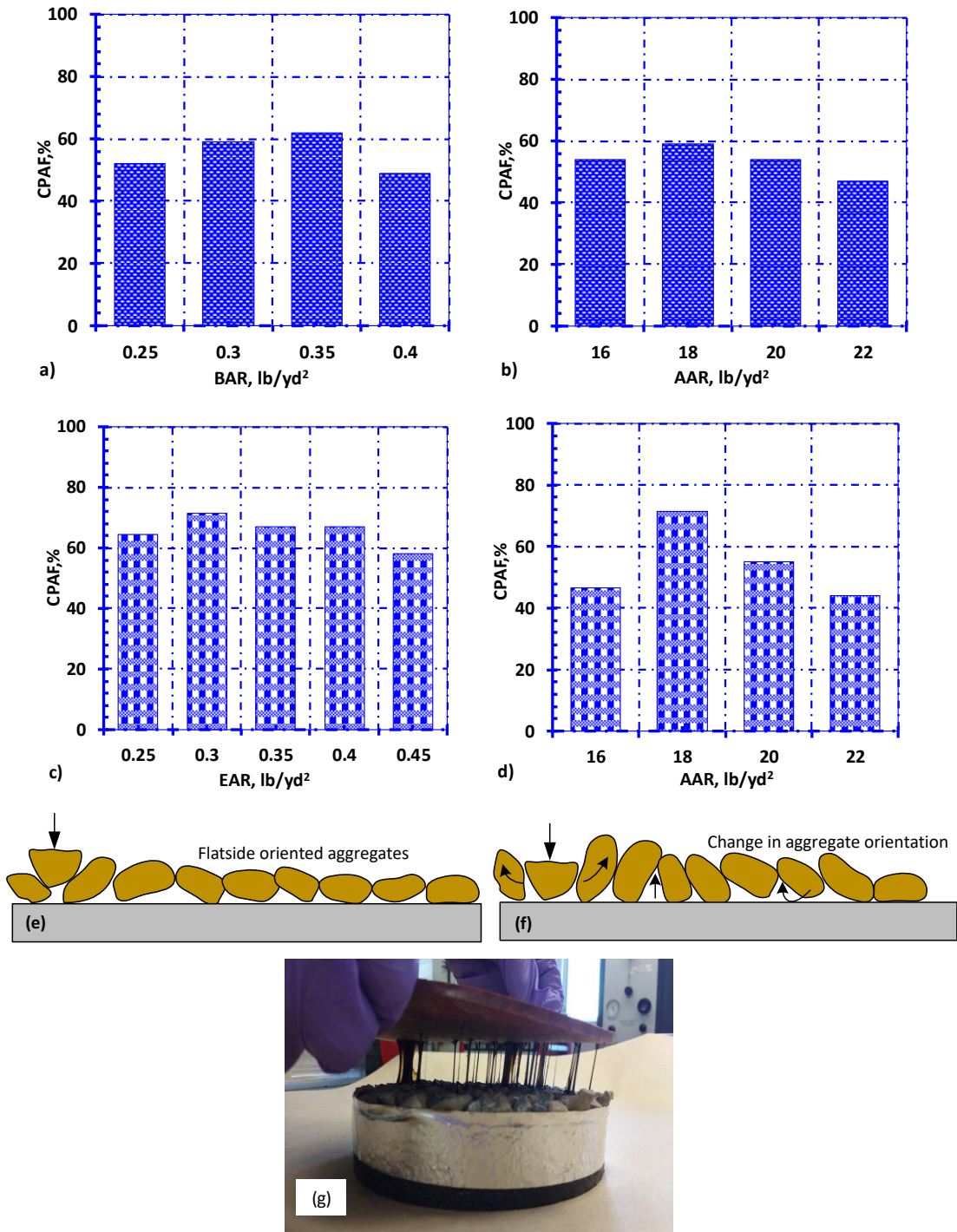


Figure 6.5 (a) CPAF vs BAR for set I-A, (b) CPAF vs AAR for set II-A, (c) CPAF vs BAR for set III-A, (d) CPAF vs AAR for set IV-A, (e) illustration of flat side orientation of aggregates, (f) illustration of change in orientation of aggregates due to lever and wedge effect, (g) a picture showing the binder sticking to the compaction rubber pad resulting in change in orientation of aggregates in case of high BAR

6.3 Comparison of hot applied and emulsion-based chip seals in terms of aggregate loss

In order to properly compare the aggregate loss in hot-applied and emulsion-based chip seals, specimens needed to be prepared at equivalent binder application rates. As mentioned previously, since about 65% of the emulsion is actually binder, the equivalent binder application rate, i.e., residual binder application rate ($\text{RBAR} = \text{EAR} \times \% \text{residue}$) was defined. Therefore, the EARs of 0.4 and 0.45 gal/yd² approximately correspond to RBARs of 0.25 and 0.3 gal/yd², respectively.

The cumulative aggregate loss (CAL) results of the specimens are presented in Figure 6.6(a). As shown, the emulsion-based chip seals performed better than the hot-applied chip seals. The ratio of CAL of emulsion and CAL of binder is about 3.35 in case of RBAR of 0.25 gal/yd² (EAR of 0.4 gal/yd²) and 1.75 in case of RBAR of 0.3 gal/yd² (EAR of 0.45 gal/yd²). Hence it can be said that, in terms of aggregate loss, emulsions outperform binders by anywhere between 75 and 200%. The reason for such a behavior is due to the physical interaction between emulsion-aggregate and binder-aggregate interface. Emulsions have water in them which helps them better spread and bind with the aggregates covering a larger part of aggregate area. It leaves a concave shape at the surface as shown in Figure 6.6(b). Whereas, hot applied binder cools and sets faster leaving a convex shape (see Figure 6.6(c)) that binds to lesser surface area of aggregates. Hence, emulsions outperform binders in terms of aggregate loss.

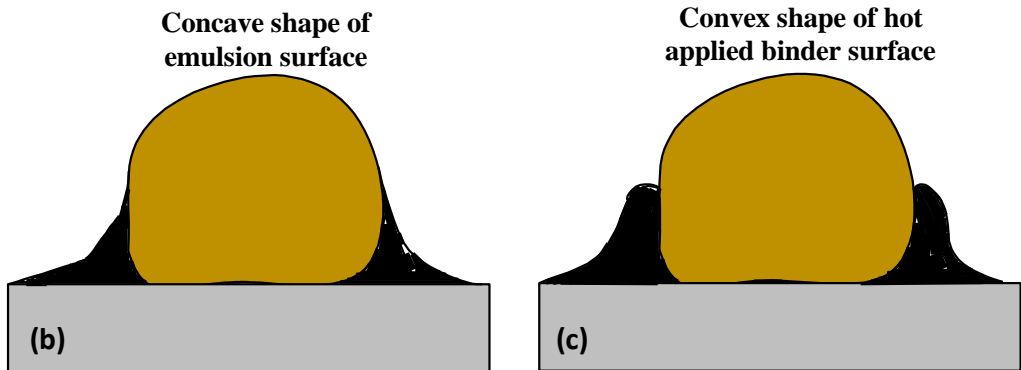
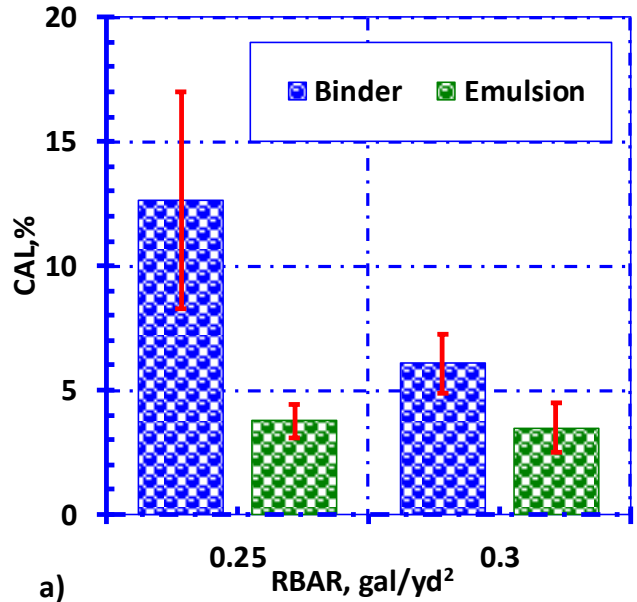


Figure 6.6 a) Comparison of Cumulative Aggregate Loss by sweep (CAL) for binder and emulsion-based chip seals at RBARs, b) sketch showing concave shape of emulsion surface, c) sketch showing convex shape of emulsion surface

6.4 Summary of chapter findings

The objective of this part of study was to investigate the effect of binder and aggregate application rates on percent embedment (PE) and aggregate orientation of chip seal aggregates via digital image analysis. In addition, the effect of the PE on aggregate loss calculated from the modified sweep test was also quantified. The major findings have been summarized as follows:

- It was observed that the cumulative aggregate loss from the sweep test should be used as a criterion to properly evaluate chip seal performance. The “Effective Percent Embedment”

(ePE) was introduced as a parameter to quantify the microstructure of the chip seals. This parameter correlated well with the cumulative aggregate loss.

- A critical evaluation of the orientation distribution of the aggregates revealed that low amounts of binder application rates or excessive amounts of aggregate application rates can cause the aggregates to disorient from their flattest sides. This was especially true when excessive aggregate application rate leads to multiple layers of aggregates, which leads to the lever and wedge effect.
- Effect of binder type on aggregate loss was evaluated. In terms of aggregate loss performance, emulsions were observed to outperform binders by anywhere between 75 and 200%.

Overall, this part of study shed light on important nuances of chip seal aggregate-binder interaction and its effects on aggregate loss performance. Findings from this study provided enhanced understanding of binder and aggregate application rates on aggregate loss as a function of aggregate-binder interaction parameters.

7. INVESTIGATION OF BLEEDING BEHAVIOR IN CHIP SEALS

The objective of this part of study was to evaluate the effect of binder and aggregate application rates on bleeding behavior of chip seals. Bleeding tests as well as image analyses were conducted on chip seal specimens prepared using hot applied binder as well as emulsion. The results and discussion have been presented in the following subsections.

7.1 Effect of Binder Application Rates (BAR) and Emulsion Application Rates (EAR) on Bleeding

The Percent Binder Area (PBA) results (see equation 4.6 for definition of PBA) for chip seal samples prepared with hot-applied binder and subjected to Hamburg Wheel Tracking (HWT) tests are presented in Figure 7.1(a). For samples at 0 cycle loading, it can be observed that there is an increase in PBA with increase in BAR. Further, the overall increase in PBA (at this stage) might not be very significant since the specimens were not yet loaded with HWT. It has to be noted that, the change in PBA is solely related to amount of extra binder that fills the voids between aggregates and attempts to ooze towards the top of the surface. For BAR of 0.25 and 0.3 gal/yd², the increase in PBA values with application of HWT cycles is gradual. A large transition in bleeding behavior was observed between BAR of 0.35 and 0.4 gal/yd², after 500 cycles. In case of chip seal specimen with BAR of 0.4 gal/yd², the samples were entirely bled with all the aggregates picked up from the surface (PBA: 100%) at 1000 cycles. Figure 7.2 shows the condition where most of aggregates in the wheel path are being picked up, (just prior to the condition mentioned above). This behavior can be analogically linked to rutting in asphalt mixtures. Figure 7.1(b) presents the change in PBA between 0 and 1500 cycles, termed as Δ PBA. It is calculated by subtracting PBA values at 1500 and 0 cycles for each application rate. It can be observed that the bleeding behavior across binder

application rates is similar to the transition from secondary to tertiary flow in asphalt mixtures, leading to excessive rutting. From these results, it can be inferred that BAR of 0.4 gal/ yd² is very high. Hence, for the given AAR of 18 lb/yd², the threshold BAR should be 0.35 gal/yd². This is an important inference in relation to chip seal design.

The PBA results for chip seal samples prepared with emulsions and subjected to HWT have been presented in Figure 7.3(a). At 0 cycle condition, the increase in PBA with increase in EAR is extremely small as expected. For EARs of 0.25, 0.3, and 0.35 gal/yd² the increase of PBA values with HWT cycles is very steady and gradual. There is a significant transition in PBA values from EAR of 0.35 to 0.4 gal/yd², especially after 1000 cycles. It is worth noting that lower threshold of recommended EAR for emulsion as per MDOT is 0.39 gal/yd², which is in close vicinity of EAR of 0.4 gal/yd² in this case. The transition is also clearly visible in Figure 7.3(b) where the Δ PBA is presented.

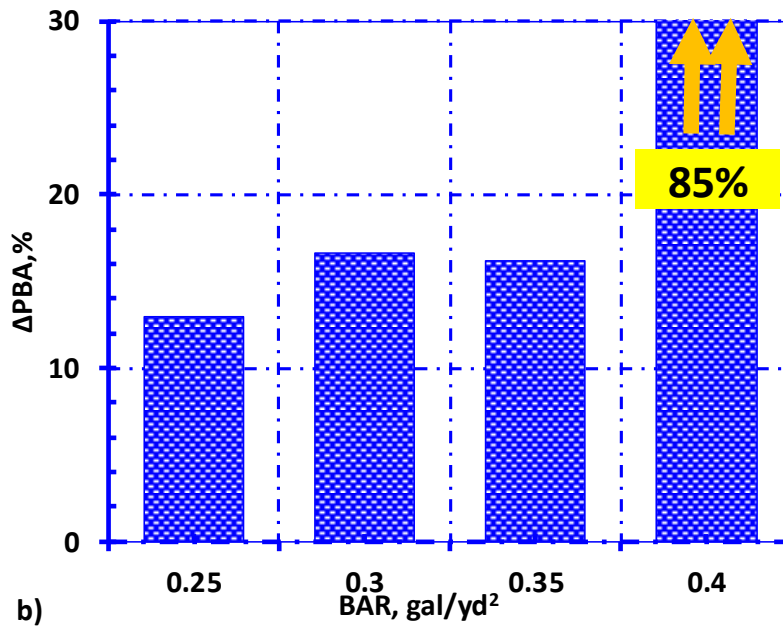
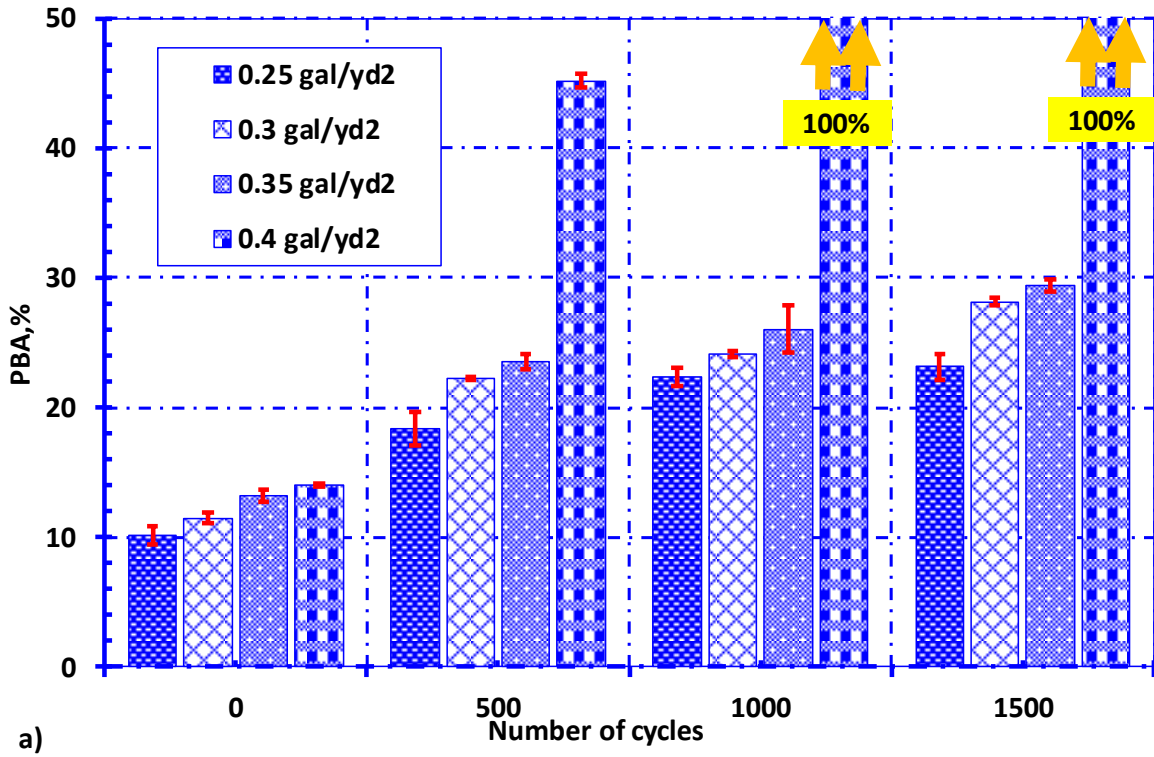


Figure 7.1 a) PBAs and b) Δ PBA for hot applied chip seals with different BARs



Figure 7.2 Aggregate pickup during HWT tests of high BAR (0.4 gal/yd²)

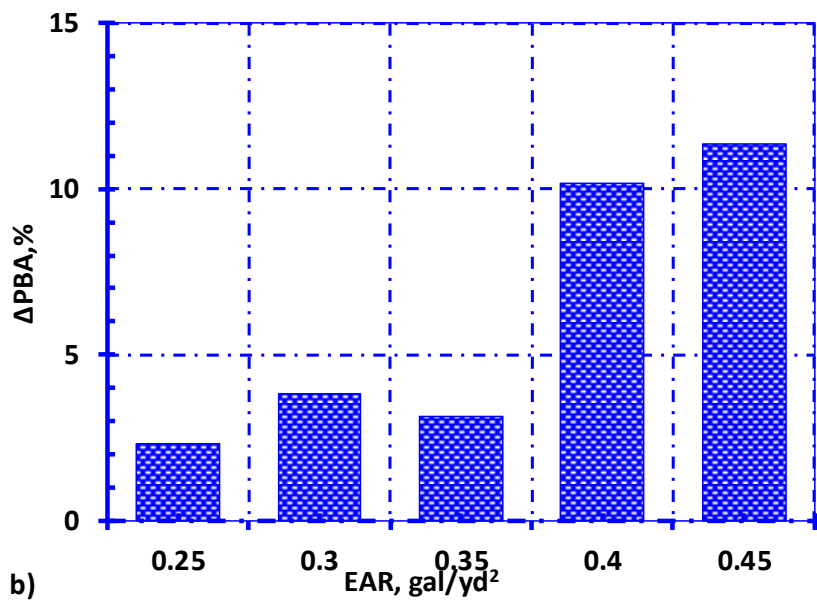
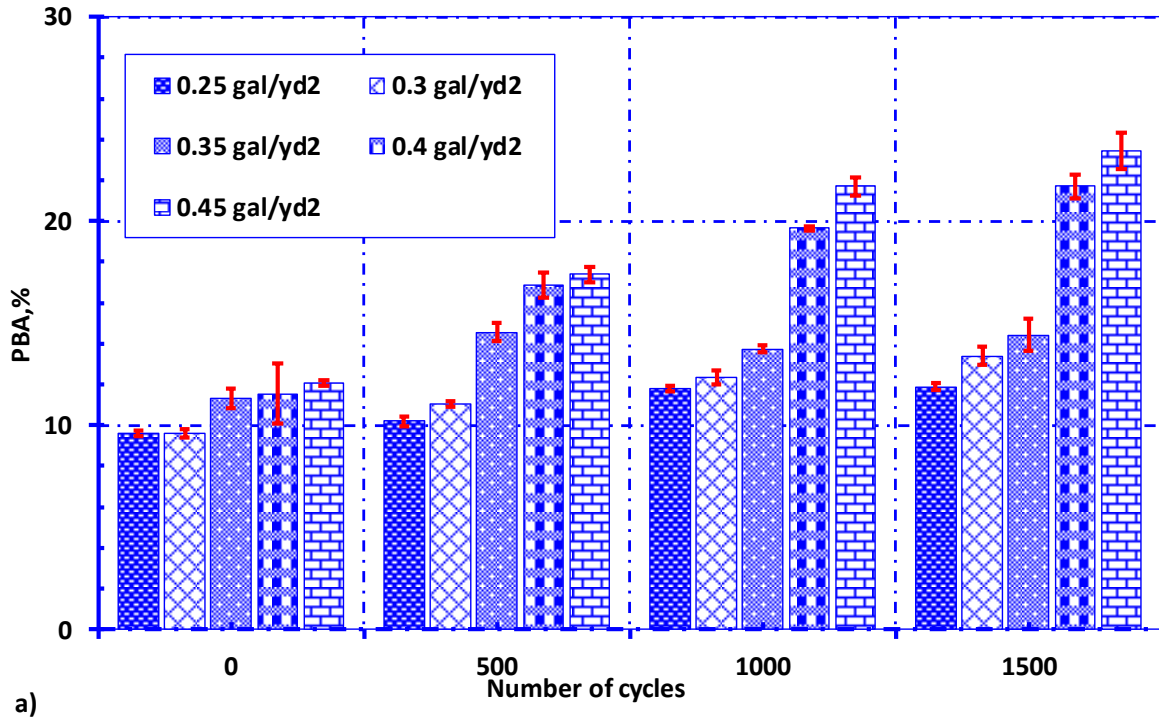


Figure 7.3 a) PBAs and b) ΔPBA for emulsion-based chip seals with different EARs

7.2 *Effect of aggregate application rate (AAR) on bleeding*

7.2.1 Characterization of effect of AAR on bleeding through 2D PBA criterion

The PBA results for hot applied and emulsion applied chip seal samples are presented in Figure 7.4(a) and Figure 7.5(a), respectively. Before HWT loading, (i.e. 0 cycle condition), although there is a slight decrease in PBA with increase in AAR, it can be observed that PBA generally remains constant. This is possibly because there was a very small difference between the residual aggregate application rates for these AARs. Residual aggregate application rate (RAR) is the amount of aggregates that is retained on the chip seal surface and is the actual component of aggregates that take part in chip seal pavement performance. Figure 7.4(b) and Figure 7.5(b) present RAR results for chip seal specimens respectively for hot applied and emulsion-based chip seals, at four different AARs. In both the cases, RAR increases significantly in the transition between AAR of 16-18 lb/ yd² and less significantly in case of 18-20 lb/ yd². No appreciable change in RAR was observed between chip seal specimens with AAR of 20 and 22 lb/ yd². AAR of 16 lb/ yd² was not subjected to HWT since visual inspection revealed its extreme susceptibility to bleeding behavior. The amount of aggregates (for AAR 16 lb/ yd²) were not enough to densely cover the whole surface, leading to a higher bleeding susceptibility.

Change in PBA between 1500 and 0 cycles are presented in Figure 7.4(c) and Figure 7.5(c). It can be clearly observed that PBA significantly decreased with increase in AAR. In order to explain this behavior, it is important to consider the orientation of aggregates at these AARs. Figure 7.4 (d) and Figure 7.5(d) present the Cumulative Percentage of Aggregates lying on Flat sides (CPAF) for hot applied and emulsion-based chip seals, respectively. CPAF is the percentage of aggregates that had orientation angle less than 20°. In other words, aggregates with angle of 20° and less are considered to be lying on their flattest side on the pavement substrate. There is an

increase in CPAF as AAR increases from 16lb/yd² to 18lb/yd², then the CPAF decreases as AAR increases. This indicates that the optimum aggregate application rate for these specimens is about 18lb/yd², after which the aggregates ‘disorient’. The increase in the AAR results in the ‘lever and wedge’ effect as noted by previous researchers (Caltrans 2003), where the excessive aggregates bridge over the single layer aggregates and push and disorient them from their flattest sides.

Though the specimens with AAR of 20 and 22 lb/yd² had very similar residual application rates (RAR), the lever and wedge effect resulted in different orientation patterns for these AARs. In case of chip seal specimens with high AAR (low CPAF), the initial HWT cycles might have resulted in forcing the aggregate particles to align and lie to their flat sides. The real bleeding action actually might have initiated and progressed only after all aggregates were aligned to their flat sides. Hence, the PBA values at the end of HWT showed a significant difference across AARs.

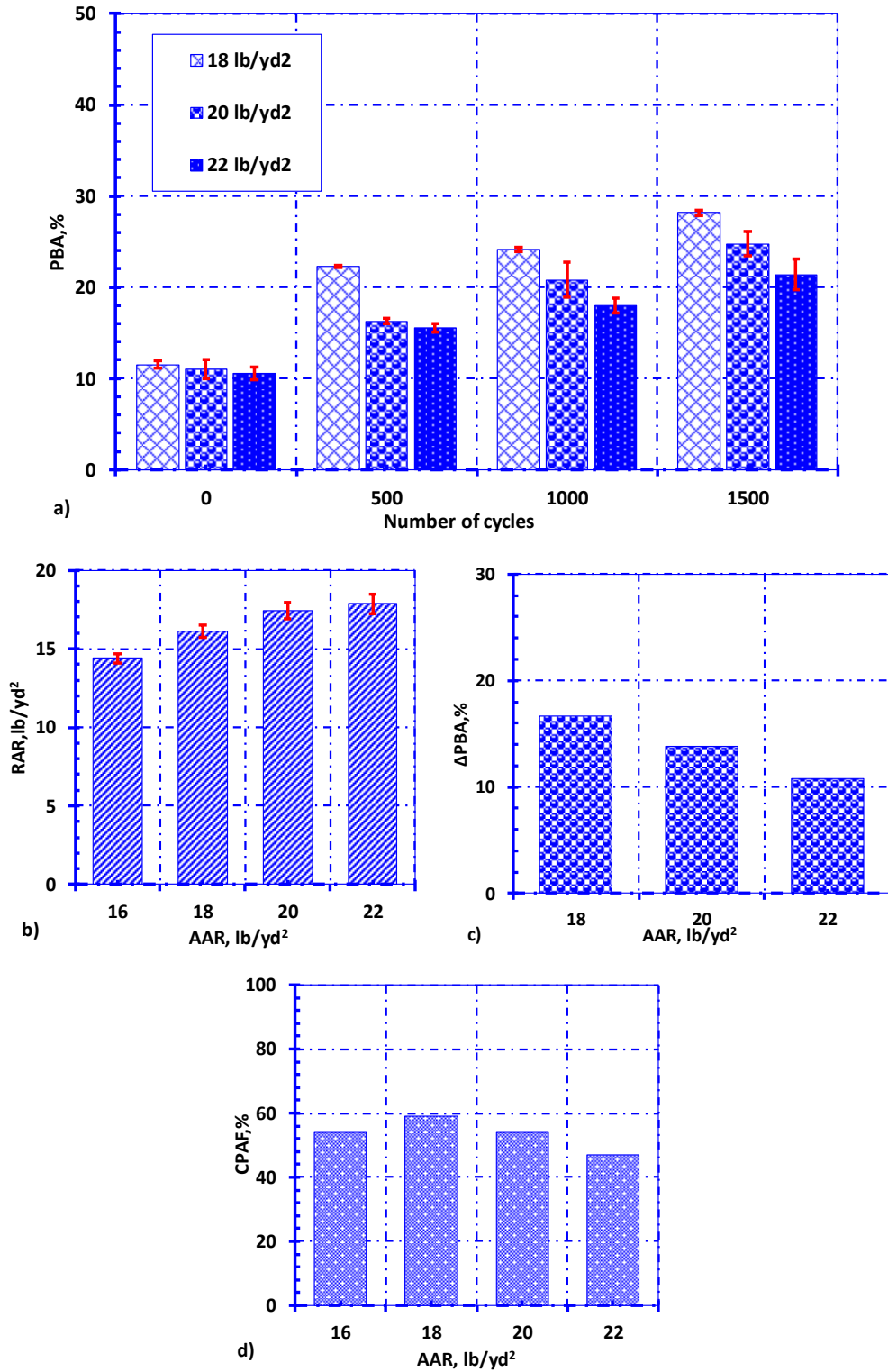


Figure 7.4 For hot applied chip seal samples: a) PBAs at different cycles b) Δ PBA, c) CPAF for different AARs

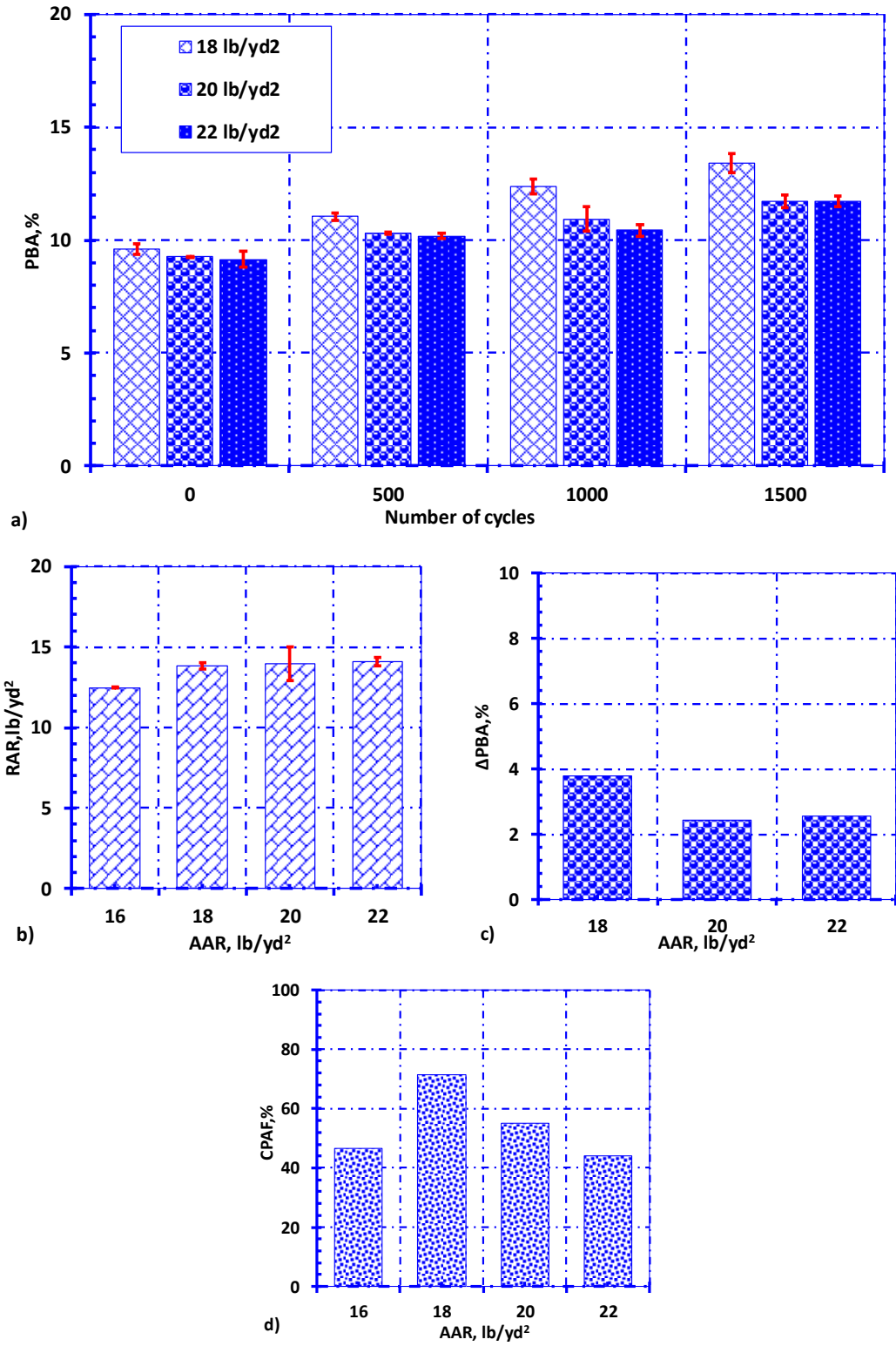


Figure 7.5 For emulsion applied chip seal samples: a) PBAs at different cycles b) ΔPBA, c) CPAF for different AARs

7.2.2 Characterization of effect of AAR on bleeding through 3D Mean Profile Depth (MPD) criterion

The mean profile depth (MPD) results for hot applied and emulsion-based chip seal samples for different AARs are presented in Figure 7.6 and Figure 7.7. For initial condition in all the cases, MPDs slightly increase with increase in AAR. MPD at 0 HWT cycles for AAR of 18 and 20 are nearly the same and MPD for AAR 22 lb/yd² is slightly higher than the other two. This observation aligns with the previous discussion on effect of addition of high amount of aggregates. Based on previous observation in terms of RAR, it was inferred that 22 lb/yd² being too high application rate, the effect of lever and wedge effect was more pronounced in this case. The resulting adverse effect on aggregate orientation has direct consequence on high initial MPD values. The trend of MPD across AARs further highlights its inverse relation with PE as depicted in Figure 4.6(b). This further assures that how chip seal micro-structure properties (PE) are very well correlated to the macro-texture properties (MPD).

Furthermore, the change in MPD with HWT cycles seems to follow a specific trend. There is drastic decrease in MPD values at the end of 500 cycles, which remains nearly same until the end of 1000 cycles. A slight decreasing trend of MPD is observed at the end of 1500 cycles. It can be inferred that, major change in macrotecture related characteristics of chip seals take place during the initial service life of chip seal pavements. Furthermore, it has to be noted that these aggregate application rates do not result in significant change in terms of increase in 2D binder area, which is a positive outcome. But the change in MPD will result in formation of localized rutting patterns in wheel path. This would cause adverse effect on safety. These effects will be worsened with addition of high amount of aggregates, because of higher amount of change in MPD resulting in deeper rut patterns at high AARs.

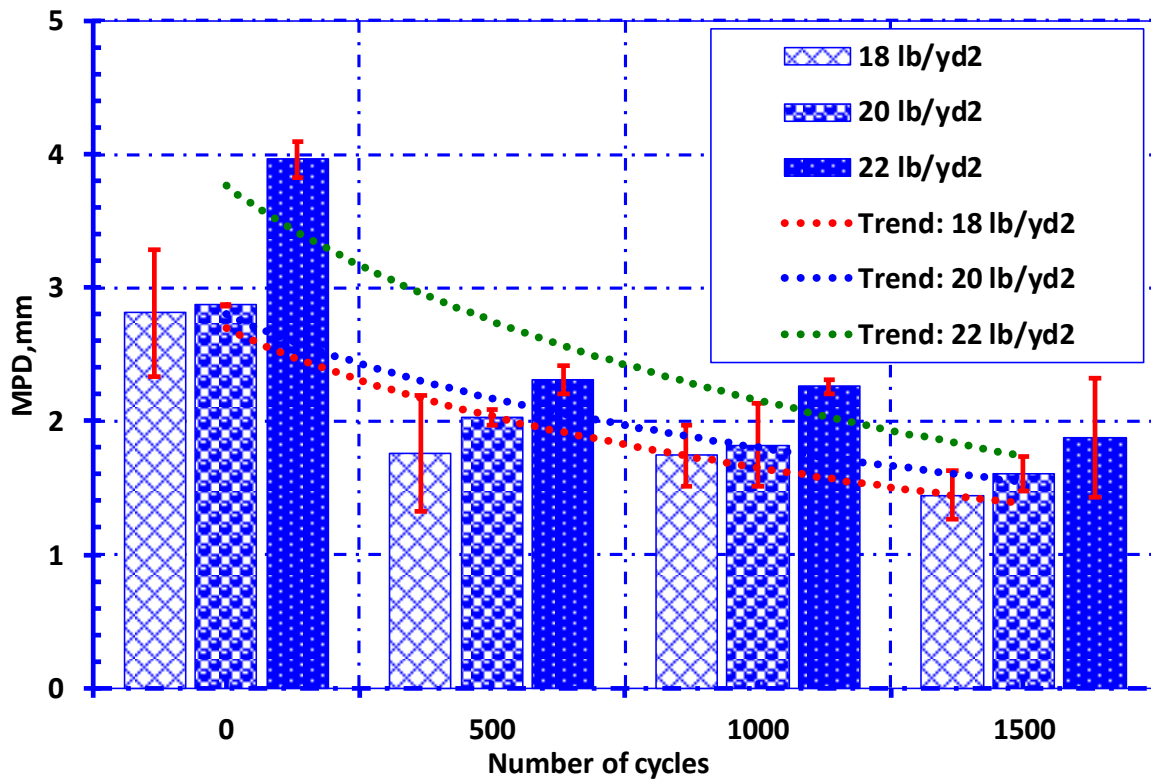


Figure 7.6 MPDs at different cycles for hot applied chip seal samples with AAR of 18 lb/yd², 20 lb/yd², and 22 lb/yd²

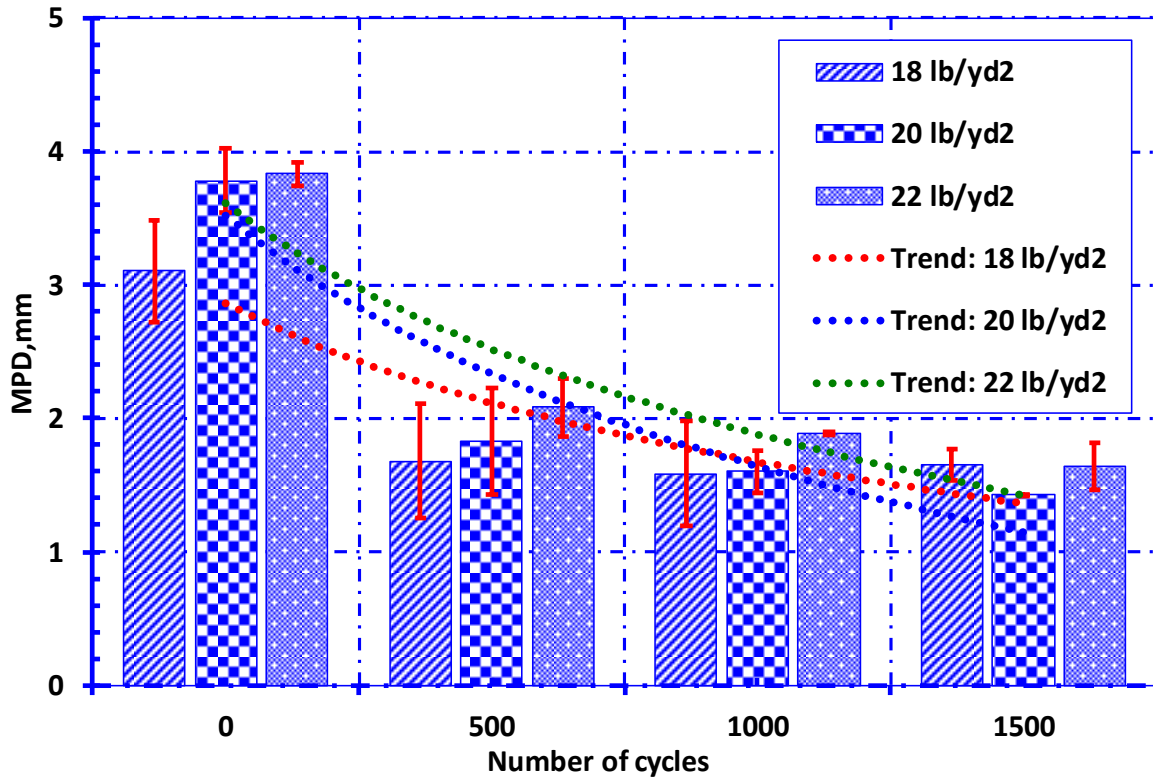


Figure 7.7 MPDs at different cycles for emulsion-based chip seal samples AAR of 18 lb/yd², 20 lb/yd², and 22 lb/yd²

7.3 Relation between PE and bleeding

Figure 7.8(a) presents the PBA results for the chip seal specimens as a function of Percent Embedment (PE), including hot applied as well as emulsion-based specimens. For the reasons discussed before regarding normalization of PE (chapter 3), effective percent embedment (ePE) was computed for these chip seal specimens. Figure 7.8(b) presents PBA results as a function of ePE. It can be observed that there is a strong correlation between ePE and PBA, therefore ePE is a good parameter to characterize bleeding behavior of chip seals. It can be observed that chip seal specimens with BAR of 0.4 gal/yd² (ePE = 78%) (in case of hot applied chip seal specimens) failed with respect to bleeding behavior. Highest ePE without failure was observed at ePE = 72.5%.

Hence, it can be inferred that maximum ePE threshold is somewhere between of 72.5% and 78%.

Conservatively, ePE =70% is perhaps a reasonable upper threshold.

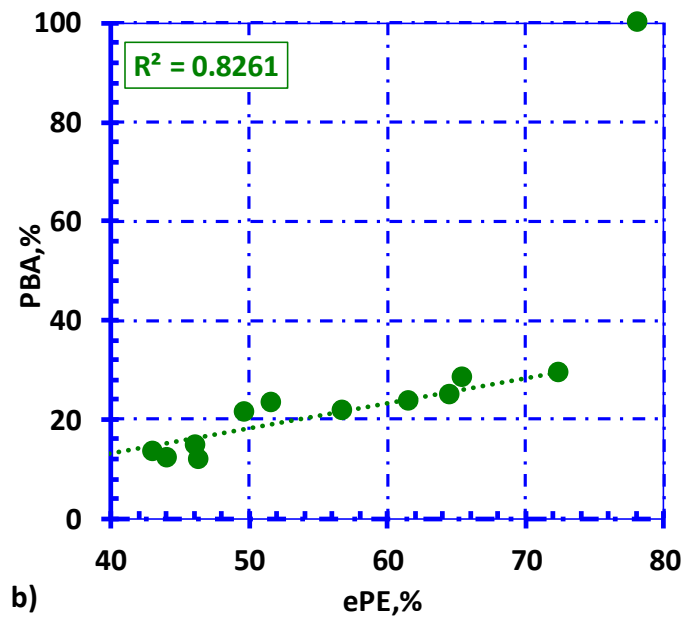
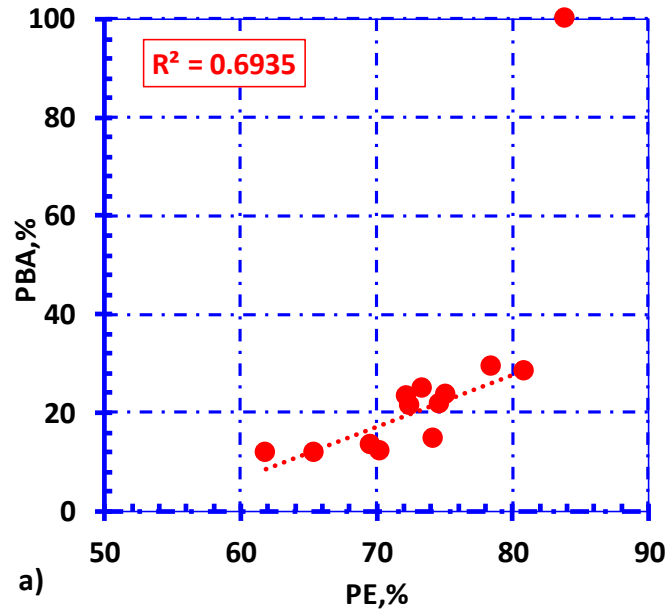


Figure 7.8 a) PBA vs ePE and b) PBA vs ePE at 1500 HWT cycles

7.4 Comparative performance of binder and emulsion with respect to bleeding

In order to properly compare the bleeding performance in hot-applied and emulsion-based chip seals, specimens needed to be prepared at equivalent binder application rates. As mentioned previously, since about 65% of the emulsion is actually binder, the equivalent binder application rate, i.e., residual binder application rate ($\text{RBAR} = \text{EAR} \times \% \text{residue}$) was defined. Therefore, the EARs of 0.4 and 0.45 gal/yd² approximately correspond to RBARs of 0.25 and 0.3 gal/yd², respectively.

The PBA results of the specimens are presented in Figure 7.9(a). As shown, the emulsion-based chip seals performed better than the hot-applied chip seals. The ratio of PBA of emulsion and PBA of binder is about 0.93 in case of RBAR of 0.25 gal/yd² (EAR of 0.4 gal/yd²) and 0.83 in case of RBAR of 0.3 gal/yd² (EAR of 0.45 gal/yd²). Hence it can be said that, in terms of bleeding, emulsions outperform binders by anywhere between 10 and 20%. ΔPBA results have been depicted in Figure 7.9(b) showing similar trend of emulsions outperforming hot applied binders in terms of bleeding performance.

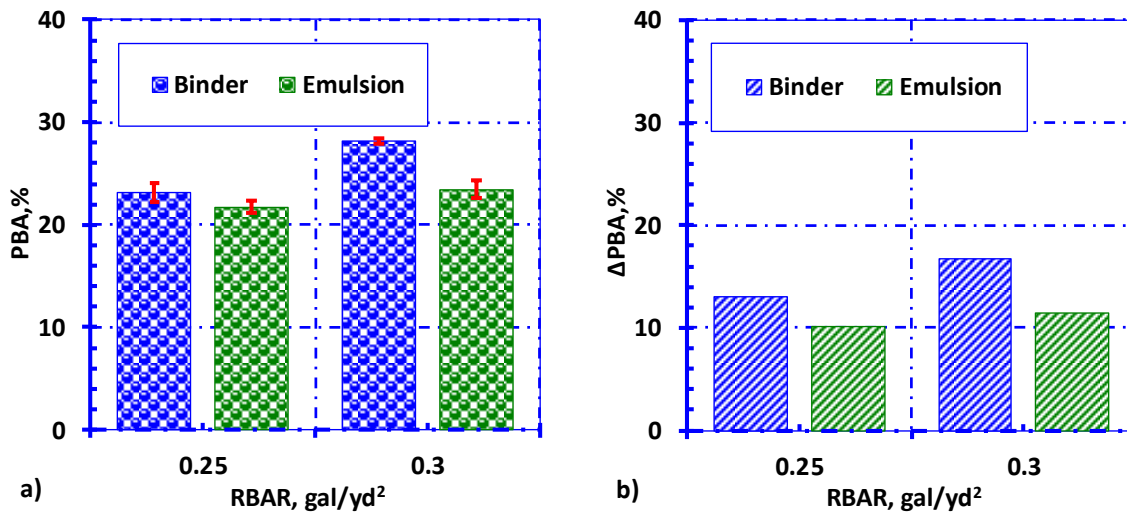


Figure 7.9 a) PBA and b) ΔPBA for binder and emulsion applied chip seals

7.5 *Summary of chapter findings*

Objective of this part of the study was to investigate effect of binder and aggregate application rates on bleeding performance through percent embedment criteria using Hamburg Wheel Tracking (HWT) test. Chip seal specimens with different BARs, EARs and AARs were prepared and tested for bleeding susceptibility. Also, image analysis was performed to compute PE and aggregate orientation. Important findings from this part of the study are presented below:

- Evaluation of Percent Binder Area (PBA) during/after HWT tests was found to be effective in characterizing the bleeding behavior of chip seals. PBA generally increased with increase in binder application rates (BAR) (in hot-applied chip seal) and emulsion application rates (EAR) (in emulsion-based chip seal). The bleeding behavior during a HWT test was found to be analogous to the rutting behavior of asphalt mixtures, specifically the concept of ‘flow number’ in repeated load permanent deformation (RLPD) tests. Similar to the change in plastic strain in asphalt mixture during a RLPD test, there is a steady increase in PBA as the HWT cycles increase. At high binder application rates, a rapid increase in PBA is observed after certain number of HWT cycles, similar to the tertiary flow in flow number tests.
- Effective percent embedment (ePE) showed excellent correlation with PBA, therefore ePE can be effectively used to characterize bleeding behavior of chip seals.
- Effect of aggregate application rate on bleeding behavior was best observed in terms of change in the aggregate orientation, which is quantified in this study using the CPAF parameter. Good correlation was observed between PBA and aggregate orientation results (CPAF).

- In terms of bleeding performance, emulsion-based chip seals outperformed hot-applied chip seals, by anywhere between 10 and 20%.
- Holistic evaluation of chip seal bleeding behavior needs 3D analysis. A unique low-cost method to evaluate chip seal 3D macrotexture was developed. Mean profile depths (MPD) at the end of various HWT cycles were computed. Results showed that there is a significant change in macrotexture with bleeding. If excessive amount of aggregates is used, then although change in PBA is negligible but a significant change in MPD (i.e. 3D macrotexture) is observed. This essentially creates a rut pattern in the wheel path. The change in MPD being high, it can potentially lead to hydroplaning and loss of friction. Furthermore, localized rut patterns will lead to difficulty in maneuvering and potential safety hazard.

8. DEVELOPMENT OF A PERFORMANCE-BASED DESIGN METHODOLOGY FOR CHIP SEALS

The objective of this part of the study was to develop a performance-based design procedure for design of chip seals. The image analysis, sweep tests and bleeding tests on group I and group II chip seal specimens (hot applied chip seals) were further analyzed to develop a performance-based design methodology. The equations used for characterizing aggregate orientation, loss and bleeding are presented in the previous chapters. These results have been briefly summarized herein and the new design procedure is proposed.

8.1 Aggregate orientation

The CPAF results as a function of the AAR are presented in Figure 8.1. It can be observed that there is an increase in CPAF with increase in the AAR until the AAR of 18 lb/yd², after which the CPAF shows a decreasing trend. After the optimum AAR, the aggregates start to disorient. If a higher amount of aggregates is added than required, then the excessive aggregates push each other and disorient them from their flattest side. Hence, the optimum AAR is the one which gives the highest CPAF value, which is 18 lb/yd² for the dataset shown Figure 8.1.

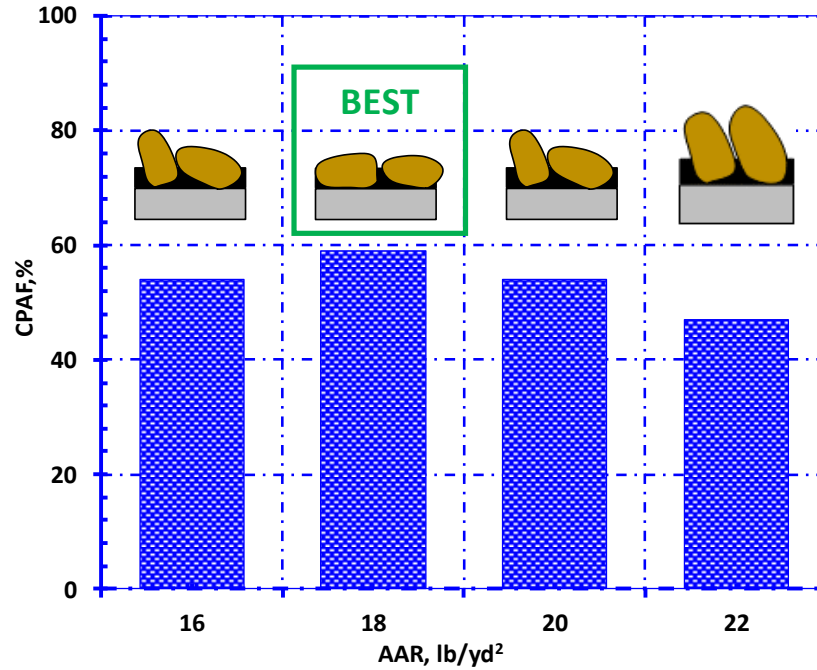


Figure 8.1 Variation of cumulative percentage of aggregates lying on their flat side (CPAF) for samples of set I-A (hot applied) with different aggregate application rates (AARs)

8.2 Aggregate loss

Figure 8.2 shows the CAL results as a function of the BAR for Set II-B samples. It has been stated in previous studies that chip seal treatments perform efficiently with respect to the aggregate loss if aggregate loss is less than 10% (Lee & Kim 2008b). As shown in Figure 8.2, the CAL decreases drastically with increase in the BAR from 0.25 to 0.3 gal/yd², after which it doesn't show an appreciable change. The CAL for the BAR of 0.25 gal/yd² being greater than 10% does not meet the requirement, however the rates 0.3, 0.35 and 0.4 gal/yd², all meet the aggregate loss criterion. These rates need to be evaluated for bleeding susceptibility.

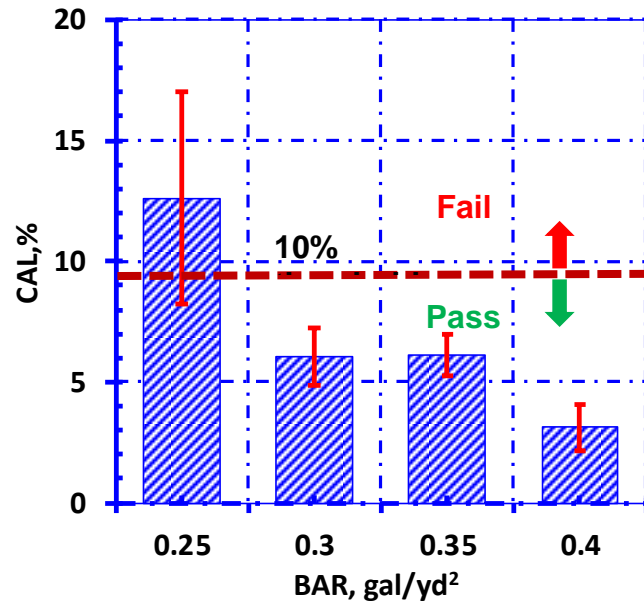


Figure 8.2 Variation of the Cumulative Aggregate Lost by sweep (CAL) for Set II-B (hot applied) samples with different binder application rates (BARs)

8.3 Bleeding

Figure 8.3 shows the relation between percent binder area (PBA) and the BAR for Set II-C, at the end of 1500 HWT cycles. It can be seen that there is a steady increase in PBA as the BAR increases, until the BAR of 0.4 gal/yd², where a 100% bleeding was observed. At the BAR 0.4 gal/yd², the binder bleeding was excessive and started adhering to the tire of the HWT device. Once the binder came into contact with the tire, the tire picked up the binder and the aggregates attached to the binder, leading to a complete failure of the sample. These results indicate that BAR < 0.35 gal/yd² yield satisfactory results with respect to bleeding.

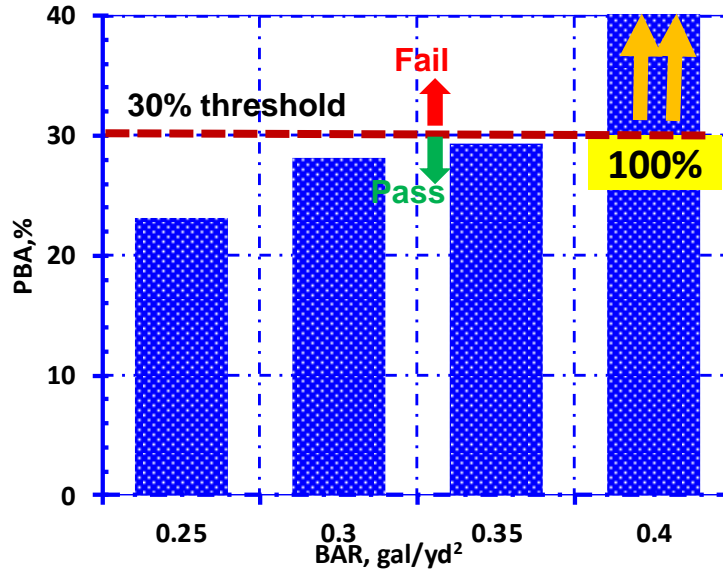


Figure 8.3 The change in the Percentage Bleeding Area (PBA) for Set II-C (hot-applied) samples with different binder application rates (BARs)

8.4 Performance-based design procedure

The results of aggregate orientation, aggregate loss and bleeding was combined to develop a performance-based design procedure, as illustrated in Figure 8.4. The first step consists of preparing chip seal samples with a seed BAR value (based on experience) and varying the AARs. The first step is to perform image analysis using the CIPS software to compute the aggregate orientation distribution and the CPAF parameter. The AAR that yields highest value for CPAF (i.e., optimal aggregate orientation) is the design AAR. The second step involves preparing several samples with different BARs (at design AAR), then running the sweep test to calculate the CAL. The BARs that yield the CAL values less than 10% can be pursued in the next step for the bleeding analysis. The third step consists of preparing the samples and testing them for the PBA in the HWT device. The lowest BAR that yields least PBA is the design BAR.

8.5 *Comparison with existing design methods*

Table 8.1 shows the design binder and aggregate application rates produced by the current popular design methodologies and the application rates produced by the performance-based design method developed in this study. The values of the binder and aggregate application rates (of the popular design methods mentioned below) were obtained by entering relevant aggregate and binder related data in the nomographs/equations provided by these design methods. It can be seen that the Modified Kearby design yields a BAR of 0.16 gal/yd², which is quite low. Extrapolating the CAL results from Figure 8.2, it can be seen that the BAR of 0.16 gal/yd² would result in a high CAL value and aggregate loss in field. Similar arguments can be made for BAR values from the McLeod Design. On the contrary, the Modified McLeod Design method yielded a higher BAR value with respect to the bleeding criteria. The AAR value computed from the Modified Kearby method was found to be very low with respect to the performance-based design rate. The McLeod Design method yielded a high value of AAR, which can be detrimental to orientation (see Figure 8.1). The AAR and BAR values given by the Modified McLeod design seemed to be comparable to those of the performance-based design methodology, but the former was a bit over-design (i.e., more expensive).

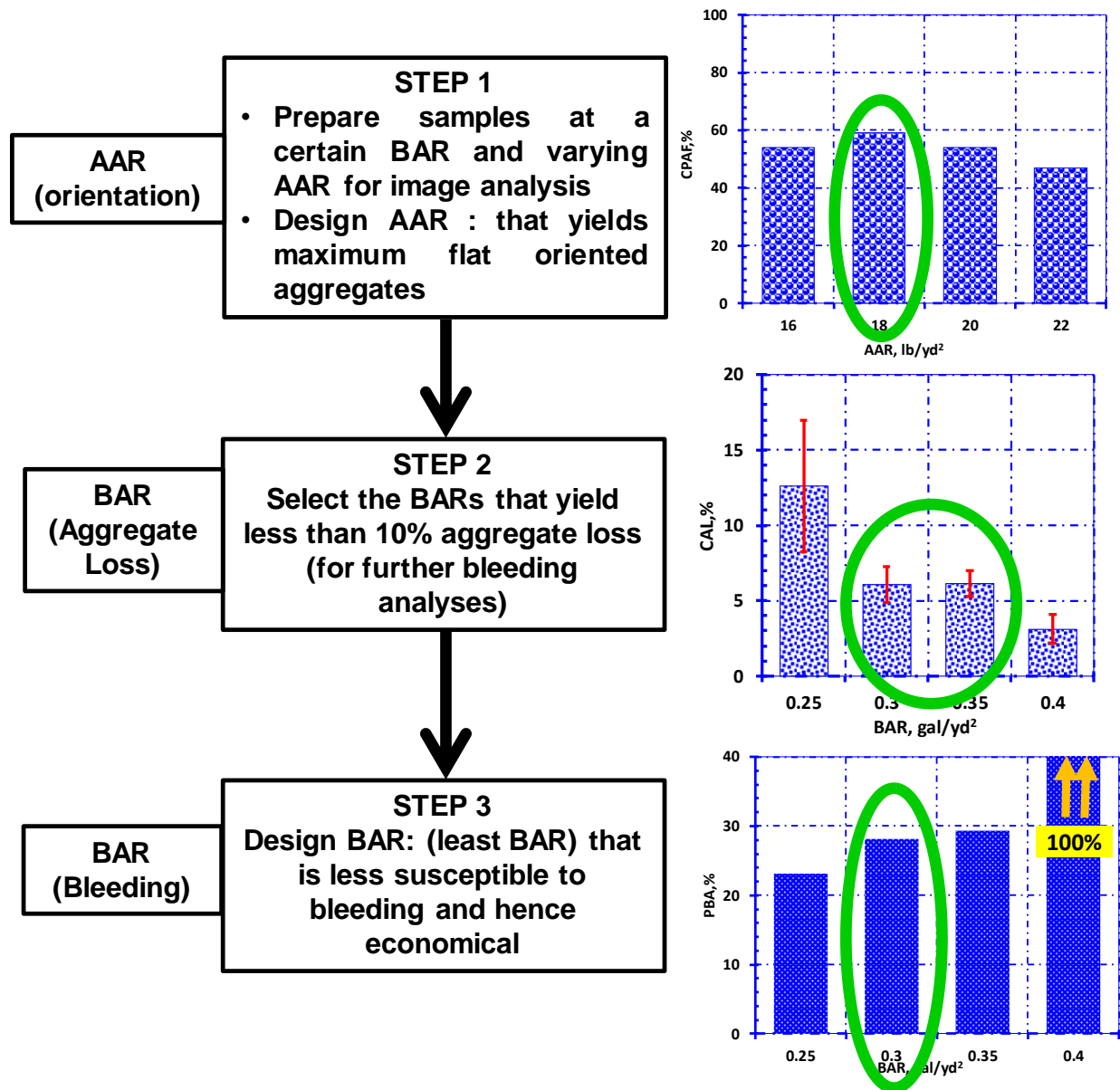


Figure 8.4 Flowchart depicting the performance-based procedure for chip seal designs

Table 8.1 Comparison of BAR and AAR values obtained by following various Chip Seal design methodologies

Method	BAR (gal/yd ²)	AAR (lb/yd ²)
Modified Kearby	0.16	11.8
McLeod	0.19	23.8
Modified McLeod	0.38	18.8
Performance based design	0.3	18

8.6 Acceptable Range of Percent Embedment

Figure 8.5(a) and Figure 8.5(b) show the relationship between the effective percent embedment (ePE) and the cumulative aggregate loss (CAL) and percent bleeding area (PBA), respectively. All the results for hot applied as well as emulsion-based chip seals have been included in these figures. As indicated earlier, the literature indicated that the acceptable threshold for aggregate loss is 10% (Lee & Kim 2012). Maximum acceptable PBA observed in this study was 30%, above which the bleeding was excessive and the binder oozed out the surface, stuck the tire and caused the entire chip seal to be lifted up by the tire. Therefore, the results of this study suggest that the acceptable range of ePE is from about 57% to 70%.

8.7 Summary of chapter findings

The objective of this part of research study was to develop a performance-based design procedure for design of chip seal treatments. The experimental program involved preparation of chip seal samples and subjecting them to image analysis, sweep test, and Hamburg Wheel Tracking (HWT) test. The research findings can be summarized as follows:

- The methodology developed in this study is based on the major performance parameters (aggregate loss and bleeding) and ensures that aggregates are oriented on their flattest side during the design and laboratory testing stage.
- The comparative analysis with respect to the existing methodologies showed the rationality of the developed design methodology.
- Based on comprehensive evaluation of hot applied binder as well as emulsion applied chip seals, it was observed that the acceptable range of ePE is from 57% to 70%.

Overall, this phase of research study helped understand the merits and drawbacks of the popular chip seal design methodologies and provided a way to achieve more optimal design for chip seals.

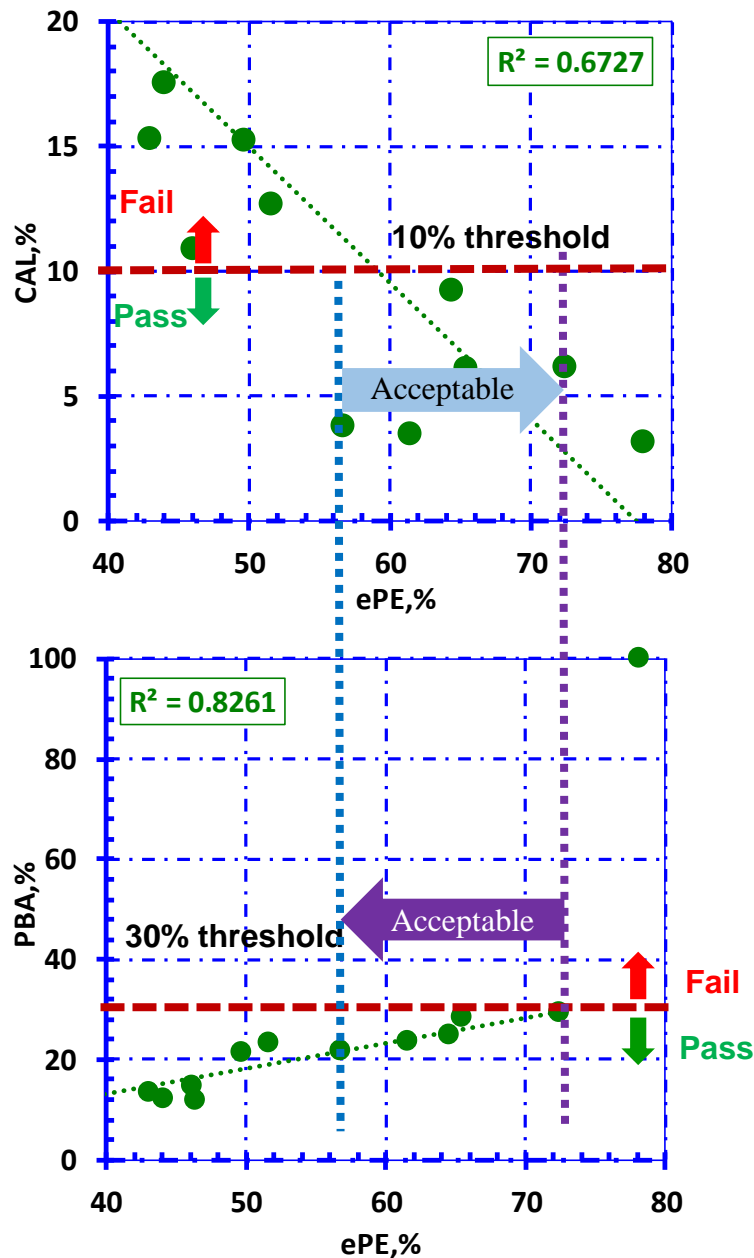


Figure 8.5 Illustration of determination of acceptable range of percent embedment

9. FINITE ELEMENT MODELLING OF CHIP SEALS

The objective of this part of the study was to evaluate the effect of percent embedment of aggregates and aggregate shape characteristics on the performance of chip seals through a two-dimensional (2-D) finite element (FE) analysis at multiple temperatures as well as the laboratory-based sweep test. Also, the effect of aggregate application rates on the performance of chip seals was investigated. Laboratory chip seal samples with cubical and flaky aggregates were prepared and subjected to sweep tests. Further, 2D finite element (FE) analysis was performed on FE meshes developed from actual chip seal specimens. Similar approach was taken to evaluate effect of aggregate application rates as well. To achieve this particular sub-objective, laboratory tests as well as FE analysis were conducted on chip seal samples with flaky aggregates (group II). It should be noted that, only hot-applied chip seals were included in this part of the study.

9.1 Chip Seals with a Single Aggregate

As described previously, 2D FE analyses were conducted on single cubical and flaky aggregates. This artificial scenario represents the worst-case scenario for chip seals where the positive effect of aggregate to aggregate interaction (i.e., interlocking) on the overall chip seal performance is not present. The FE analyses on chip seals with the cubical and flaky aggregate were performed at four different, artificially generated, aggregate embedment levels (25, 50, 72, and 94%) and three different temperatures (25, 30, and 35°C). The strain distributions around the binder-aggregate interface were plotted for each aggregate embedment and temperature combination for the chip seals with the cubical and flaky aggregates. Figure 9.1 shows the principal strain contours at 25°C around the binder-aggregate interface at a range of percent embedment levels for the cubical aggregate. As expected, the highest values of the tensile strains were observed

at the lowest percent embedment, 25%. As the percent embedment level increases, the magnitude of the tensile strains around the binder-aggregate interface decreases. Figure 9.2 depicts the magnitudes of the maximum tensile strain (ϵ_T^{max}) at a range of temperatures and percent embedments for the cubical aggregate. It is evident from Figure 9.2 that the maximum tensile strain doubles at every 5°C increments of temperature, regardless of the percent embedment levels. A close examination of Figure 9.2 reveals that the magnitude of the maximum tensile strain exhibits a relatively steady trend after the aggregate embedment level of 50%. Similar trend was also observed in another study (Boz et al. 2019). This trend is somewhat consistent with a general rule of thumb in chip seal practices that, for good aggregate retention, chip seal aggregates should be embedded into emulsion/binder by at least 50 %.

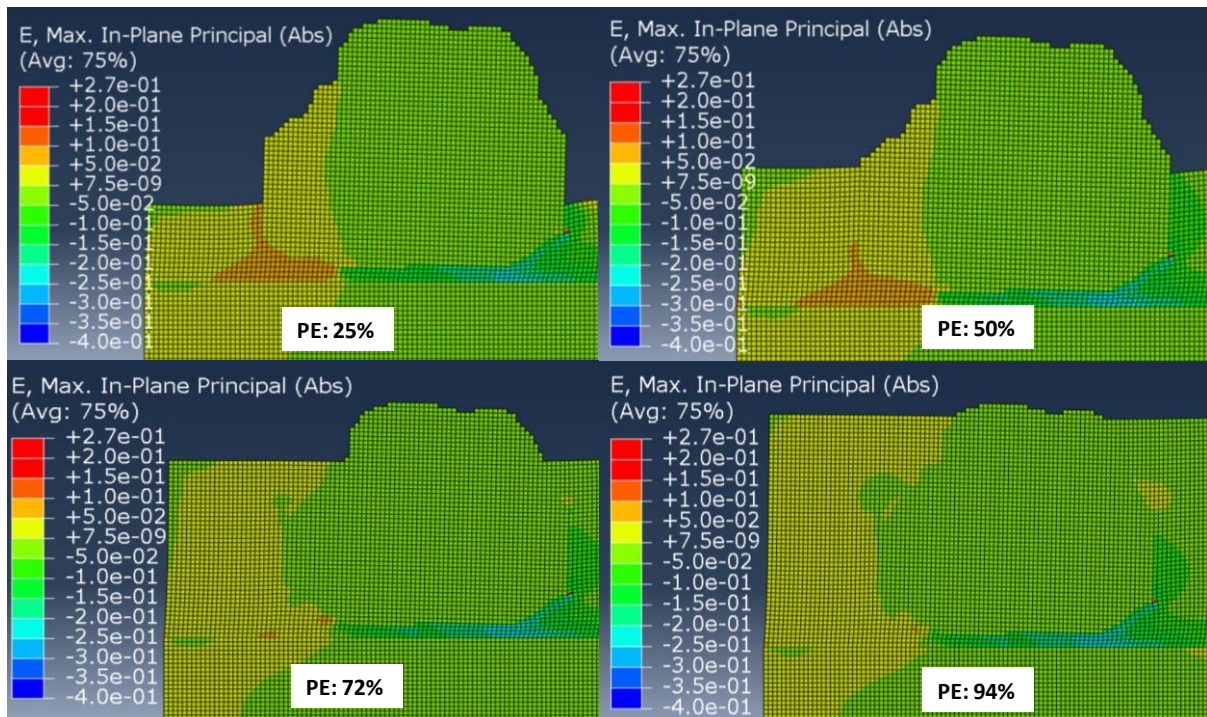


Figure 9.1 Tensile strain distributions at 25°C around the binder-aggregate interface at various percent embedment for the chip seal with the cubical aggregate

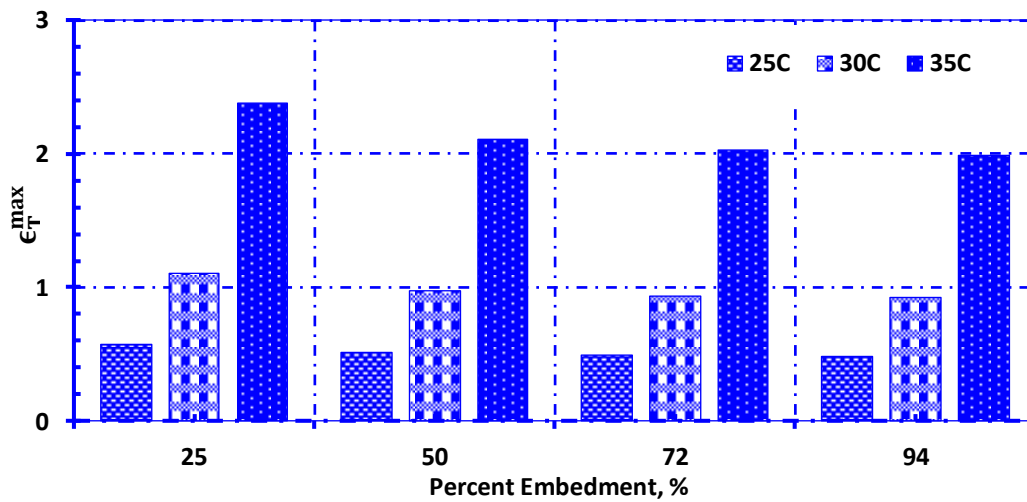


Figure 9.2 Maximum tensile strain (ϵ_T^{max}) at the binder-aggregate interface as a function of temperature and percent embedment for the chip seal with the cubical aggregate

The principal strain contours at 25°C around the binder-aggregate interface at a range of percent embedment levels for the flaky aggregate are plotted in Figure 9.3. The magnitudes of the maximum tensile strain (ϵ_T^{max}) for the flaky aggregate is shown in Figure 9.4. It can be observed that tensile strains at the binder-aggregate interface decrease (with increase in PE) at a higher rate in case of flaky aggregates as compared to the cubical aggregates.

Figure 9.5 shows the $\Delta\epsilon_T^{max}$ values for cubical and flaky aggregates at 25 °C. It is evident from Figure 9.5 that flaky aggregates are more susceptible to change in PE than the cubical aggregates. This is because greater $\Delta\epsilon_T^{max}$ values are observed in flaky aggregates as compared to that of cubical aggregates. Also, the change in $\Delta\epsilon_T^{max}$ values attain a steady state for PE values greater than 50%.

It is also worth noting that the critical strain levels shown in Figure 9.4 for flaky aggregate are significantly higher than those shown in Figure 9.2 for the cubical aggregate at all temperatures and percent embedment levels. The ratio of the maximum tensile strain of the chip seal with the flaky aggregate to the maximum tensile strain of the chip seal with the cubical aggregate ranges from 2 to 4, depending on the temperature and percent embedment level combination. This is expected since the flaky aggregate in Figure 9.3 is positioned about 45° from the horizontal, which is possibly the worst possible scenario for this type of aggregate, and the cubical aggregate, due to its shape, has a better stability and better bonding with the binder. As a result, the strain levels in the flaky aggregate are quite high as compared to those in the cubical aggregate. This indicates that, for flaky aggregates, if the aggregate application rate in the field is not enough, where some of the aggregates do not have adjacent aggregates to provide lateral support (i.e. interlocking), chip seal aggregates would be very susceptible to dislodging. Although such outcome is also most likely

the case for chip seals with cubical aggregates, the extent of such outcome would be more severe for chip seals with flaky aggregates.

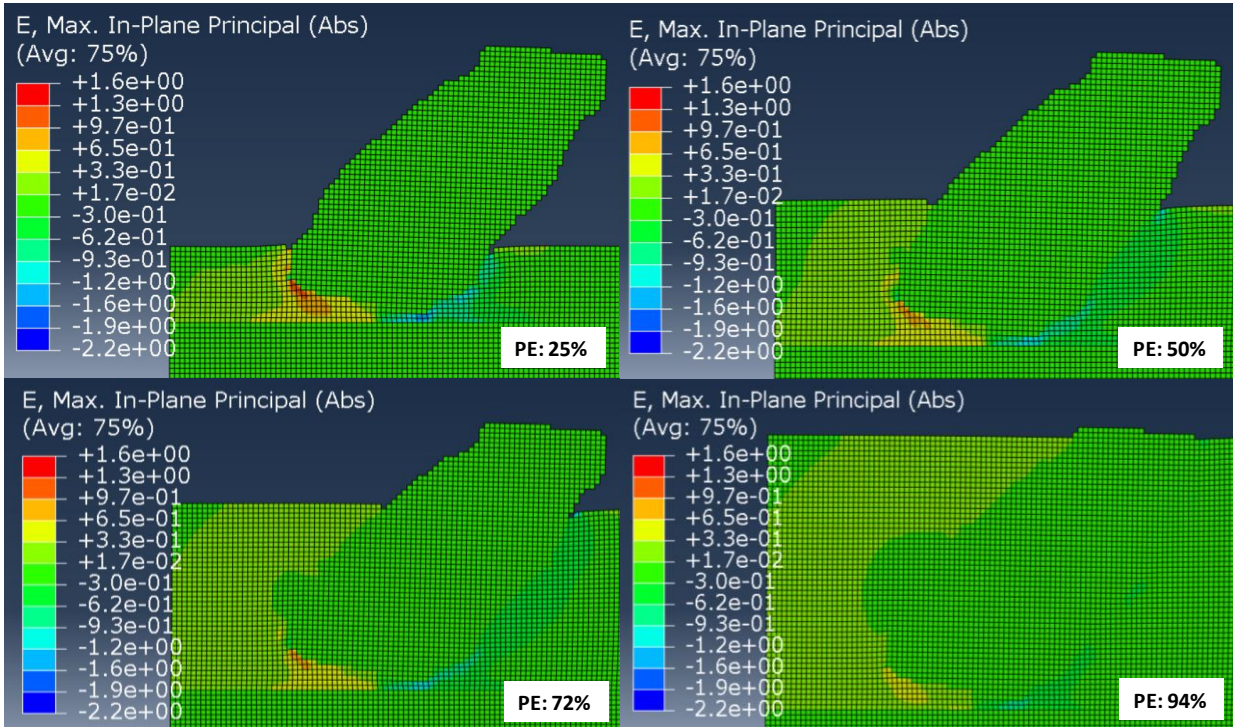


Figure 9.3 Tensile strain distributions at 25°C around the binder-aggregate interface at various percent embedment for the chip seal with the flaky aggregate

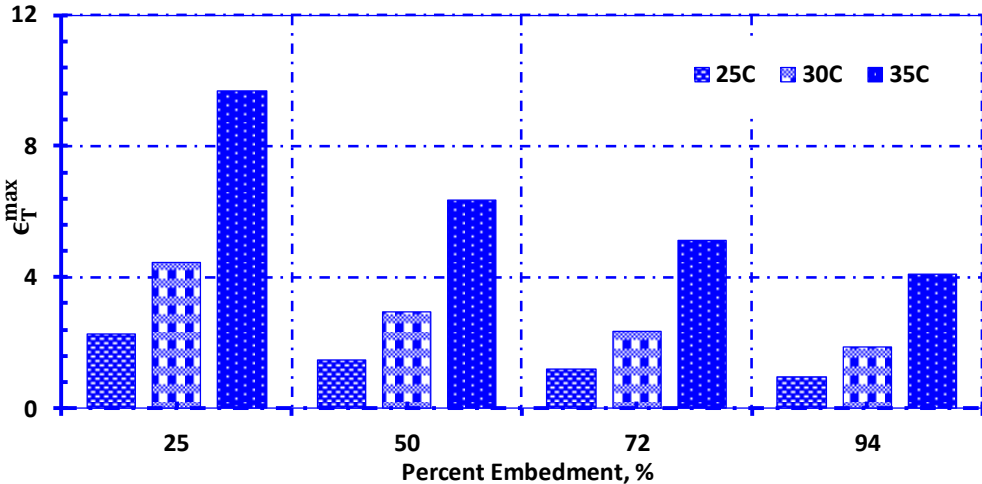


Figure 9.4 Maximum tensile strain (ϵ_T^{max}) at the binder-aggregate interface as a function of temperature and percent embedment for the chip seal with the flaky aggregate

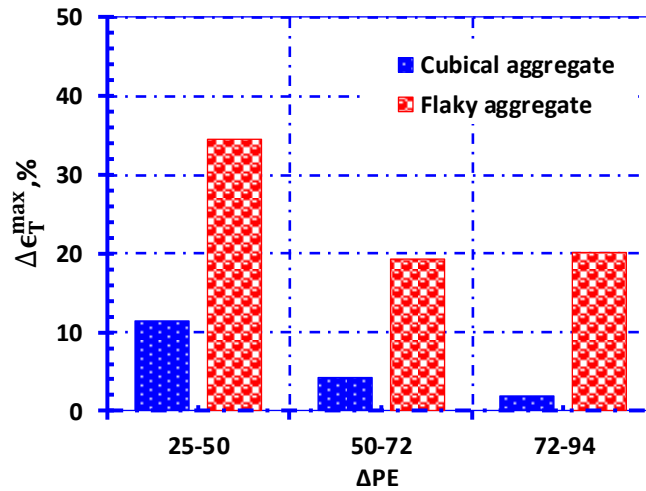


Figure 9.5 Percent Change in ϵ_T^{\max} with change in PE, for single aggregate at 25°C

9.2 Chip Seals with two Aggregates

In this phase, the effect of aggregate interlocking (i.e., bridging) on the critical strain levels of chip seals was studied. The 2D FE simulations for each aggregate type were repeated on chip seals with two aggregates standing side by side. The simulations were performed at a single temperature (25°C) in this part of the study. **Error! Reference source not found.** and Figure 9.7 illustrate the tensile strain contours at 25°C around the binder-aggregate interface at a range of percent embedment levels for the chip seal with two cubical and two flaky aggregates, respectively. It can be seen from these figures that the interlocking (i.e., bridging) effect in the chip seal with flaky aggregates is quite pronounced. Figure 9.8 shows the maximum tensile strain levels at the binder-aggregate interfaces for the chip seals with cubical and flaky aggregates, where the critical strain in the flaky aggregates are consistently lower than those of the cubical aggregates. This is complete opposite trend as compared to the results shown in Figure 9.2 and Figure 9.4, where the chip seal with the cubical aggregate exhibited lower strain levels. This essentially shows one of best possible scenarios, where a very good aggregate interlock results in a stronger chip seal sample, especially in the case of the flaky aggregates. Similar phenomenon has also been observed

in another experimental research study (Boz et al. 2018), where aggregate bridging has been attributed to be one of the main reasons for flaky aggregates showing better performance, apart from other possible reasons. In the field, some of the aggregates will be standing alone and some of them will be bridged. Therefore, the ranking of the performance of the flaky aggregates and cubical aggregates can be reversed, depending on the aggregate interlocking. This emphasizes the importance of microstructural configuration of compacted aggregates in chip seals.

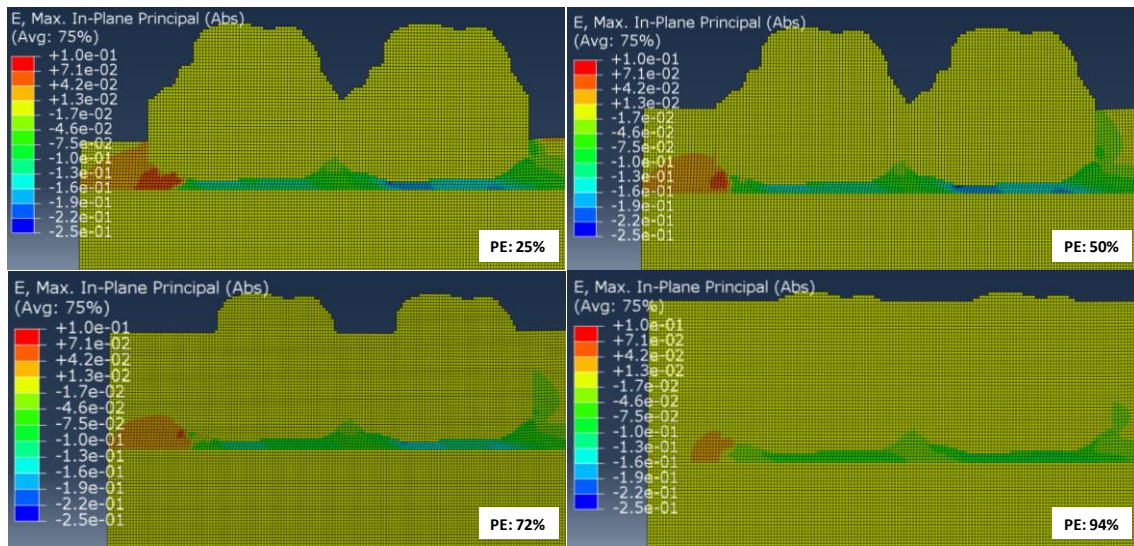


Figure 9.6 Tensile strain distributions at 25°C around the binder-aggregate interface at various percent embedment levels for the chip seal with two cubical aggregates

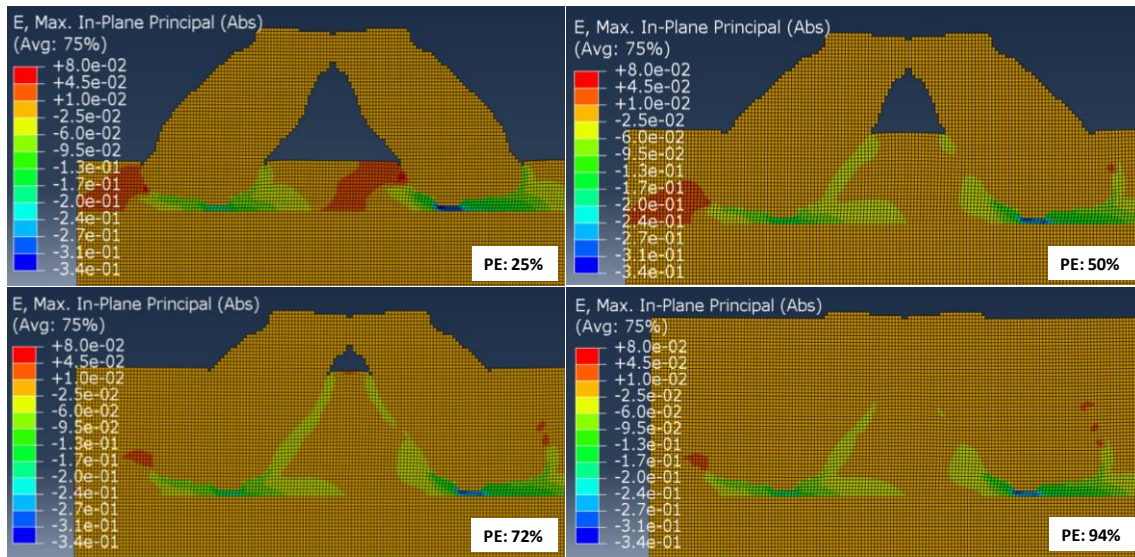


Figure 9.7 Tensile strain distributions at 25°C around the binder-aggregate interface at various percent embedment levels for the chip seal with two flaky aggregates

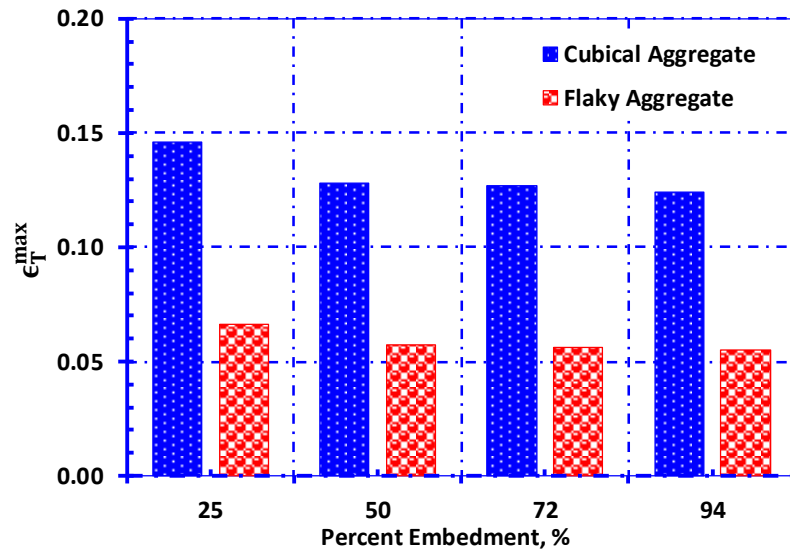


Figure 9.8 Maximum tensile strain (ϵ_T^{max}) at the binder-aggregate interface at 25°C as a function of percent embedment for the chip seals with two aggregates

9.3 *Chip Seals with Multiple Aggregates (Full Spectrum)*

9.3.1 Evaluation of Percent Embedment and Aggregate Shape Characteristics

In the first two phases of the study, artificial scenarios representing extreme cases for chip seals consisting of two distinct aggregate shape characteristics (cubical vs flaky) were analyzed. In this phase of the study, the effect of percent embedment and aggregate shape characteristics on the performance of chip seals were studied through the FE simulations on images obtained from the cross-sectional planes of chip seal specimens.

The tensile strain distributions at the binder-aggregate interface at 25°C at various percent embedment levels are shown in Figure 9.9 and Figure 9.10 for the chip seals with the cubical and flaky aggregates, respectively. The average maximum tensile strains (ϵ_T^{max}) at the binder-aggregate interface at 25°C as a function of percent embedment are plotted in Figure 9.11 for both chip seals. It is important to note that the error bars in Figure 9.11 represent one standard deviation around the average maximum tensile strain, as calculated from the interface of each aggregate in the chip seal cross section. Figure 9.11 indicates that the tensile strains decrease with an increase in the percent embedment levels for both chip seals, as expected. Additionally, the magnitude of the maximum tensile strain reaches a steady state for the chip seals with cubical aggregates after the aggregate embedment level of 50% is achieved, an observation consistent with the observation made on the chip seals scenarios with single and two aggregates. Also, the change in ϵ_T^{max} is more susceptible in the case of flaky aggregates than that of cubical aggregates. This observation is consistent in case of single aggregate as well as the full specimen FE analysis.

An important observation from Figure 9.11 is that the maximum tensile strains are significantly higher (about three times more in the magnitude) in the case of the chip seals with flaky aggregates compared to that of the chip seals with cubical aggregates. In comparison with

the previously exhibited worst-case (no interlock) and one of the best-case (excellent interlock, especially in the case of flaky aggregates) scenarios, it can be stated that the ranking of the actual full chip seal specimens is in alignment with the observations from the worst-case scenario. Also, it has to be noted that, different scenarios of interlocking arrangements were not included in this study. Different interlocking arrangements can lead to variations in the tensile strain results.

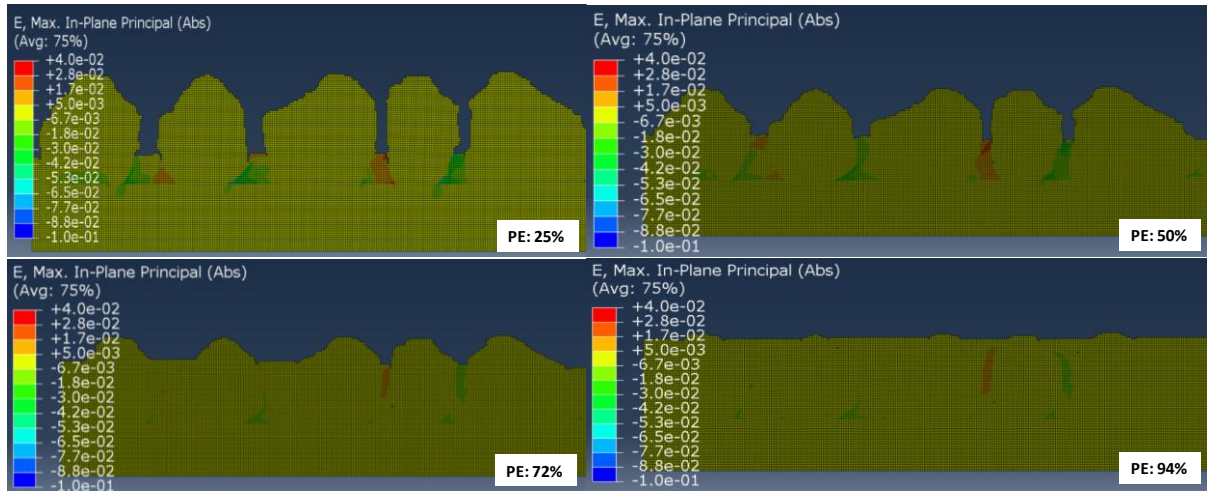


Figure 9.9 Tensile strain distributions at 25°C around the binder-aggregate interface at various percent embedment levels for the chip seal with multiple aggregates (cubical)

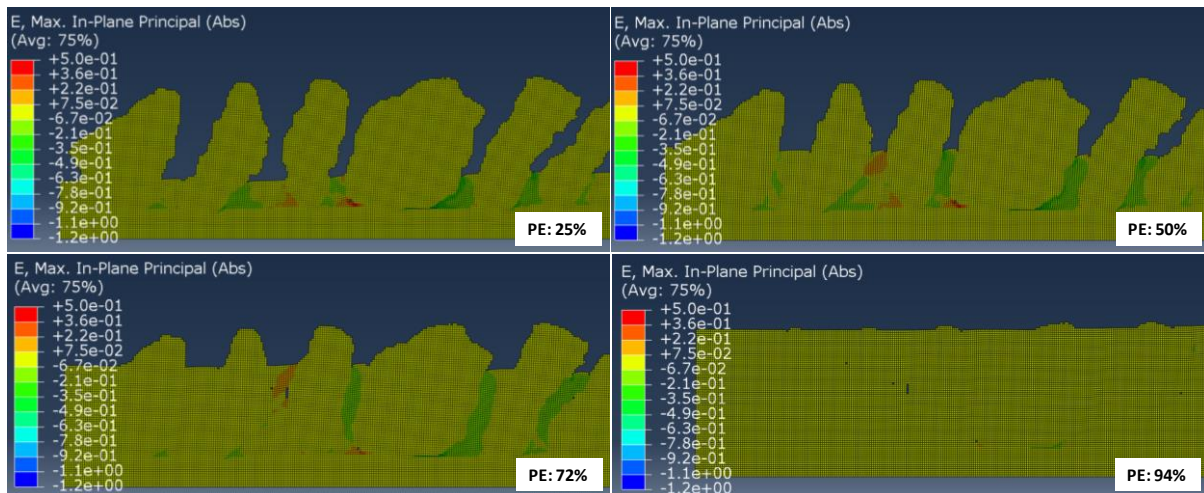


Figure 9.10 Tensile strain distributions at 25°C around the binder-aggregate interface at various percent embedment levels for the chip seal with multiple aggregates (flaky)

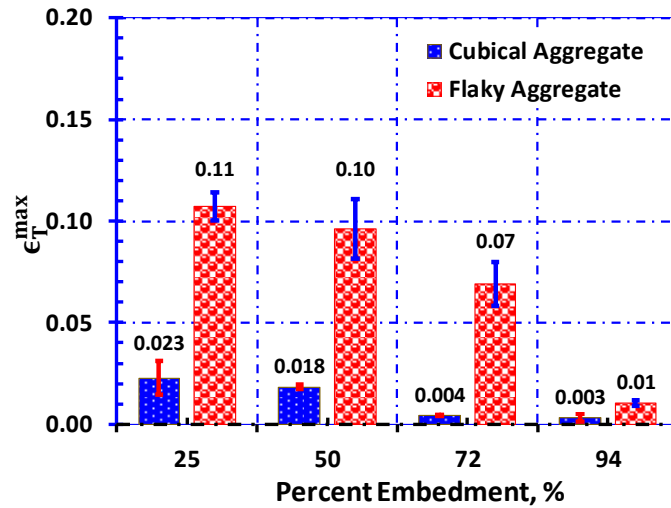


Figure 9.11 Maximum tensile strain (ϵ_I^{\max}) at the binder-aggregate interface at 25°C as a function of percent embedment for the chip seals with multiple aggregates

9.3.2 Evaluation of Aggregate Application Rate

One of the sub-objectives of this phase of study was to numerically evaluate the impact of aggregate application rates (AAR) on the performance of chip seals. The digital images of chip seals prepared at four different AAR (16, 18, 20, and 22 lb/yd² respectively) using flaky aggregates were obtained and processed for the FE analysis (see Figure 9.12).

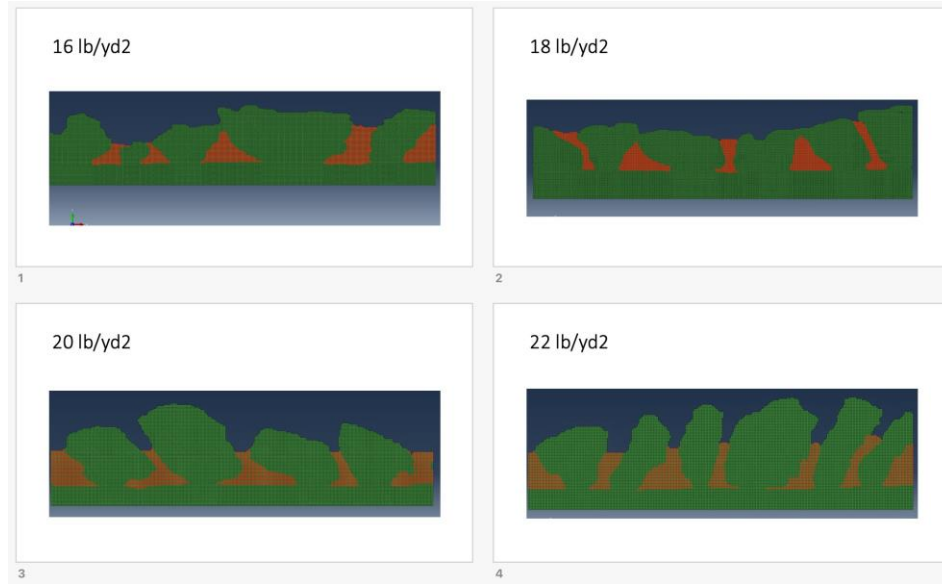


Figure 9.12 Snapshots of FEM meshes of chip seal samples prepared at several AARs.

The average maximum tensile strains (ϵ_T^{max}) for each AAR are depicted in Figure 9.13. As shown in the figure, the maximum tensile strain increases with an increase in AAR at all three temperatures, with an especially significant jump in ϵ_T^{max} as the AAR transitions from 18 to 20 lb/yd². In a previous study (Y. Kumbarger et al. 2018), it was reported that the optimum AAR for this aggregate was 18 lb/yd². Any increase in AAR greater than the optimum AAR would result in a trigger of the lever and wedge effect. Thus, as explained before, this would consequently lead to an increase in tensile strains at aggregate-binder interface. This fact is clearly supported by the data shown in Figure 9.13. The sudden increase at 30 and 35°C when the AAR transitioned from 18 to 20 lb/yd² is due to the confounding effects of temperature and the lever and wedge effect, where the binder becomes softer with an increase in temperature and, upon loading, the lever and wedge effect exacerbates the chip seals' ability to resist aggregate loss.

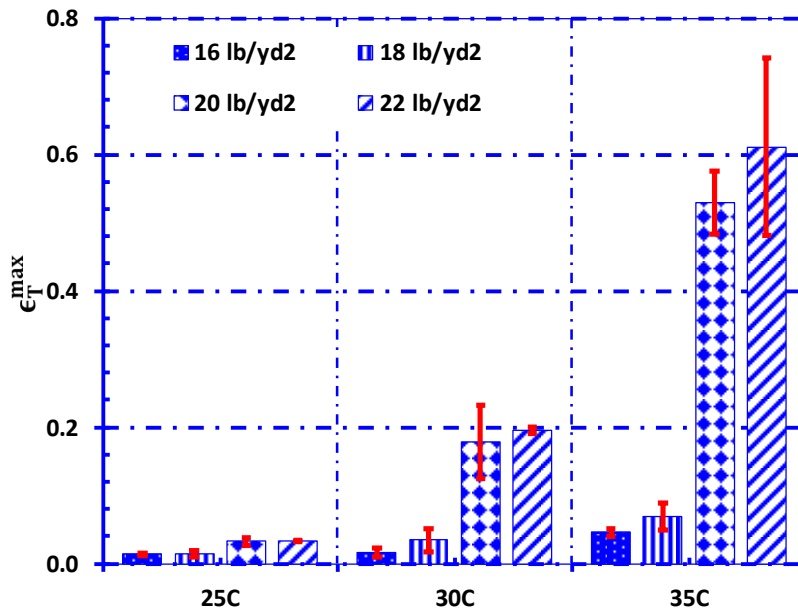


Figure 9.13 Maximum tensile strain (ϵ_T^{max}) at the binder-aggregate interface as a function of temperature for the chip seals with different aggregate application rates

In order to experimentally investigate effect of AAR on aggregate loss performance, sweep tests were carried out for the chip seal samples with flaky aggregates at 25, 30, and 35°C. The cumulative aggregate loss (CAL) results have been depicted in Figure 9.14. The figure indicates that the CAL increases with an increase in AAR. Further, CAL values for AAR of 22 lb/yd² are much higher than the CALs of the other AARs. This further supports the observation that adding too much aggregates is detrimental to chip seal performance. Furthermore, CAL generally increases with an increase in temperature, although the percentage change of CAL with temperature is lower than that of the trend in FE simulation results.

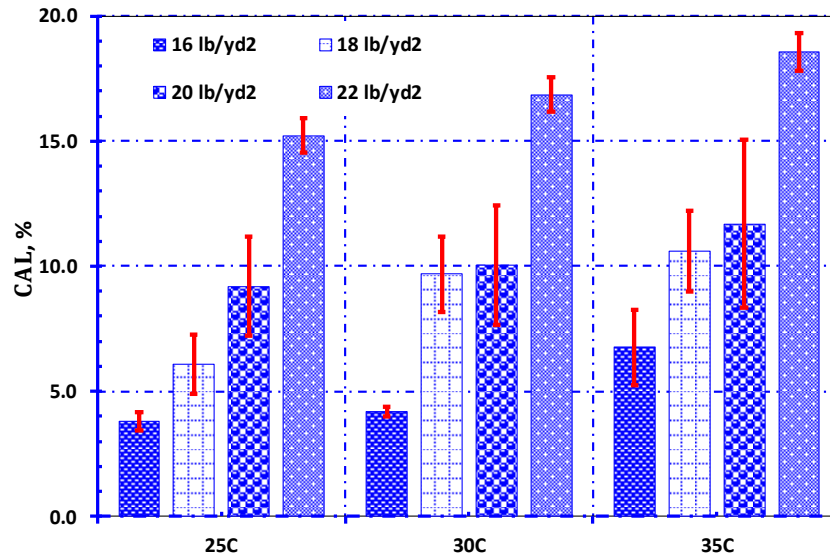


Figure 9.14 Cumulative Aggregate loss from the sweep test at a range of temperatures for the chip seals with cubical and flaky aggregates.

It must be noted that the comparison between the tests results from the FE analyses and the sweep test was done based on general trends observed in the two sets of data. This is due to the fact that the aggregate loss from the sweep test is a result of the nylon brush abrading on the entire chip seal specimens, where the interaction of multiple aggregates in all directions (3D) plays a key role in aggregate loss behavior. On the other hand, the FE analyses were performed on an aggregate-binder structure obtained from the 2D images of an actual truck traffic loading was simulated. The induced strains due to abrasive forces from the nylon brush in the sweep test were not as high as those in the FE analyses. Nevertheless, FE simulations as well as sweep test results show that it is extremely important not to add more aggregates than the optimum. This will ensure good performance of chip seals as well as lower the material costs associated with aggregates.

9.4 Summary of chapter findings

The part of the study presented in this chapter focused on investigation of the effect of percent embedment and aggregate shape characteristics on chip seal performance via a two-

dimensional (2D) viscoelastic finite element model simulations performed at multiple temperatures. The scope also included laboratory sweep tests. Additionally, the effect of the aggregate application rate on the performance of chip seals was also investigated. The simulations were performed on actual aggregate images processed from laboratory-produced chip seal specimens. The main findings can be summarized as follows:

- The results indicated that the level of change in maximum tensile strains at the binder-aggregate interfaces depends on the aggregate shape and interlocking. Both the FE simulations and sweep test results revealed that chip seals with cubical aggregates provide better aggregate retention characteristics; however, there might be cases in which chip seals with flaky aggregates might form a good interlock structure and perform better than the cubical aggregates.
- Furthermore, chip seals with cubical aggregates exhibit more stable aggregate retention characteristics (steady-state maximum tensile strain) for the aggregate embedment levels higher than 50%. However, such a trend is not necessarily observed for chip seals with flaky aggregates due to the lever and wedge effect. Flaky aggregates are more susceptible to change in percent embedment than that of cubical aggregates. This probably means that the performance of a chip seal with a flaky aggregate can be quite variable, depending on the percent embedment distribution.
- Excess aggregate application rate is detrimental to chip seal performance as it leads to increase in tensile strains at the aggregate-binder interface. This was especially true for the chip seals with flaky aggregates, primarily due to increased confounding impacts of temperature and lever and wedge effect. Hence, it is crucial not to add excessive aggregates

than the optimal amount. Therefore, careful design of chip seals to find the optimal application rates is important.

10. CONCLUSIONS

The primary objective of this study was to investigate factors responsible for chip seal performance and development of performance-based methods and related guidelines with a focus on fundamental parameters to achieve efficiently performing chip seal pavements. Two types of binders (hot applied and emulsion) and two types of aggregates (cubical and flaky) were used in this study. Chip seal samples with various binder, emulsion and aggregate application rates were prepared and tested for aggregate loss and bleeding performance. Image analysis was also performed on these chip seal samples to investigate the effects of aggregate-binder interaction and microstructural parameters (such as aggregate orientation) on performance. Furthermore, an innovative image based finite element analysis approach was used to evaluate chip seal performance. The findings of this study can be summarized as follows:

- New image analysis-based parameters for quantifying chip seal microstructure were developed. These included Cumulative Percentage of Aggregates lying on Flattest side (CPAF) and effective percent embedment (ePE).
- In terms of aggregate loss, it was observed that the cumulative aggregate loss (CAL) from the sweep test is a reasonable criterion to evaluate chip seal performance. Also, the ePE correlated very well with the cumulative aggregate loss.
- Evaluation of Percent Binder Area (PBA) during/after HWT tests was found to be effective in characterizing the bleeding behavior of chip seals. PBA generally increased with increase in binder application rates (BAR) (in hot-applied chip seal) and emulsion application rates (EAR) (in emulsion-based chip seal). The bleeding behavior during a HWT test was found to be analogous to the rutting behavior of asphalt mixtures,

specifically the concept of ‘flow number’ in repeated load permanent deformation (RLPD) tests. Similar to the change in plastic strain in asphalt mixture during a RLPD test, there is a steady increase in PBA as the HWT cycles increase. At high binder application rates, a rapid increase in PBA is observed after certain number of HWT cycles, similar to the tertiary flow in flow number tests.

- Effective percent embedment (ePE) showed excellent correlation with PBA, therefore ePE can be effectively used to characterize bleeding behavior of chip seals.
- Based on comprehensive evaluation of hot applied and emulsion-based chips seals, performance-based percent embedment limits were established for chip seals. The acceptable range of ePE was concluded to be between 57% and 70%.
- A critical evaluation of the orientation distribution of the aggregates (i.e. CPAF) revealed that low amounts of binder application rates or excessive amounts of aggregate application rates can cause the aggregates to disorient from their flattest sides. This was especially true when excessive aggregate application rate leads to multiple layers of aggregates, which leads to the lever and wedge effect. Good correlation was observed between CPAF and aggregate loss and bleeding results.
- In terms of bleeding performance, emulsion-based chip seals outperformed hot-applied chip seals, by anywhere between 10 and 20%.
- A unique low-cost method (using smart phones) to evaluate chip seal 3D macrotecture was developed. Mean profile depths (MPD) at the end of various HWT cycles were computed. Results showed that there is a significant change in macrotecture with bleeding. If excessive amount of aggregates is used, then although change in PBA is negligible but a significant change in MPD (i.e. 3D macrotecture) is observed. This essentially creates a

rut pattern in the wheel path. The change in MPD being high, it can potentially lead to hydroplaning and loss of friction. Furthermore, localized rut patterns will lead to difficulty in maneuvering and potential safety hazard.

- A performance-based design methodology was developed as part of this research study. The methodology based on major performance parameters (aggregate loss and bleeding) and ensures that aggregates are oriented on their flattest side during the design and laboratory testing stage. The comparative analysis with respect to the existing methodologies showed the rationality of the developed design methodology.
- A unique mechanistic approach to analyze chip seals was developed in this study. The actual 2D images of chip seals were subjected to image processing and were converted to FE meshes for further analysis. For efficient chip seal performance, the bond between aggregate and binder is extremely important. In order to capture this aspect mechanistically, maximum tensile strains at aggregate-binder interface was evaluated. Furthermore, this approach was used to characterize effect of aggregate types and aggregate application rates on chip seal performance.
- Results from FE analysis indicated that the extent of change in maximum tensile strains at the binder-aggregate interfaces depends on the aggregate shape and interlocking. Both the FE simulations and sweep test results revealed that chip seals with cubical aggregates provide better aggregate retention characteristics; however, there might be cases in which chip seals with flaky aggregates might form a good interlock structure and perform better than the cubical aggregates.
- Furthermore, chip seals with cubical aggregates exhibit more stable aggregate retention characteristics (steady-state maximum tensile strain) for the aggregate embedment levels

higher than 50%. However, such a trend is not necessarily observed for chip seals with flaky aggregates due to the lever and wedge effect. Flaky aggregates are more susceptible to change in percent embedment than that of cubical aggregates. This probably means that the performance of a chip seal with a flaky aggregate can be quite variable, depending on the percent embedment distribution.

- Excess aggregate application rate is detrimental to chip seal performance as it leads to increase in tensile strains at the aggregate-binder interface. This was especially true for the chip seals with flaky aggregates, primarily due to increased confounding impacts of temperature and lever and wedge effect. Hence, it is crucial not to add excessive aggregates than the optimal amount. Therefore, rigorous design of chip seals to find the optimal application rates is important.

REFERENCES

AASHTO-PP82, 2016. Standard Practice for Emulsified Asphalt Chip Seal Design. , 3(August 2016), pp.16–19.

AASHTO:T59, 2016. Standard Method of Test for emulsified asphalts. , 96.

Abedini, M. et al., 2017. Low-temperature adhesion performance of polymer-modified Bitumen emulsion in chip seals using different SBR latexes. *Petroleum Science and Technology*, 35(1), pp.59–65. Available at: <https://www.tandfonline.com/doi/full/10.1080/10916466.2016.1238932>.

Adams, J.M. & Kim, Y.R., 2014. Mean profile depth analysis of field and laboratory traffic-loaded chip seal surface treatments. *International Journal of Pavement Engineering*, 15(7), pp.645–656. Available at: <http://dx.doi.org/10.1080/10298436.2013.851790>.

Adams, J.M. & Kim, Y.R., 2014. Mean profile depth analysis of field and laboratory traffic-loaded chip seal surface treatments. *International Journal of Pavement Engineering*, 15(7), pp.645–656. Available at: <http://dx.doi.org/10.1080/10298436.2013.851790>.

Aktaş, B. et al., 2013. Effect of aggregate surface properties on chip seal retention performance. *Construction and Building Materials*, 44, pp.639–644.

ASTM-C29, 2009. Standard Test Method for Bulk Density (“ Unit Weight ”) and Voids in Aggregate. *ASTM International*, i(c), pp.1–5.

ASTM-D6372, 2005. Standard Practice for Design , Testing , and Construction of Micro-Surfacing 1. , i, pp.1–7.

ASTM-D7000, 2011. Standard Test Method for Sweep Test of Bituminous Emulsion Surface Treatment Samples. *Astm D7000*, 11(C), pp.1–4. Available at: <http://www.astm.org/Standards/D7000.htm>.

ASTM-E965, 2015. Standard Test Method for Measuring Pavement Macrotexture Depth Using a. *ASTM International*, i, pp.1–4.

ASTM D4541, 2009. Standard Test Method for Pull-Off Strength of Coatings Using Portable Adhesion. *ASTM International*, (April), p.16 p.

Austroroads, 2018. *Austroroads Selection and design of sprayed seals*,

Bhattacharjee, S. et al., 2004. Use of MMLS3 scaled accelerated loading for fatigue characterization of Hot Mix Asphalt (HMA) in the laboratory. *2nd International Conference on Accelerated Pavement Testing*, (September 2004). Available at: http://www.mrr.dot.state.mn.us/research/MnROAD%7B_%7DProject/index%7B_%7Dfiles/pdfs/Bhattacharjee%7B_%7DS.pdf.

Bitelli, G. et al., 2012. Laser scanning on road pavements: A new approach for characterizing

- surface texture. *Sensors (Switzerland)*, 12(7), pp.9110–9128.
- Boz, I. et al., 2018. *Establishing Percent Embedment Limits to Improve Chip Seal Performance*, Available at: https://www.michigan.gov/documents/mdot/SPR-1679_635048_7.pdf.
- Boz, I., Kumbarger, Y.S. & Kutay, M.E., 2019. Performance-Based Percent Embedment Limits for Chip Seals. *Transportation Research Record: Journal of the Transportation Research Board*, p.36119811882137. Available at: <http://journals.sagepub.com/doi/10.1177/0361198118821370>.
- Buttlar, W.G. et al., 2014. Digital image correlation techniques to investigate strain fields and cracking phenomena in asphalt materials. *Materials and Structures*, (47), pp.1373–1390.
- Caltrans, 2003. *Caltrans maintenance Advisory Guide*,
- Čelko, J., Kováč, M. & Kotek, P., 2016. Analysis of the Pavement Surface Texture by 3D Scanner. *Transportation Research Procedia*, 14, pp.2994–3003.
- Chaturabong, P., Hanz, A.J. & Bahia, H.U., 2015. Development of Loaded Wheel Test for Evaluating Bleeding in Chip Seals. *Transportation Research Record: Journal of the Transportation Research Board*, pp.48–55.
- Ejsmont, J.A. et al., 2017. Road texture influence on tyre rolling resistance. *Road Materials and Pavement Design*, 18(1), pp.181–198.
- Epps-Martin, A., Glover, C.J. & Barcena, R., 2001. *A performance-graded binder specification for surface treatments*,
- Epps, J.A. & Gallaway, B.M., 1972. Synthetic Aggregate Seal Coats- Current Texas Highway Department Practices. *Research report 83-1, Texas Highway Department*, (May).
- Epps, J., Chaffin, C.W. & Hill, A.J., 1980. *FIELD EVALUATION OF A SEAL COAT DESIGN METHOD*,
- Epps, J., Chaffin, C.W. & Hill, A.J., 1980. *FIELD EVALUATION OF A SEAL COAT DESIGN METHOD*,
- Escalada, L.T., 1995. an Investigation on the Effects of flaky particles on the properties of asphaltic mixtures. *Analyzer*, 4791(October 2014), pp.865–871.
- Flintsch, G. et al., 2003. Pavement Surface Macrotexture Measurement and Application. *Transportation Research Board 2003 Annual meeting*, 34(540), p.107.
- Gerber, J. & Jenkins, K., 2017. Finite element modelling and damage quantification of chip seals. *Road Materials and Pavement Design*, 18(2), pp.350–361. Available at: <https://doi.org/10.1080/14680629.2016.1213512>.

- Gransberg, D. & James, D.M.B., 2005. *Chip seal best practices*,
- Gransberg, D.D., 2005. Chip Seal Program Excellence in the United States. *Transportation Research Record: Journal of the Transportation Research Board*, 1933(1933), pp.72–82.
- Gransberg, D.D. & James, D.M., 2005. *Chip seal best practices*,
- Gransberg, D.D. & Zaman, M., 2005a. Analysis of emulsion and hot asphalt cement chip seal performance. *Journal of Transportation Engineering-Asce*, 131(3), pp.229–238.
- Gransberg, D.D. & Zaman, M., 2005b. Analysis of emulsion and hot asphalt cement chip seal performance. *Journal of Transportation Engineering-Asce*, 131(3), pp.229–238.
- Guirguis, M. & Buss, A., 2017. Performance Evaluation of Emulsion and Hot Asphalt Cement Chip Seal Pavements. *Journal of Materials in Civil Engineering*, 29(11)(11), pp.1–10. Available at: <https://ascelibrary-org.ezproxy.lib.vt.edu/doi/pdf/10.1061/%28ASCE%29MT.1943-5533.0002057>.
- Haider, S.W. et al., 2019. Development of performance related specifications for chip seal treatments. *International Journal of Pavement Engineering (in press)*.
- Hanson, F., 1934. *Bituminous surface treatment of rural highways*,
- Hanson, F.M., 1934. BITUMINOUS SURFACE TREATMENT OF RURAL HIGHWAYS. Available at: <http://trid.trb.org/view.aspx?id=97948>.
- Henry, J., 2000. *Evaluation of pavement friction characteristics, NCHRP Synthesis 291*,
- Herrington, P.R. & Henderson, R., 2004. Bitumen Film Thicknesses and Confinement Ratios in Chip Seal Surfacing. *Road Materials and Pavement Design*, 5(2), pp.251–264. Available at: <http://www.tandfonline.com/doi/abs/10.1080/14680629.2004.9689972>.
- Howard, I.L. et al., 2009. Chip and Scrub Seal Binder Evaluation by Frosted Marble Aggregate Retention Tes. *Transportation Research Board 88th Annual Meeting*.
- Howard, I.L. et al., 2017. Material selection and traffic opening guidance for chip or scrub seals. *Road Materials and Pavement Design*, 0(0), pp.1–23. Available at: <https://www.tandfonline.com/doi/full/10.1080/14680629.2017.1340327>.
- Huurman, M. et al., 2003. Development of a Structural FEM for Road Surfacing Seals.
- Huurman, M., 2010. Developments in 3D surfacing seals FE modelling. *International Journal of Pavement Engineering*, 11(1), pp.1–12. Available at: <http://www.tandfonline.com/doi/abs/10.1080/10298430600949852>.
- IDOT-guide, 2017. The Idaho Transportation Department ' s Chip Seal Coat Warranty Guide. ,

(January).

- Johannes, P.T., Mahmoud, E. & Bahia, H., 2011. Sensitivity of ASTM D7000 Sweep Test to Emulsion Application Rate and Aggregate Gradation. *Transportation Research Record: Journal of the Transportation Research Board*, 2235, pp.95–102. Available at: <http://trrjournalonline.trb.org/doi/10.3141/2235-11>.
- Jordan, W.S. & Howard, I.L., 2010. Applicability of Modified Vialit Adhesion Test for Seal Treatment Specifications. *Transportation Research Board 89th Annual Meeting*.
- Kandhal, P.S. & Motter, J.B., 1991. Criteria for Accepting Precoated Aggregates for Seal Coats and Surface Treatments. *Transportation Research Record Journal of the Transportation Research Board Transportation Research Board of the National Academies*, (January), pp.80–89. Available at: <https://www.google.com.my/url?sa=t&rct=j&q=&esrc=s&source=web&cd=164&cad=rja&uact=8&ved=0CCsQFjADOKAB&url=http://www.ncat.us/files/reports/1991/rep91-02.pdf&ei=AZ7JVKmlN6LQmwXu5YLwAQ&usg=AFQjCNHhU8mQ1wFcNKpVkul7uH4eYZkLvA&sig2=6XsZUySRZqAJAJolwoOoPQ&bvm=b>.
- Kathirgamanathan, P. & Herrington, P.R., 2014. Numerical modelling of road with chip seal surfacing layer. , (Juice), pp.370–376.
- Kearby, J., 1953. Tests and theories on penetration surfaces. In *Highway research board*.
- Kim, H. et al., 2013. Measurement of Texture Depth of Pavement Using Potable Laser Profiler. *Journal of the Eastern Asia Society for Transportation Studies*, 10, pp.1576–1589.
- Kim, Y.R. et al., 2012. Development of a New Chip Seal Mix Design Method. *Final Report for HWY-2008-04. FHWA, North Carolina Department of Transportation*, (FHWA/NC/2008-04), p.104.
- Kim, Y.R. et al., 2017a. *Performance-Related Specifications for Emulsified Asphaltic Binders Used in Preservation Surface Treatments*, Available at: <https://www.nap.edu/catalog/24694>.
- Kim, Y.R. et al., 2017b. *Performance-Related Specifications for Emulsified Asphaltic Binders Used in Preservation Surface Treatments*, National Academies Press. Available at: <https://www.nap.edu/catalog/24694>.
- Kumbarger, Y., Boz, I. & Kutay, M.E., 2018. Quantifying the effect of binder/aggregate application rates on chip seal characteristics via digital image processing and sweep tests. *Transportation Research Board 2018 Annual Meeting*.
- Kumbarger, Y.S., Boz, I. & Kutay, M.E., 2018. Performance based design procedure for chip seal projects. *International Conference on Advances in Materials and Pavement Performance Prediction, Qatar*.

- Kumbarger, Y.S., Kutay, M.E. & Boz, I., 2018. Effect of percent embedment on chip seal performance using FE modeling. *International Conference on Advances in Materials and Pavement Performance Prediction, Qatar*, (April).
- Kutay, M.E. et al., 2017. *Development of an Acceptance Test for Chip Seal Projects, Michigan Department of Transportation, report no. SPR 1649*, Available at: http://www.michigan.gov/documents/mdot/SPR1649_554816_7.pdf.
- Lee, J. et al., 2013. Calibration of Seal Coat Application Rate Design. *Journal of Testing and Evaluation*, 41(2), p.20120021. Available at: <http://www.astm.org/doiLink.cgi?JTE20120021>.
- Lee, J. & Kim, R.Y., 2012. Evaluation of polymer-modified chip seals at low temperatures. *International Journal of Pavement Engineering*, 15(3), pp.1–10.
- Lee, J. & Kim, Y., 2008a. Understanding the Effects of Aggregate and Emulsion Application Rates on Performance of Asphalt Surface Treatments. *Transportation Research Record: Journal of the Transportation Research Board*, 2044, pp.71–78. Available at: <http://trrjournalonline.trb.org/doi/10.3141/2044-08>.
- Lee, J. & Kim, Y., 2008b. Understanding the Effects of Aggregate and Emulsion Application Rates on Performance of Asphalt Surface Treatments. *Transportation Research Record: Journal of the Transportation Research Board*, 2044, pp.71–78.
- Lee, J., Kim, Y.R. & McGraw, E.O., 2006. Performance Evaluation of Bituminous Surface Treatment Using Third-Scale Model Mobile Loading Simulator. *Transportation Research Record Journal of the Transportation Research Board Transportation Research Board of the National Academies*, 1958, pp.59–70.
- Lee, S., 2003. *Long-term performance assessment of asphalt concrete pavements using the third scale model mobile loading simulator and fiber reinforced asphalt concrete*. North Carolina State University. Available at: <http://repository.lib.ncsu.edu/ir/handle/1840.16/3887>.
- Louw, K., Rossman, D. & Cupido, D., 2004. The Vialit Adhesion Test: Is It An Appropriate Test To Predict Low Temperature Binder/Aggregate Failure? *8th Conference on Asphalt Pavements for Southern Africa (CAPSA'04)*, 12(September 2004).
- Mcleod, N. et al., 1969. A general method of design for seal coats and surface treatments. In *Association of Asphalt Paving Technologists*.
- Mcleod, N., 1969. A General Method of Design for Seal Coats and Surface Treatments. *Proceedings of the Association of Asphalt Paving Technologists*, 38.
- MDOT-warrantyguidelines, 2017. *Guidelines for administering Warranties on road and bridge construction contracts*,

- Meegoda, J.N. & Gao, S., 2015. Evaluation of pavement skid resistance using high speed texture measurement. *Journal of Traffic and Transportation Engineering (English Edition)*, 2(6), pp.382–390. Available at: <http://dx.doi.org/10.1016/j.jtte.2015.09.001>.
- Miller, T., Arega, Z. & Bahia, H., 2010. Correlating Rheological and Bond Properties of Emulsions to Aggregate Retention of Chip Seals. *Transportation Research Record: Journal of the Transportation Research Board*, 2179, pp.66–74. Available at: <http://trrjournalonline.trb.org/doi/10.3141/2179-08>.
- NCDOT-manual, 2016. NCDOT Chip Seal Best Practices manual. *North Carolina Department of Transportation*, (June).
- Noyce, D.A. et al., 2005. INCORPORATING ROAD SAFETY INTO PAVEMENT MANAGEMENT : MAXIMIZING ASPHALT PAVEMENT SURFACE FRICTION FOR ROAD SAFETY IMPROVEMENTS DRAFT Literature Review & State Surveys. *Midwest Regional University Transportation Center*, p.110.
- Ozdemir, U. an et al., 2018. Quantification of aggregate embedment in chip seals using image processing. *Journal of Transportation Engineering-Part B: Pavements*, 144(4). Available at: <https://doi.org/10.1061/JPEODX.0000068>.
- Pierce, L.M. & Kebede, N., 2015. Chip Seal Performance Measures — Best Practices Chip Seal. , (March).
- Potter, J.E. & Church, M., 1969. The Design of Sprayed Single Seals. *Proceedings of the Association of Asphalt Paving Technologists*, 38, pp.537–630.
- Praticò, F.G. & Vaiana, R., 2015. A study on the relationship between mean texture depth and mean profile depth of asphalt pavements. *Construction and Building Materials*, 101, pp.72–79.
- Praticò, F.G., Vaiana, R. & Iuele, T., 2013. Acoustic absorption and surface texture : an experimental investigation. , (September), pp.1–9.
- Praticò, F.G., Vaiana, R. & Iuele, T., 2016. Surface Performance Characterization of Single-Layer Surface Dressing: A Macrotecture Prediction Model. In *8th RILEM International Symposium on Testing and Characterization of Sustainable and Innovative Bituminous Materials*. pp. 459–470.
- Puzzo, L. et al., 2017. Three-dimensional survey method of pavement texture using photographic equipment. *Measurement: Journal of the International Measurement Confederation*, 111(July), pp.146–157.
- Ran, M. et al., 2015. Measurement method of asphalt pavement mean texture depth based on multi-line laser and binocular vision. *International Journal of Pavement Engineering*, 18(5), pp.459–471. Available at: <http://dx.doi.org/10.1080/10298436.2015.1095898>.

- Rizzutto, S.J. et al., 2015. Use of a Variable Rate Spray Bar to Minimize Wheel Path Bleeding for Asphalt-Rubber Chip Seal Applications. *Journal of Materials in Civil Engineering*, 27(3), pp.1–8.
- Roberts, C. & Nicholls, J.C., 2008. *Design Guide for Road Surface Dressing*,
- Sakhaeifar, M. et al., 2018. Tyre–pavement interaction noise levels related to pavement surface characteristics. *Road Materials and Pavement Design*, 19(5), pp.1044–1056. Available at: <https://doi.org/10.1080/14680629.2017.1287770>.
- Seitllari, A. & Kutay, M.E., 2018. Soft Computing Tools to Predict Progression of Percent Embedment of Aggregates in Chip Seals. *Transportation Research Record, Journal of Transportation Research Board*, in press.
- Senadheera, S., Gransberg, D.D. & Kologlu, T., 2000. *Statewide Seal Coat Constructability Review*,
- Sendheera, S. et al., 2006. *A testing and evaluation protocol to assess seal coat binder-aggregate compatibility*,
- Serigos, P.A., Prozzi, J.A. & Street, G., 2017. Performance of Preventive Maintenance Treatments for Flexible Pavements in Texas. *Final report, Texas Department of Transportation*.
- Shuler, S. et al., 2011. *Manual for Emulsion-Based Chip Seals for Pavement Preservation*, Available at: <http://www.nap.edu/catalog/14421>.
- South-african-national-road-agency-report, 2007. Technical Recommendations for Highways.
- Texas Department of Transportation, 2010. Seal Coat and Surface Treatment Manual. , (July).
- TNZ, 1981. Standard Test Procedure for Measurement of Texture By the Sand Circle Method. , pp.4–5.
- TNZ-report, 2005. *Chipsealing in New Zealand*, Available at: <https://www.nzta.govt.nz/resources/chipsealing-new-zealand-manual/chipsealing-in-new-zealand/>.
- Tutumluer, E., Pan, T. & Carpenter, S.H., 2005. *Investigation of aggregate shape effects on hot mix performance using an image analysis approach, Federal highway Administration report*,
- Wang, W. et al., 2011. Design and verification of a laser based device for pavement macrotexture measurement. *Transportation Research Part C: Emerging Technologies*, 19(4), pp.682–694. Available at: <http://dx.doi.org/10.1016/j.trc.2010.12.001>.
- Wasiuddin, N.M. et al., 2013. Use of Sweep Test for Emulsion and Hot Asphalt Chip Seals: Laboratory and Field Evaluation. *Journal of Testing and Evaluation*, 41(2), p.20120051.

Available at: <http://www.astm.org/doiLink.cgi?JTE20120051>.

Zhou, F. et al., 2014. Laboratory Evaluation of Asphalt Binder Rutting, Fracture, and Adhesion Tests. *Texas Department of Transportation, Report no. SWUTC/14/0-6674-1*.